THE UNIVERSITY *of* EDINBURGH

The exploration of bio-renewable solvents in membrane fabrication for applications in alcohol recovery and water purification

Ammara Akram

A thesis submitted for the degree of Doctor of Philosophy

The University of Edinburgh

2022

Declaration

The author declares that the work undertaken in this thesis has been carried out and composed by her, unless stated or acknowledged otherwise. This work has not been submitted or accepted in the fulfilment of any other degree or qualification, at any other university.

Thesis Supervisors

Dr. Andrea Joana Correia Semiao, University of Edinburgh, Edinburgh

Dr. Cher Hon Lau, University of Edinburgh, Edinburgh

Dr Santiago Romero-Vargas Castrillon, University of Edinburgh, Edinburgh

Thesis Examiners

Dr. Vitor Magueijo, University of Strathclyde, Glasgow

Dr. Francisco R Garcia Garcia, University of Edinburgh, Edinburgh

Abstract

Membrane separation is one of the most widespread sustainable and ecological technologies for purifying and separating waste streams. This process can substitute thermal separation processes such as distillation, evaporation, and crystallisation. Membrane separation has been proven to be promising for liquid separations due to the high efficiency, low operation cost and energy-saving performance in numerous applications of this process.

Nanofiltration (NF) is a pressure-driven membrane separation process that employs membranes for molecular separation and purification in liquid applications. Organic solvent nanofiltration (OSN) is a membrane process for molecular separation in harsh organic media. It excludes molecules dissolved in organic solvents based on shape, charge and size, allowing the reuse of solvents. NF membranes are typically produced as thin-film composite (TFC) membranes comprising of a thin porous selective layer typically derived from amines and acyl chlorides deposited on a porous substrate created from petroleum-derived synthetic polymers. The materials used in both layers are toxic, hazardous, petroleum-derived and non-biodegradable contributing to landfill and pollution. In recent years, works reported in the literature have been invested in embedding sustainability into membrane fabrication through the use of bio-renewable solvents and the use of sustainable raw materials. Although considerable progress has been made in the past few years with the production of green solvents from renewable feedstock, the use of these solvents for membrane fabrication has not been fully explored as new solvents are constantly emerging.

The work in this thesis aims to replace conventional materials used for membrane fabrication to create membranes that have lower environmental impact and health and safety concerns through the use of bio-renewable solvents and sustainable fabrication methods. The work in this thesis extends current research in green solvents through the exploration of Cyrene™ and 2-Methyltetrahydrofuran (2-MeTHF) for TFC membrane fabrication, two solvents that have not yet been explored. The work also investigated the application of these bio-renewable membranes in aqueous and organic solvent nanofiltration.

The thesis starts with the development of support that is stable in a wide range of organic solvents, allowing it to become the foundation of a thin film composite membrane that could be utilised in OSN applications. A comparative study was carried out, and supports were produced using Dimethylformamide, (DMF) (the conventionally used solvent) which were compared to supports produced using Cyrene™ (the bio-renewable alternative). The study looked at investigating the effects of using a bio-renewable solvent on the resultant support characteristics. The thermal and chemical stability, solvent filtration and morphology of the two supports were investigated. An important aspect considered in this project was the operating conditions for membrane fabrication. Traditional membranes are produced using complicated lengthy sixteen-hour energy-intensive procedures, the work in this project aimed to produce membranes using benign room temperature conditions. The fabrication of polyimide (PI) the most conventional polymer used in OSN membrane fabrication and Cyrene™ were explored and the combination of the polymer/solvent/non-solvent was unsuccessful in creating support. The polymer was changed to a renewable polymer, cellulose acetate (CA), and quick room temperature fabrication methods for 90 minutes were utilised to produce supports stable in harsh organic environments. The bio-renewable supports exhibited excellent permeance of solvents, and a 115% increase in water permeation was experienced compared to the traditional support produced using DMF. Protocols in this work were established that produced supports that maintained structural integrity and excellent stability in DMF immersion at 100 °C and performed well in different solvent environments.

The second part of this thesis was to fabricate polyamide, the selective layer used in a TFC membrane using 2-MeTHF. The polymer was studied and fully characterised and compared to the traditional polyamide produced using the petroleum-derived n-hexane solvent. The two polyamide layers were deposited onto the support produced using Cyrene™, and a TFC membrane was created using only bio-renewable solvents. Ethanol permeance of 2.5 L m^{-2} h^{-1} bar^{-1} was experienced when using the n-hexane derived polyamide, and this increased to 11.2 L m^{-2} h^{-1} bar^{-1} when 2-MeTHF was utilised as the solvent for interfacial polymerisation. A further 900% increase of ethanol permeance was experienced after DMF activation, reaching 25 L m^{-2} h^{-1} bar^{-1}. A detailed study was carried out to test for OSN applications with a range of dyes with varying molecular weights and charges and the molecular dye rejection rates of the bio-renewable TFC membrane reached 98%, higher than the n-hexane derived polyamide TFC membrane at 94%. The membrane produced solely from bio-renewable solvents outperformed current state-of-the-art membranes and mixed matrix membranes that incorporate fillers into the membrane for enhanced separation performance.

The final part of the thesis explored the potential of the bio-renewable TFC membranes being utilised in aqueous NF applications using a feed solution of different salts. The performance capabilities of the bio-renewable membrane were compared with a commercially available NF TFC membrane, NF 270. The bio-renewable TFC membrane experienced a higher water permanence compared to the NF 270 TFC membrane at 17.8 L m^{-2} h^{-1} bar^{-1} and 11.8 L m^{-2} h^{-1} bar^{-1} respectively. Further to this, magnesium chloride rejection for the bio-renewable TFC membrane reached 39% while the NF 270 TFC membrane reached 36%. The bio-renewable membrane outperformed the commercial membrane, and this opens up an interesting avenue of research, as the use of sustainable materials and benign operating conditions could compete with the current state-of-the-art membranes.

The results presented in this thesis make a valuable contribution to the exploration of the two bio-renewable solvents for membrane fabrication. The fabrication strategies developed in this work are time-saving, energy-efficient and cost-effective and protocols

were established that have improved health, safety and environmental impact. Next-generation membranes can be fabricated with sustainable materials to produce membranes that potentially have higher through-puts and require less energy for separations to occur which could potentially transform polymer membrane fabrication into a more sustainable process.

Acknowledgements

I would first like to express my deepest thanks and gratitude to my supervisors, Dr. Andrea Semiao and Dr. Sam Lau. The guidance and support that was received to produce this work was invaluable, and I am very grateful to have had the opportunity to work with you both - thank you.

The experimental work that has taken place in this thesis would not have been possible without the support of Mr.Fergus Dingwall, Mr. Stuart Martin and Mr. Gordon Patterson. Thank you for going above and beyond what was required and for your help with the experimental and characterisation aspect of the thesis.

I would also like to acknowledge, with gratitude, the financial support from the University of Edinburgh that I received to complete the PhD. A special thanks to the engineering graduate school, in particular, Dr. Kartina Tait, Ms Katherine Moore and Prof. Prashant Valluri for their help and support during the PhD, it would not have been possible to reach the end without this support.

To all the friends that became family along this journey, thank you. This has truly been a life-changing experience, and I am grateful that I got to meet you, travel with you and share the past four years with you. Finally, I would like to thank my family for their support during my PhD journey. Nani and Nanajee, thank you for everything you did for me, I hope I made you proud.

Contents

List of Tables

List of Figures

Nomenclature

2-MeTHF 2-Methyltetrahydrofuran

BET Brunauer-Emmett-Teller

CA Cellulose acetate

DMAc Dimethylacetamide

DMF Dimethylformamide

DMSO Dimethyl sulfoxide

FGF Fast Green F

FTIR Fourier Transform Infrared Spectroscopy

HSP Hansen solubility parameters

IP Interfacial polymerisation

IPC Isophthaloyl chloride

KOH Potassium hydroxide

MB Methylene Blue

MO Methyl Orange

MPD m-phenylenediamine

MWCO Molecular weight cut-off

NaOH Sodium hydroxide

NF Nanofiltration

NiPS Non-solvent induced phase inversion

NMP N-Methyl-2-pyrrolidone

OSN Organic solvent nanofiltration

PAN Polyacrylonitrile

PANi Polyaniline

PBI Polybenzimidazole

PEEK Poly(ether–ether–ketone)

PEG Polyethylene glycol

PI Polyamide

PIP Piperazine

PPD p-Phenylenediamine

PSf Polysulfone

PVDF Polyvinylidene difluoride

RB Rose Bengal

RhB Rhodamine B

RO Reverse osmosis

SEM Scanning electron microscopy

TFC Thin film composite membrane

Nomenclature

TGA Thermal gravimetric analysis

TMC Trimesoyl chloride

UV-Vis Ultraviolet-visible spectroscopy

XPS X-ray Photoelectron Spectroscopy

Chapter 1

Introduction

1.1 Project background and motivation

Separation processes are essential in numerous industries, however, the energy consumption of these processes contributes to 40% of the global energy output. A phase change in thermal separation processes such as distillation, evaporation, and crystallisation is required, resulting in high-energy consumption [1]. The removal of this phase change through membrane technology is an ecological solution that can be applied to transform the current industrial processes [1]. The use of membrane technology can help reach the target of zero emissions of greenhouse gases in 2050 in an attempt to stop or revert the global temperature increase [2].

Membranes have the capability for separating media at the industrial level with applications in food engineering, desalination and pharmaceutical industries with the potential of replacing distillation and crystallisation [3]. Recently, the fabrication of organic solvent nanofiltration membranes has opened up a new avenue of application exploration as these membranes are stable in harsh organic media. OSN membranes have the capability to be used in numerous applications such as hydrocarbon separation, catalyst recovery and product purification [1].

Many conventional separation and purification processes in oil refining, chemical and pharmaceutical industries use large amounts of organic solvents which require purification and involve high-energy consumption, utilising membrane technology in these processes could compete or complement these processes [1]. Employing this sustainable separation process in industries has the potential to reap major benefits: reduced energy consumption by an order of magnitude, increased separation performance, simplification of solvent renewable processes, the transformation of processes from batch to continuous, lower spatial requirements and cost of equipment [1]. In addition to this, incorporating membrane technology yields significant environmental benefits in waste minimisation as industrial chemical processes generate large amounts of waste, thus imposing an increased burden on

the environment [1], [4]. Recycling this waste through membrane technology presents many advantages, such as a substantial reduction of solvents released into the atmosphere which can significantly diminish environmental pollution, and health risks. Solvent recovery through a sustainable means allows for a considerable reduction in CO_2 emitted during processes which are in line with the target of zero emissions of greenhouse gases in 2050 [2].

Polymeric membranes are the most commonly used separation media at the industrial level for applications in the food, and water treatment industries [5]. Polymeric membranes exhibit good performance, are easy to fabricate, low cost and have a wide operating range [6]. Membrane technology has been recognised as a green sustainable process, however, the fabrication of polymeric membranes offsets the green credential of membrane technology as the materials chosen for fabrication are derived from major chemical building blocks of the petrochemical industry, obtained by the fractional distillation of crude oil and natural gas [4]. Further to this, the solvents used in fabrication are volatile, highly flammable, toxic to reproduction and carcinogenic and are listed as substances of very high concern [2].

The membrane manufacturing industry itself needs to be part of the transition to minimise the environmental impact of membrane manufacture and look for alternative biodegradable and sustainable materials that do not compromise the performance of membranes [4]. The design criteria for an effective membrane include: adequate sized pores, a narrow pore size distribution, a thin active layer, a high level of chemical and physical stability, robust mechanical strength, and simple fabrication methods [6]. Producing membranes from green alternative materials that offer the same performance is a great challenge.

In 2010 Paul Anastas developed the 12 Principles of Green Chemistry, which looked at the molecular level to achieve sustainability [7]. From this, many industries adopted their own principles, such as the pharmaceutical industry applying solvent selection guides to

change the current solvent usage to benign alternatives [8]. The development of new 'green' bio-renewable solvents which are derived from the processing of agricultural crops has opened up extensive works recently to see if the green bio-renewable solvents can be used in membrane fabrication [9]–[13]. Solvent waste from membrane fabrication accounts for up to 85 % of the waste derived from membrane fabrication [4]. The need to replace hazardous, toxic and petroleum-derived solvents is of great advantage. Further to this, extensive work has also been carried out using the principles of Green Chemistry to investigate different fabrication techniques, such as using alternative bio-materials in conjunction with the bio-renewable solvents or carrying out fabrication at room temperature and recycling waste materials for fabrication [14]–[20].

Although great progress has been made in the development of the fabrication of membranes using bio-renewable materials in the last few years, the emergence of new green solvents in the market allows for further exploration in this field. This PhD project looks at the application of two bio-renewable solvents for membrane fabrication.

1.2 Aim and objectives

The aim of this thesis is to assess the suitability of bio-renewable solvents for the fabrication of membranes and to determine the suitability of these membranes in nanofiltration applications. The bio-renewable solvents were compared to their petroleum-derived counterparts to determine if the use of the green bio-renewable solvent can produce membranes that exhibit similar properties whilst offering a sustainable alternative to current solvent systems.

Cyrene™ is a benign bio-renewable solvent derived from waste cellulose in a two-step process first developed by Circa Group in partnership with Professor James Clark at the University of York. It has demonstrated the capability of substituting toxic petroleum-

derived solvents such as DMF and N-Methyl-2-pyrrolidone (NMP), the two most commonly used solvents for membrane fabrication due to the similarities in density and polarity the solvent exhibits [21], [22]. Cyrene™ offers a safer alternative to the current solvents used, as the only hazardous risk associated with the solvent is that it is flammable.

2-Methyltetrahydrofuran is a bio-renewable solvent produced from corncobs which has limited miscibility with water and can potentially be used as an alternative to the traditional solvent n-hexane used for interfacial polymerisation to produce polyamide [23], [24]. Polyamide is the selective layer that is deposited onto support to produce a thin film composite membrane. The two parts of the membrane: the support and the selective layer, were produced through bio-renewable solvents and the membranes were tested for nanofiltration applications in both aqueous and organic feed solutions. The membranes were compared to a membrane produced using traditional solvents to explore the feasibility of successfully substituting the solvents.

1.3 Thesis structure

The thesis is structured into seven chapters. Chapter 1, is an introduction to the project background and the motivation for this thesis. The main objective and the contribution of this PhD project were also stated. Chapter 2, provides the literature review relevant to this project, background information about membrane fabrication, the design principles, fabrication methods, and applications in separation processes, were provided. In Chapter 3, details about the different materials that have been used in this work were stated. Further to this, the main methodologies that were developed for different experiments in this work were provided, as well as the different characterisation techniques used to characterise the materials were given.

Contents in Chapter 4 to Chapter 6 were the main body of this thesis and present

the experimental work that was carried out during the PhD. In these four chapters, the experimental work, results and discussions on the preparation of membranes using green solvents for nanofiltration applications were presented.

In Chapter 4, a comparative study of Cyrene™ and DMF membrane fabrication is presented. Supports were fabricated that were stable in organic solvents, allowing them to be utilised in organic solvent nanofiltration applications. Protocols were established to produce supports in quick and benign fabrication conditions. Different characterisation techniques were conducted to investigate the difference in structure and morphology that the two supports had, and the influence of the fabrication solvent on the resultant support is presented.

In Chapter 5, a comparative study was carried out producing polyamide - the conventional selective layer used in thin film composite membranes. The traditional petroleum-derived n-hexane solvent conventionally used for interfacial polymerisation to produce polyamide was compared to the polyamide fabricated using 2-MeTHF. Different characterisation techniques were employed to characterise the two polymers. The two selective layers were then deposited onto the support produced in chapter 4 and the two thin film composite membranes were tested for organic solvent applications with a feed solution of ethanol and different dyes of different molecular weights and charges.

In Chapter 6, the two selective layers established in chapter 5 were deposited onto a cellulose acetate support and were tested for aqueous nanofiltration with a feed solution consisting of different salt solutions. As the support for aqueous nanofiltration does not require cross-linking, supports using Cyrene™ and methanol were produced at room temperature. Methanol was used as this solvent is commonly used with CA support fabrication. The two thin film composite membranes were then compared to NF 270 a commercially available membrane to test the performance of the bio-renewable thin film composite membrane with a commercial membrane.

Chapter 7 presents the major conclusions and highlights the significance of this work. The limitations of this study are addressed, and suggestions for future work are also proposed.

References

[1] P. Marchetti, M. F. Jimenez Solomon, G. Szekely, and A. G. Livingston, "Molecular separation with organic solvent nanofiltration: A critical review," *Chemical reviews*, vol. 114, no. 21, pp. 10 735–10 806, 2014.

[2] D. Kim and S. P. Nunes, "Green solvents for membrane manufacture: Recent trends and perspectives," *Current Opinion in Green and Sustainable Chemistry*, p. 100 427, 2020.

[3] G. Szekely, J. Bandarra, W. Heggie, B. Sellergren, and F. C. Ferreira, "A hybrid approach to reach stringent low genotoxic impurity contents in active pharmaceutical ingredients: Combining molecularly imprinted polymers and organic solvent nanofiltration for removal of 1, 3-diisopropylurea," *Separation and purification technology*, vol. 86, pp. 79–87, 2012.

[4] G. Szekely, M. F. Jimenez-Solomon, P. Marchetti, J. F. Kim, and A. G. Livingston, "Sustainability assessment of organic solvent nanofiltration: From fabrication to application," *Green Chemistry*, vol. 16, no. 10, pp. 4440–4473, 2014.

[5] R. J. Petersen, "Composite reverse osmosis and nanofiltration membranes," *Journal of membrane science*, vol. 83, no. 1, pp. 81–150, 1993.

[6] R. W. Baker, *Membrane technology and applications*. John Wiley and Sons, 2012.

[7] P. Anastas and N. Eghbali, "Green chemistry: Principles and practice," *Chemical Society Reviews*, vol. 39, no. 1, pp. 301–312, 2010.

[8] D. Prat, O. Pardigon, H.-W. Flemming, *et al.*, "Sanofi's solvent selection guide: A step toward more sustainable processes," *Organic Process Research and Development*, vol. 17, no. 12, pp. 1517–1525, 2013.

[9] M. Doble and A. K. Kruthiventi, "Alternate solvents," *Green Chemistry and Engineering*, pp. 93–104, 2007.

[10] M. A. Rasool, P. P. Pescarmona, and I. F. Vankelecom, "Applicability of organic carbonates as green solvents for membrane preparation," *ACS Sustainable Chemistry and Engineering*, vol. 7, no. 16, pp. 13 774–13 785, 2019.

[11] M. A. Rasool, C. Van Goethem, and I. F. Vankelecom, "Green preparation process using methyl lactate for cellulose-acetate-based nanofiltration membranes," *Separation and Purification Technology*, vol. 232, p. 115 903, 2020.

[12] M. A. Rasool and I. Vankelecom, "Use of γ-valerolactone and glycerol derivatives as bio-based renewable solvents for membrane preparation," *Green chemistry*, vol. 21, no. 5, pp. 1054–1064, 2019.

[13] A. Figoli, C. Ursino, S. Santoro, *et al.*, "Cellulose acetate nanofiltration membranes for cadmium remediation," *Journal of Membrane Science and Research*, vol. 6, no. 2, pp. 226–234, 2020.

[14] S.-H. Park, A. Alammar, Z. Fulop, B. A. Pulido, S. P. Nunes, and G. Szekely, "Hydrophobic thin film composite nanofiltration membranes derived solely from sustainable sources," *Green Chemistry*, 2021.

[15] S. Hermans, E. Dom, H. Marien, G. Koeckelberghs, and I. F. Vankelecom, "Efficient synthesis of interfacially polymerized membranes for solvent resistant nanofiltration," *Journal of Membrane Science*, vol. 476, pp. 356–363, 2015.

[16] L. Paseta, M. Navarro, J. Coronas, and C. Tellez, "Greener processes in the preparation of thin film nanocomposite membranes with diverse metal-organic frameworks for organic solvent nanofiltration," *Journal of Industrial and Engineering Chemistry*, vol. 77, pp. 344–354, 2019.

References

[17] F. Fei, H. A. Le Phuong, C. F. Blanford, and G. Szekely, "Tailoring the performance of organic solvent nanofiltration membranes with biophenol coatings," *ACS applied polymer materials*, vol. 1, no. 3, pp. 452–460, 2019.

[18] K. Vanherck, A. Cano-Odena, G. Koeckelberghs, T. Dedroog, and I. Vankelecom, "A simplified diamine crosslinking method for pi nanofiltration membranes," *Journal of membrane science*, vol. 353, no. 1-2, pp. 135–143, 2010.

[19] J. da Silva Burgal, L. Peeva, and A. Livingston, "Towards improved membrane production: Using low-toxicity solvents for the preparation of peek nanofiltration membranes," *Green Chemistry*, vol. 18, no. 8, pp. 2374–2384, 2016.

[20] B. A. Pulido, O. S. Habboub, S. L. Aristizabal, G. Szekely, and S. P. Nunes, "Recycled poly (ethylene terephthalate) for high temperature solvent resistant membranes," *ACS Applied Polymer Materials*, vol. 1, no. 9, pp. 2379–2387, 2019.

[21] R. A. Milescu, C. R. McElroy, T. J. Farmer, P. M. Williams, M. J. Walters, and J. H. Clark, "Fabrication of pes/pvp water filtration membranes using cyrene, a safer bio-based polar aprotic solvent," *Advances in Polymer Technology*, vol. 2019, 2019.

[22] H. J. Salavagione, J. Sherwood, V. Budarin, G. Ellis, J. Clark, P. Shuttleworth, *et al.*, "Identification of high performance solvents for the sustainable processing of graphene," *Green Chemistry*, vol. 19, no. 11, pp. 2550–2560, 2017.

[23] E. Yara-Varon, A.-S. Fabiano-Tixier, M. Balcells, R. Canela-Garayoa, A. Bily, and F. Chemat, "Is it possible to substitute hexane with green solvents for extraction of carotenoids? a theoretical versus experimental solubility study," *RSC Advances*, vol. 6, no. 33, pp. 27 750–27 759, 2016.

[24] A.-G. Sicaire, M. A. Vian, A. Filly, Y. Li, A. Bily, and F. Chemat, "2-methyltetrahydrofuran: Main properties, production processes, and application in extraction of natural products," in *Alternative Solvents for Natural Products Extraction*, Springer, 2014, pp. 253–268.

Chapter 2

Literature review

This review aims to provide insight into current state-of-the-art research in thin film composite membranes for both aqueous and organic nanofiltration applications. It will focus on membrane fabrication, the different parameters in membrane formation and the materials currently employed. A future challenge of membrane fabrication is to develop membranes using materials that have lower toxicity and better health, safety and environmental impact and the current work focused on this will also be presented.

2.1 Background

A membrane is a molecular sieve that allows the separation of solutes and employs a driving force to push a feed stream through a membrane [1]. The fraction of the feed stream that passes through the membrane is known as the permeate, and the fraction that cannot pass through the membrane produces the retentate stream, as shown in Figure 2.1 [1]. Membrane separation is one of the most widespread sustainable technologies for purifying and separating waste streams and can be utilised in a wide range of industries such as desalination, wastewater treatment, chemical production, pharmaceutical and food engineering [1], [2]. Membrane technology is considered a sustainable process when compared with conventional separation methods such as evaporation and distillation, which are widely used in industry, due to the improved energy efficiency, reduced environmental impact, and the ease of scale up this technology offers [1]–[3].

2.1.1 Pressure driven membranes

Pressure-driven membranes utilise pressure as a driving force for separation and the separation process can be categorised according to (1) the pressure required for the separation; (2) the size of the rejected solute or, the size of the pore; (3) the molecular weight cut off (MWCO); and (4) the transport mechanism governing the separation [1].

These categories include: microfiltration (MF), ultrafiltration (UF), nanofiltration (NF), and reverse osmosis (RO) membranes, see Figure 2.2 for the pore size classification for these membrane processes. [1].

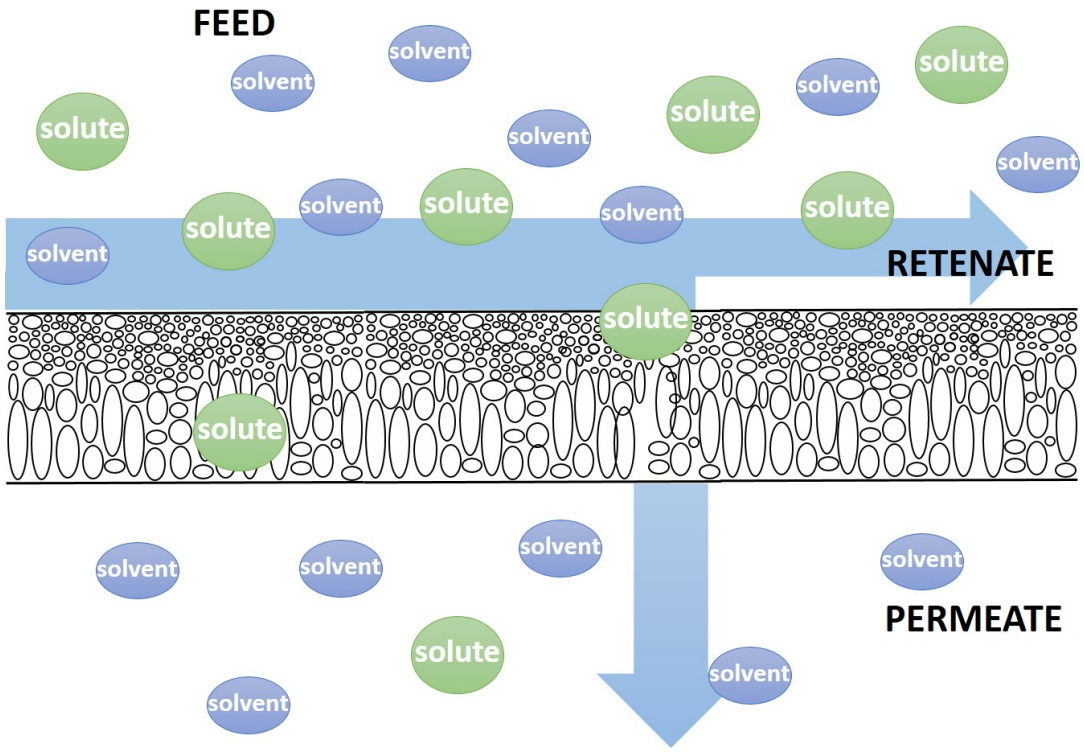

Figure 2.1: Diagram depicting a pressure-driven membrane separation process

MF membranes have pore sizes ranging from 0.1 - 10 μm and are used for the removal of large particulates, colloids, and bacteria from feed streams [1]. UF membranes have smaller pore sizes ranging from 0.1 - 0.01 μm and are used for rejecting viruses and polypeptides, and are widely used in protein concentration and wastewater treatment [1]. The pressure employed for UF separation ranges from 1-5 bar [4], [5]. The composition of MF and UF membranes are predominantly of asymmetric configuration, as the size of the contaminants are able to be rejected by the pore size in the asymmetric membranes [1], [6].

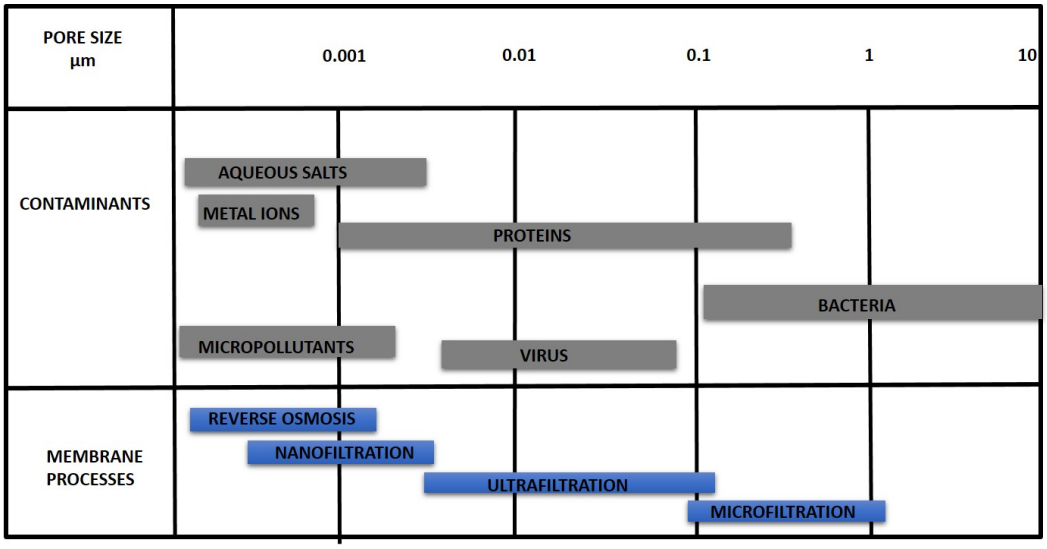

Figure 2.2: Overview of pressure driven membrane processes available for wastewater treatment, adapted from [1]

Nanofiltration membranes are able to reject multivalent salts, uncharged solutes and various organic molecules with pore sizes in the range of 0.01 - 0.001 μm with operating pressures ranging from 5 to 60 bar [5], [6]. Due to the relatively low operating pressures, NF membranes experience high flux and high rejection to contaminants. Reverse osmosis membranes are tighter than NF membranes and are able to reject monovalent ions while allowing water molecules to pass through in aqueous solutions. Common applications for reverse osmosis include seawater desalination and industrial water treatment [1]. Nanofiltration and reverse osmosis membranes can be asymmetric membranes with a dense highly rejecting top layer (50-150 nm) or composite membranes where a polymer layer (<1 μm) is derived on top of a porous asymmetric layer [1]. These membrane configurations allow the membranes to be suitable for small ion selectivity. [1], [4], [6].

2.1.2 Membrane performance

Membrane functional characterisation is a measure of the membrane's performance and is determined by permeability and solute/particle rejection. Permeability is a measure of the flux that permeates the membrane as a function of transmembrane pressure (ΔP). The flux (J) is calculated by measuring the permeate volume (V) per unit area (A) per unit time (t) and is expressed in terms of Equation 2.1. The flux is proportional to the applied pressure to the membrane, and the permeability of the membrane is expressed as Equation 2.2 with the units L m^{-2} h^{-1} bar^{-1}.

Selectivity is a measure of the membrane's capability to reject solutes and is conventionally measured as rejection. It is calculated as a function of the solute concentration in the permeate C_P and the feed streams, C_F which is expressed as Equation 2.3.

$$Flux = \frac{V}{At} \tag{2.1}$$

$$Permeance = \frac{V}{At\Delta P} * 100\% \tag{2.2}$$

The rejection of the membranes was calculated using the following equation:

$$Rejection\% = (1 - \frac{C_P}{C_F}) * 100\% \tag{2.3}$$

The separation performance of a membrane can also be defined by the molecular weight cut-off (MWCO). MWCO is defined as the lowest molecular weight at which greater than 90% of a solute with a known molecular weight is rejected by the membrane [1]. The MWCO measures the rejection to selected solutes with different molecular weights under

controlled conditions [1]. The solutes cover the expected size range for the membrane with 0% to 100% rejection, and ideally should not interact with the membrane. Typical oligomers used for MWCO experiments include polyethylene glycol and polystyrene [6]. The MWCO of a membrane is derived from an MWCO curve, which features the membrane's rejection of solutes over a range of molecular weights as shown in the example in Figure 2.3, (in this membrane the MWCO would be determined to be 360 g/mol) [6], [7].

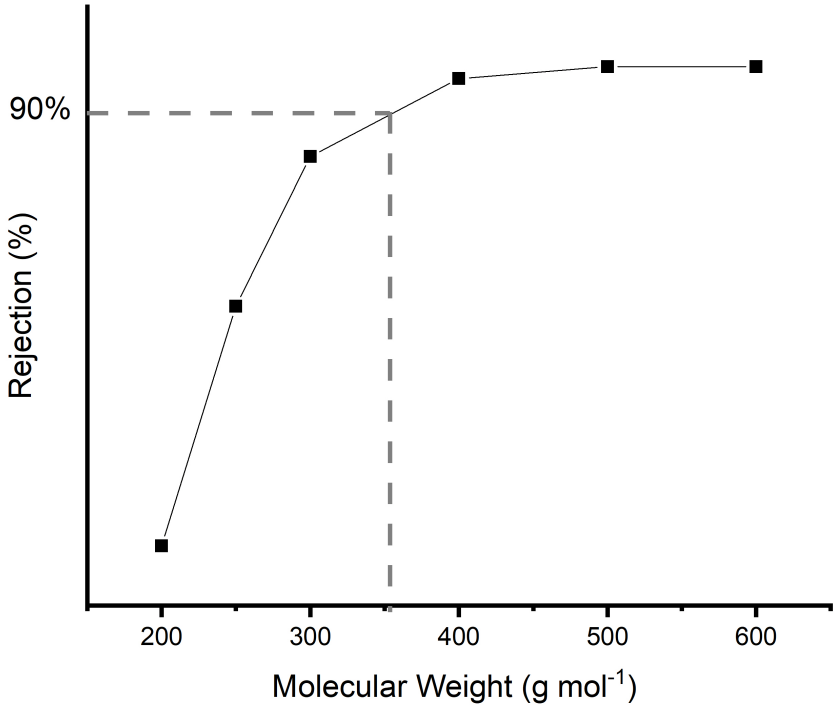

Figure 2.3: Example of molecular weight cut-off curve

2.2 Nanofiltration

Nanofiltration membranes are a type of pressure-driven membrane process with properties in between reverse osmosis and ultrafiltration membranes [1]. NF membranes have the capability to reduce the ionic strength of solutions and remove hardness, organics and particulate contaminants [2]. The key distinguishing characteristics of NF membranes are that they offer low rejection of monovalent ions, high rejection of divalent ions and higher flux compared to RO membranes [8]. Further to this, nanofiltration offers several advantages over reverse osmosis, such as relatively lower investment and lower operation and maintenance costs [1]. Due to the number of advantages that this technology offers, the use of nanofiltration membranes has increased [2], [9]. Further to this, NF has grown rapidly in the last few decades as this technology has the unique ability to separate and fractionate ionic and low molecular weight organic species. NF is used in aqueous separations such as desalination, wastewater treatment, pharmaceutical purification and biomedical applications, but also organic solvent-based separations emerging in the chemical, and petrochemical industries [1], [10], [11].

The separation mechanism of nanofiltration membranes can be attributed to a combination of size-based and Donnan exclusion principles [8]. The Donnan exclusion describes the equilibria and potential interactions between a charged species and the charged interface of the membrane [1]. The membrane charge originates from the dissociation of ionisable groups at the membrane surface and from within the membrane pore structure [1], [8]. As the Donnan exclusion effect is much stronger for multivalent ions than for monovalent ions, the selective layer is able to reject multivalent ions but allows the monovalent ions to pass relatively unhindered [1]. The transport of neutral solutes is via size-based exclusion [1].

2.2.1 Aqueous nanofiltration

Nanofiltration membranes are used in the treatment of groundwater [12], surface water [13] and wastewater reclamation [14] [1]. Another application for nanofiltration membranes is in the textile industry. The textile industry consumes large amounts of water and chemicals for the processing of textiles. The concentrations of dyes in the effluent are undesirable, and the application of nanofiltration membranes to remove these dyes is advantageous. The removal of dyes from wastewater has been studied extensively by many researchers [15]–[19]. Commercially available membranes that are used for nanofiltration and the properties are listed in Table 2.1.

Table 2.1: Commercial NF membranes and their characteristics

Membrane	Manufacturer	Selective layer	Salt rejection
SW30 HRLE-400	Dow Filmtec	PA TFC	99.8% NaCl
NF270-400/34i	Dow Filmtec	alkanes, PA TFC	97% NaCl
TrisepTS40	Trisep	Polypiperazineamide TFC	99% MgCl
T880 Trisep	Trisep	PA TFC	99.2 % MgSO4
4040-HR	Koch	PA TFC	99.2% NaCl
8040-SW-400-34	Koch	PA TFC	99.5% NaCl

2.2.2 Organic solvent nanofiltration

Recently, the development of membranes suitable for organic solvent nanofiltration has opened up a wide range of potential applications for NF membranes in separations involving non-aqueous solutions. The operating range of these membranes is similar to that of NF membranes used in aqueous membranes, but the support has to be modified for enhanced applications involving alcohols and polar aprotic solvents [11]. Applications

for this technology can replace distillation, crystallisation, chromatography and adsorption in the food, chemical, pharmaceutical and petroleum industry [20]–[25].

Compared to traditional separation processes, the use of OSN membranes offers sustainable advantages such as high efficiency, and reduced energy consumption as distillation and crystallisation operations are no longer required. In a study conducted by Rundquist *et al.*, it was found that OSN membranes are able to use 25 times less energy per volume of the recovered solvent when compared to distillation for solvent recovery from crystallisation [26]. Further to this, other authors affirm that the energy required when using OSN membranes can be as little as 10% of that required by distillation, and operations can proceed at room temperature with no vacuum requirement [7], [27]. OSN allows for low operating temperatures as separation can proceed at room temperature and membranes can be easily installed as a continuous process or combined with existing processes to form a hybrid process [7], [27].

OSN requires solvent-resistant membranes that are able to preserve their separation characteristics while processing a large range of solvents with defect-free morphology and controlled molecular weight cut-off [11]. To meet the industrial requirement, membranes should exhibit high permeance, increased rejection, excellent solvent resistance and long-term stability [11]. Commercially available OSN membranes that are available, and the operating ranges, are listed in Table 2.2.

Table 2.2: Commercial OSN membranes and their characteristics

Membrane	Material	Stability range	MWCO Da
Evonick MET Germany, Duramem & Puramem	Lenzing P84	Alcohols, aromatics, esters, ketones, polar aprotic	150 - 900 & 280 - 600
Borsig Membranes Technology Germany, GMT-oNF	PDMS based composites	alkanes, alcohols, aromatics, ethers, esters, ketones	unspecified

2.3 Membrane fabrication

Membranes can be classified into different categories depending on the material, structure and application [1]. Membrane materials can include organic materials such as in polymer membranes or inorganic materials such as in ceramic membranes [1]. Polymeric membranes lead the membrane separation industry and market due to the straightforward pore-forming mechanism, higher flexibility, smaller footprints required for installation, and relatively low cost compared to inorganic membrane equivalents [1]. Polymeric membranes can be classified into two groups based on membrane structures: asymmetric membranes and thin film composite (TFC) membranes [1], [28].

The most common and versatile process employed to produce polymeric membranes is through phase inversion using the Loeb–Sourirajan method [3]. Phase inversion is a demixing process in which a homogeneous polymer dope solution is transformed from a liquid phase to a solid phase through different stages to produce an asymmetric membrane, (see Figure 2.4a for the illustration) [3]. The most widely adopted method to fabricate membranes through phase inversion is using the Non-solvent Induced Phase Separation (NIPS) process [1]. A polymer dope solution containing a polymer dissolved in a suitable solvent at typical concentrations ranging from 10 to 25 wt% is used [2]. An even film of the polymer dope solution is spread across a non-woven support material taped to a glass plate with a casting knife at a thickness between 50-500 μm [1]. After casting, the solution is left to stand for a few seconds (10-100 s) before being submerged into a coagulation bath using a non-solvent to precipitate the film and form a membrane. The non-solvent precipitates in the top surface of the cast film rapidly to form a dense surface layer of approximately 100 nm thick [1]. This layer then slows the entry of the non-solvent into the underlying polymer solution, which precipitates much slower to form a more porous substructure to produce an asymmetric membrane.

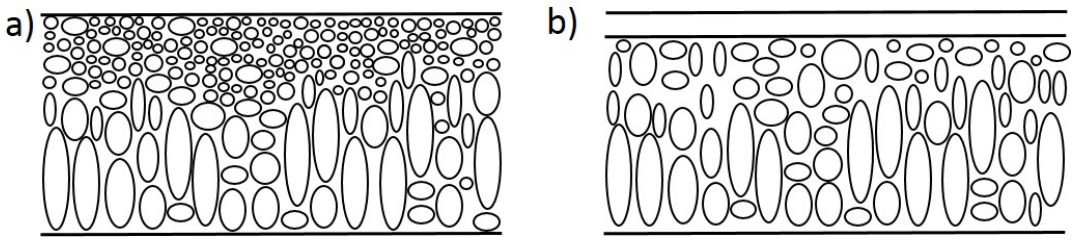

Figure 2.4: Schematic diagram representing polymeric membranes a) integrally skinned asymmetric membrane b) thin film composite membrane adapted from [1].

Thin film composite membranes typically consist of at least three components: (1) a top thin selective layer; (2) a bottom porous sublayer (e.g. an asymmetric membrane as described above); and (3) a non-woven backing material, [29] (see Figure 2.4b for the illustration). The porous support provides the required mechanical stability for the whole membrane structure to operate under high pressures (5-40 bar), while the ultrathin top surface layer plays the principal role in the rejection of contaminants [1], [29]. The multilayer feature of TFC membranes exploits the highly desirable advantage that each layer in the composite membrane can be independently optimised with the choice to tailor materials and preparation methods to target specific applications [9]. Thin film composite membranes experience extremely high salt rejections at over 99.5% and are widely used for industrial applications in RO and NF [1], [29]–[31]. The membranes are also stable over a larger pH range (pH 5-13) and are able to withstand high temperatures as they are stable up to 70° C [32], [33]. The disadvantage to this membrane is that it is more expensive compared to asymmetric membranes, as more materials are required for fabrication [2].

The most widely adopted technique to prepare TFC membranes is interfacial polymerisation (IP) due to the high manufacturing efficiency and the robust separation performance of the resulting TFC membrane [1]. Key for IP is the interface between two immiscible solvents, water and an organic solvent [9]. Monomers that are only soluble in each phase diffuse towards the interface and polymerise in this region of significant chemical potential difference to produce a thin film, (see Figure 2.5 for the diagram of this process) [9]. During IP, an aqueous amine solution is deposited onto an asymmetric support of ultrafiltration

performance characteristics. This amine solution penetrates the pores of the support, and then the amine-loaded support is immersed into an organic solution containing an acyl chloride. The two monomers react instantly at the interface of the two immiscible solvents until a thin ($\sim$ 200 nm) highly cross-linked polyamide (PA) film is produced on the support [1], [9]. The chemical and physical characteristics of the interfacially formed polyamide film are dependent on a number of important variables such as: monomer type, concentration and partition coefficient of monomer, type of organic solvent, overall kinetics and diffusion rates of monomer, reaction time, presence of additive/surfactant and post-treatment of the resulting polymer film [9].

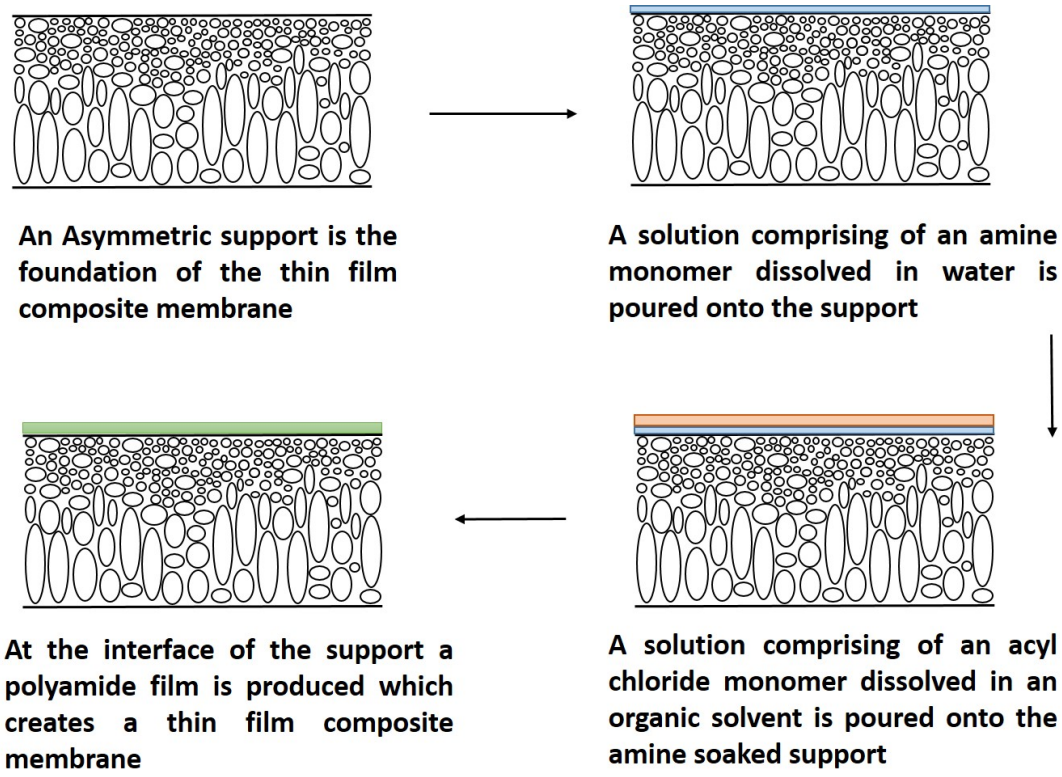

Figure 2.5: Schematic diagram representing the process of interfacial polymerisation to create a thin film composite membrane

There are five parameters that influence membrane fabrication: (1) solvents used for support fabrication; (2) solvents used for IP; (3) polymer used for support fabrication; (4) monomers used for IP; (5) fabrication conditions (temperature of the dope solution, coagulant used for phase inversion, operating temperatures). All five parameters will be

presented and discussed in this chapter.

2.3.1 Solvents used for membrane fabrication

The choice of solvent for membrane fabrication is based on several factors: a solvent is selected for the capability to dissolve the polymer at either room temperature or high temperatures suitable for use in NIPS or TIPS [1]. The characteristics of the solvent will influence the membrane morphology, as membranes prepared with different solvents will exhibit different properties [1], [34]. The most commonly used solvents employed for membrane fabrication are aprotic solvents such as dimethylformamide, N-Methyl-2-pyrrolidone and dimethylacetamide (DMAc) [2], [35]–[39]. These solvents dissolve a wide range of polymers, and polymer dope solutions based on these solvents precipitate rapidly when immersed in a coagulation bath containing water to produce porous anisotropic membranes [1]. Producing dope solutions using low solubility-parameter solvents, such as tetrahydrofuran, acetone, or dioxane are generally not appropriate as they slow the precipitation and produce non-porous membranes [1], [2].

2.3.2 Monomers used during interfacial polymerisation

The physicochemical properties of the selective layer are an important factor in determining the membrane separation efficiencies [40]. For high permeability and selectivity, the selective layer of the TFC membrane should be very thin with a highly cross-linked structure [9]. The structure of the PA is an important factor in determining the permeation characteristics of the membrane. The pore size and the free volume of the selective layer influence the MWCO and permeation rate [9]. Generally, membrane performance is tailored to meet the required application by adjusting the IP parameters and these include: the reactive monomers, additives, monomer concentration, reaction time, temperature,

and post-treatment conditions [9], [34].

The commonly used reactive amines to produce polyamide are aliphatic or aromatic diamines such as piperazine (PIP), m-phenylenediamine (MPD) or p-phenylenediamine (PPD) respectively [41]. The commonly used acyl chloride monomers used include trimesoyl chloride (TMC), isophthaloyl chloride (IPC) or terephthaloyl chloride (TPC) [9].

Amines used during Interfacial polymerisation

The most commercially successful method employed to produce a polyamide selective layer is to use MPD in an aqueous solution reacting with TMC in an organic solvent. Membranes produced using aromatic diamines such as MPD produce a more cross-linked polyamide selective layer compared to an aliphatic amine such as PIP and are able to reject NaCl at 99.5 % [29]. This method is used to produce FT-30, a reverse osmosis membrane produced by Filmtec [29].

Alternatively, an aliphatic monomer such as PIP can also react with aromatic TMC to form a semi-aromatic poly(piperazinamide) [29]. Membranes based on this chemistry exhibit low rejections of NaCl (50%) [29], [42]. Commercial membranes that employ this selective layer include NF270 from Filmtech [29]. The membranes produced in this work were carried out using this chemistry, as this is the most commonly used monomer for nanofiltration applications.

The concentration of the monomer is crucial for the performance of the membrane. A study conducted by Khorshidi *et al.* investigated the effect of the monomer concentration on the salt rejection and water flux of the TFC membrane. It was found that increasing the MPD concentration from 1% to 2% increased the salt rejection from 95% to 97% and decreased the water flux from 45 L m^{-2} h^{-1} to 15 L m^{-2} h^{-1} at 15 bar [30].

Acyl chlorides used during interfacial polymerisation

The structure and the number and position of the acyl halide group on the aromatic ring influence the structure of the resulting polyamide [9]. In addition to the most commonly used trifunctional monomer TMC, membranes have also been prepared from bifunctional acyl chlorides such as IPC or TPC [41], [43], [44]. The use of these bifunctional acyl chlorides reduces the amount of unreacted acyl chloride group and also produces a linear polyamide rather than a more cross-linked structure when reacted with amines [41]. This difference in the degree of cross-linking results in lower rejections in membranes produced using IPC and TMC, as Saha *et al.*, found that a PIP-IPC PA TFC membrane had a water flux of 25 L m^{-2} h^{-1} and NaCl rejection of 40 % compared to a water flux of 90 L m^{-2} h^{-1} at 10 bar and a NaCl rejection of 50 % when using a PA fabricated using PIP-TMC [42].

The concentration of acyl chloride is also crucial for the performance of the membrane. Khorshidi *et al.*, also investigated the effect of increasing the acyl chloride concentration from 0.15 % to 0.35 %. It was found that the increase in concentration resulted in higher water flux 13 L m^{-2} h^{-1} to 45 L m^{-2} h^{-1} at 15 bar. However, the salt rejection decreased from 97.5 % to 95 % [30].

2.3.3 Solvents used during interfacial polymerisation

The organic solvent used for IP must be immiscible in water, and n-hexane is the most widely used solvent for IP [1]. Studies have also been carried out using heptane, cyclohexane, isopar G, benzene and 1,2-Dichloroethane [30], [40], [45], [46]. A study, carried out by Hu *et al.*, investigated the effect of the organic solvent used during interfacial polymerisation and the effect this solvent has on the resulting TFC membrane in terms of salt rejection and water flux [47]. PIP and TMC were used as the monomers, and the feed solution comprised of an aqueous Na_2SO_4 solution. Cyclohexane, (68.1 L m^{-2} h^{-1}, 96.9 %) n-hexane, (57.5 L m^{-2} h^{-1}, 97.7 %), toluene, (43.9 L m^{-2} h^{-1}, 87.2 %) and xylene, (34.6 L m^{-2} h^{-1}, 91.8 %) were tested at 10 bar, and it was found that from the four solvents, cyclohexane performed the best in terms of water flux and salt rejection [47].

The addition of solvents to the aqueous or organic phase can alter the interfacial properties and improve the polymerisation efficiency. Solvents employed for this include n-propanol, i-propanol and DMF as they have good solubility towards polyamide [48]. Akbari *et al.*, added dimethyl sulfoxide (DMSO) in the aqueous phase during interfacial polymerisation and the resultant TFC membranes experienced a flux increase of 46 % and the salt rejection remained unaltered [49].

2.3.4 Current protocols and chemicals used in membrane fabrication

Organic Solvent Nanofiltration Membrane Fabrication

Different to membranes that are employed for aqueous applications, OSN membranes require stability in harsh organic media for them to be utilised in a wide range of solvents [11]. Conventional TFC membranes, when in contact with organic solvents, swell or undergo dissolution as the structure of the polymer is not able to withstand the harsh organic nature of solvents [11]. To overcome this, a cross-linking step is required to enhance membrane stability [7]. Polymer cross-linking can take place using chemical cross-linking, plasma cross-linking or UV cross-linking [50]. Chemical cross-linking is the most widely adopted technique for OSN membranes due to the relative ease of the method compared to the use of UV or plasma crosslinking, covalent bonds are formed to join polymer chains together, which allow for stability in polar aprotic solvents [11].

The polymer chosen for a membrane affects the pore size, morphology and chemistry of the membrane. The support is the foundation of the TFC membranes and the interface where IP occurs. Polymer choice for membrane fabrication is determined by the polymer's chemical and thermal stability, film forming properties, tolerance to a wide range of pH, availability and price [1], [7]. Polymers undergo dissolution in organic solvents at temperatures above 50 °C to form a polymer dope solution suitable for casting, and consequently, high glass transition temperatures are required [1]. Common synthetic polymers utilised for membrane fabrication typically include polyacrylonitrile (PAN) [51]–[54], polybenzimidazole (PBI) [39], [51], polyimide (PI) [37], [51], [55]–[57], polyaniline (PANI) [36], [58]–[61], polythiosemicarbazide (PTSC), polysulfone (PSf), polyvinylidene difluoride (PVDF) [38], [51], [62], [63] and poly(ether–ether–ketone) (PEEK) [64]–[66].

Current membrane protocols for fabricating OSN membranes require lengthy fabrication

procedures and produce substantial amounts of hazardous waste. To begin with, polymer solutions are heated at temperatures greater than 70 °C for over 8 hours to form a dope solution [27]. Membrane supports are fabricated using phase inversion and then undergo chemical cross-linking, a procedure based on the polymer type. The most commonly employed polymer for OSN is polyimide and supports undergoing a sixteen-hour cross-linking procedure in a hexanediamine and isopropanol solution to allow stability in organic solvents [37], [55]. Other common polymers used to produce membranes used in OSN and the common cross-linking procedures are shown in Table 2.3.

Table 2.3: Common polymers and solvents used for OSN membrane fabrication

Polymer	Dope Solution Solvent	Cross-linking reagent	Cross-linking Reaction conditions	Ref
PAN	DMF	Hydrazine hydrate/water	8 h, 80 °C	[35]
PANI	NMP/maleic acid	α, α-dichloro-p-xylene in acetone/hexane	144 h, 25 °C	[36]
PI	DMF	hexanediamine in isopropanol	16 h, 25 °C	[37]
PBI	DMA	α, α -dibromo-p-xylene in acetonitrile	24 h, 80 °C	[39]
PVDF	NMP/THF	Methanol solution of sodium hydroxide, para-xylenediamine and magnesium oxide	24 h, 25 °C	[38]

Solvent activation

A common post-treatment method employed to enhance flux and selectivity is solvent activation [67]. The solvent is passed through the membrane for a duration of time to remove any contaminants or oligomers within the membrane [37]. An increase in flux and selectivity is experienced after solvent activation, and this can be attributed to the

opening of the membrane pores that may have been previously blocked [68]. Activating the membrane with a solvent irreversibly modifies the membrane surface [69].

The solvent choice for activation is determined by the similarities in the Hildebrand solubility parameters of the activating solvent and the selective polyamide layer [37]. The Hildebrand solubility parameter of different solvents and polyamide can be seen in Table 2.4. Polar aprotic solvents have a better affinity to polyamide compared to alcohols and the top 3 solvents for activation are NMP, DMAc and DMF. Solvent activation has been applied to RO and NF membranes where the use of alcohols such as ethanol, methanol or isopropanol are used [69], [70]. These solvents are chosen as the membrane is able to interact with the solvent without dissolution [69], [70]. Kulkarni *et al.* reported the use of ethanol for solvent activation and this increased water permeance from 6 L m^{-2} h^{-1} bar^{-1} to 20 L m^{-2} h^{-1} bar^{-1} and increased NaCl rejection slightly from 70 % to 75 % [70].

Table 2.4: Hildebrand solubility parameter of different solvents, values taken from [71]

Solvent	Hildebrand Solubility Parameter $(MPa)^{1/2}$
NMP	22.9
DMAc	22.7
DMF	24.8
DMSO	26.6
. Methanol	29.7
Ethanol	26.2
PA	23.0

The use of solvent activation has been extended to OSN membranes and as these membranes are stable in harsh organic media, polar aprotic solvents can be used for activation. The use of DMF for solvent activation has been widely reported in literature and different studies have been carried out using different activation protocols [67], [68], [72]. These include treating the membrane with DMF at 80 °C for 30 min [73]–[75], DMF

filtration for 25 min [76] and 10 min [37], [55]. The studies have all reported a significant increase in flux and selectivity after DMF activation. Mertenes *et al.*, experienced an increase of permeance in acetonitrile by a factor of 11 after DMF activation in PVDF membranes and the activation had no effect on the Rose Bengal rejection, as it remained the same as prior to activation [38]. Solomon *et al.* explored solvent activation for PI membranes, where acetone permeance increased to 71 L m^{-2} h^{-1} bar^{-1} compared to 0.3 L m^{-2} h^{-1} prior to activation when using DMF as the activation solvent [37]. Solomon *et al.* also reported that membrane flux can be improved by eight times, with an 11 % increase in rejection when using DMF as an activating solvent [55].

Further work has been carried out using different solvents for activation, Guo *et al.* used an ionic liquid to treat a commercial PA TFC RO membrane (DOW BW30LE) and the results indicated that solvent activation improved the flux by 62 % with a 2.6 % decrease in salt rejection [77]. Shi *et al.,* investigated the use of hexane as an activating solvent and found the flux experienced an increase of 63 % after activation, however, the rejection decreased by 0.48 % [78]. Solomon *et al.* also looked at DMSO for activation, prior to activation, the membrane experienced no tetrahydrofuran, (THF) flux and after activation with DMSO the same membrane experienced a flux of 49 L m^{-2} h^{-1} at 30 bar [37].

2.4 Sustainability in membrane fabrication

Fabrication methods employed for OSN membranes, in particular, are lengthy and conventional fabrication methods use solvents that are generally synthesised from the fractional distillation from crude oil and natural gas, see Table 2.3 [27]. The use of petroleum-derived solvents and synthetic polymers offsets the green credentials of membrane processes and has a negative impact on the environment [27].

The use of petroleum-derived solvents carry great health and safety risks and the use of common solvents used in fabrication such as DMF, NMP, DMAc, heptane and hexane are all deemed 'hazardous' and carry considerable hazards [79]. These hazards include explosiveness, flammability, volatility, and health hazards such as acute and chronic toxicity, carcinogenicity, mutagenicity, reproduction/developmental [79]. Due to the hazards associated with these solvents, they are highly regulated by the European Chemical Agency [Regulation (EC) no. 1907/2006]. The hazards associated with the solvents for polymer dope solutions and interfacial polymerisation are shown in Table 2.5.

Membrane fabrication generates a substantial amount of hazardous waste which has to undergo targeted disposal. Usually, up to 75–85 wt% of the petroleum-derived solvent and any additives present in the dope solution are transferred to the non-solvent bath during phase inversion [27]. This process can produce up to 100-500 L of liquid waste to fabricate one square meter of a membrane [27]. Globally, it is estimated that membrane production annually generates more than 50 billion litres of wastewater with toxic solvents. OSN membranes require a chemical cross-linking step for enhanced stability in organic solvents, which further generates a large number of liquid waste [10]. The disposal of this waste not only incurs an environmental burden as treatment is required before disposal but also comes at a substantial cost [65].

Table 2.5: Hazards associated with solvents typically used for membrane fabrication

Solvent	Hazard statements	CHEM21 ranking
N-Methyl-2- pyrrolidone NMP 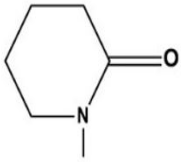	H315 - Causes skin irritation H319 - Causes serious eye irritation H335 - May cause respiratory irritation H360D - May damage the unborn child	Red
N,N Dimethylformamide DMF 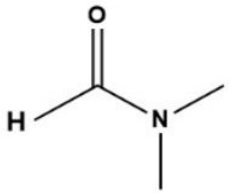	H226 - Flammable liquid and vapour H312 + H332 - Harmful when in contact with skin and toxic if inhaled H319 - Causes serious eye irritation	Red
Hexane 	H225 - Flammable liquids H315 - Skin irritation H361f - Reproductive toxicity H336 - Specific target organ toxicity - single exposure central nervous system H373 - Specific target organ toxicity - repeated exposure nervous system H304 - Aspiration hazard H411 - aquatic hazard	Red
Heptane 	H225 - Flammable liquids H315 - Skin irritation H336 - Specific target organ toxicity - single exposure Central nervous system H304 - Aspiration hazard H400 - Short-term (acute) aquatic hazard H410 - Long-term (chronic) aquatic hazard	Red

As previously discussed in section 2.2 there are five main parts that affect membrane fabrication - monomer for IP, solvent for IP, solvents for membrane fabrication, polymer for membrane fabrication and fabrication methods. To produce membranes that have a better environmental footprint and fewer health and safety risks associated with the fabrication all five parts should be investigated to explore the feasibility of producing membranes with safer and sustainable materials.

2.4.1 Greener membrane fabrication procedures

Green Chemistry is defined as the 'design of chemical products and processes to reduce or eliminate the use and generation of hazardous substances. [80]. It aims to utilise efficiently raw materials that are preferably renewable and to eliminate waste. It also aims to avoid the use of toxic and/or hazardous reagents and solvents in the manufacture and application of chemical products [80]. There are five principles that can be adopted to improve the sustainability of membrane fabrication, and they are:

1. 'Less hazardous chemical synthesis: wherever practicable, synthetic methods should be designed to use and generate substances that possess little or no toxicity to human health and the environment';

2. 'Safer solvents and auxiliaries: The use of auxiliary substances (e.g. solvents, separation agents, etc.) should be made unnecessary wherever possible and innocuous when used';

3. 'Design for energy efficiency: The energy requirements of chemical processes should be recognised for their environmental and economic impacts and should be minimised. If possible, synthetic methods should be conducted at ambient temperature and pressure';

4. 'Use of renewable feedstocks: A raw material or feedstock should be renewable rather

than depleting wherever technically and economically practicable';

5. 'Inherently safer chemistry for accident prevention: Substances and the form of a substance used in a chemical process should be chosen to minimise the potential for chemical accidents, including releases, explosions, and fires' [80].

In addition to the principals mentioned, a framework developed by Szekly *et al.* highlighted the different methods that can be adopted to embed sustainability in membrane fabrication [27]. This can include:

1. The use of bio-based green solvents - this is in line with principles of green chemistry (a) substituting conventional solvents with greener solvents as solvents account for the bulk of liquid waste during fabrication and; (b) using low toxicity chemicals, this will improve health and safety of fabrication as the risk for explosions and fires is reduced. The substitution of the chemicals to greener alternatives will reduce the environmental impact of solvents;

2. Reducing the number of steps involved in membrane fabrication which will reduce the amount of toxic waste generated and reduce the cost and energy consumption associated with membrane fabrication;

3. The use of renewable materials for membrane fabrication which will improve sustainability;

4. The energy consumption associated with membrane fabrication comes from the dissolution of the polymer in the solvent to form a dope solution. Producing dope solutions at room temperature will allow for a reduction in the energy consumption, costs and also carbon footprint of membranes. In addition to this, membranes for OSN require cross-linking to enhance chemical stability, and establishing protocols that are able to proceed at room temperature will also have similar benefits;

5. The use of materials that are degradable, which will allow membranes to degrade naturally and reduce landfill waste.

2.4.2 Solvents for fabrication

Solvent selection guides are tools employed by the pharmaceutical industry to facilitate the use of the most sustainable solvent in processes [81], [82]. The purpose of the guide is to reduce the consumption of hazardous solvents and offer alternatives where possible [81]. Solvent guides are currently employed by several pharmaceutical companies including GlaxoSmithKlein, Astrazenca and Sanofi [83]–[85]. Solvents are objectively categorised and ranked based on different criteria such as environment health and safety (EHS), process safety, physical properties, toxicology, health hazard and waste management [83], [86]–[88]. Each area is given an assessment score and these are compiled, and a final ranking is determined for the solvent. The layout of the guides are similar, employing a traffic light system: green 'preferred' yellow 'usable' and red 'undesirable.' [81], [83].

The CHEM21 - (Chemical Manufacturing Methods for the 21st Century Pharmaceutical Industries) is a consortium consisting of multiple stakeholders of pharmaceutical companies and academics aiming to improve the sustainability of the European pharmaceutical industry [79]. CHEM21 classifies 51 solvents both classical and neoteric into four systematic categories: recommended, problematic, hazardous and highly hazardous. The criteria for the ranking is chosen from EHS principals and similarly to solvent selection guides, a traffic light system is employed, red for 'highly hazardous and hazardous', yellow for 'problematic' and green for 'recommended.' Table 2.5 have listed the CHEM 21 rankings of the solvents used for phase inversion and interfacial polymerisation, and they are all ranked as hazardous [79].

The use of solvent selection guides offers benign alternatives to hazardous and toxic solvents and present safer alternatives such as alcohols, ionic liquids and bio-renewable

green solvents. By definition, bio-renewable solvents refer to solvents derived from a renewable feed stock such as biomass and the use of alternative bio-renewable solvents in membrane fabrication posses many advantages compared to petroleum derived solvents as they are (1) less hazardous; (2) are derived from renewable materials; and (3) less toxic to the environment [89].

Ionic liquids are organic salts that exist as liquids at low temperatures (<100 °C) and have low vapour pressure, and thus are deemed as green solvents [90]. Ying *et al.*, reported the use of the ionic liquid 1-butyl-3-methylimidazolium thiocyanate ([BMIM]SCN) as an alternative solvent used in phase inversion [91]. Compared to membranes produced using NMP, the ionic liquid-based membrane had lower water permeance at 983 L m^{-2} h^{-1} bar^{-1} and 114 L m^{-2} h^{-1} bar^{-1} respectively. The use of ionic liquids resulted in denser membranes, as the polymer dope solution had a higher viscosity than the NMP solution, which accounted for the difference in water permeability [91]. The study also investigated the recycling of the coagulation bath; the water was evaporated, the solvent was reused to produce a dope solution and membranes were cast using the recycled solvent dope solution. Interestingly, the membrane produced using the recycled solution had a higher porosity and pure water permeability than the original dope solution membranes at 7.0 % and 6.2 % respectively and 119 L m^{-2} h^{-1} bar^{-1} and 114 L m^{-2} h^{-1} bar^{-1} respectively. This study presents many interesting concepts, the use of the ionic liquid as an alternative to NMP was presented and the recycling of the waste derived from fabrication, leading to a circular economy of membrane fabrication.

The use of ionic liquids has also been extended to interfacial polymerisation. Marien *et al.* used the immiscible ionic liquid for the organic phase [1-butyl-3-methylimidazolium(C4mim)], [90]. TFC Membranes were produced using the new polyamide layer and were compared with the conventional polyamide using n-hexane. The water permeance for the TFC membrane produced using the ionic liquid for IP was three times higher than n-hexane at 1.09 L m^{-2} h^{-1} bar^{-1} and 0.31 L m^{-2} h^{-1} bar^{-1}, respectively. The membrane was also tested in reverse osmosis applications and experienced comparable sodium chloride

rejections at 96.8 % and 96.7 % respectively [90].

Further to this work, Haranto *et al.* also used an ionic liquid for the organic phase for interfacial polymerisation [92]. 1-butyl-3-methylimidazolium bis(trifluoromethylsulfonyl)imide (C4MIM Tf2N) was used, and the membranes had comparable water flux at 8.88 L m^{-2} h^{-1} for the synthesised PA in ionic liquid and 8.85 L m^{-2} h^{-1} at 14 bar for the n-hexane synthesised PA. The use of ionic liquid shows that the use of sustainable alternatives can produce comparable results with improved health and safety and environmental benefits.

Dimethyl sulfoxide is a petroleum-derived polar solvent that has no associated hazards and can also be used as an alternative solvent for membrane fabrication compared to NMP and DMF [37]. An example of the use of this solvent for membrane fabrication was reported by Soroko *et al.* where they substituted the conventional DMF/1,4-dioxane solvent mixture used to produce polyimide OSN membranes with an environmentally friendly DMSO/acetone solvent mixture [93]. In this work, the membranes prepared from DMSO/acetone had similar performance in terms of rejection compared to membranes prepared from DMF/1,4-dioxane as the MWCO of the membranes were 380 g/mol and 350 g/mol respectively. In addition to the similarity in MWCO, the flux of the membranes was also similar at 129 L m^{-2} h^{-1} and 137 L m^{-2} h^{-1} respectively at 30 bar. The study demonstrates that alternative solvent systems can be employed in membrane fabrication, replacing conventional systems without compromising the separation characteristics.

Membranes have also been fabricated using the bio-renewable solvents methyl lactate and 2-Methyltetrahydrofuran.[94]. Rasool *et al.* reported the use of a solvent mixture containing methyl lactate and 2-MeTHF and the polymer cellulose acetate to produce asymmetric membranes that were suitable for nanofiltration [94]. Another study conducted by Rasool *et al.* employed G-valerolactone (GVL) and a set of glycerol derivatives as a replacement for petroleum-derived solvents [94]. The study produced different polymer solutions using a wide range of solvents and commonly used polymers employed for membrane fabrication, PI, CA, PVDF, PES. In total, eleven different bio-renewable

solvents were explored, and it was found that cellulose acetate dissolved well in the green solvents and produced asymmetric membranes that were suitable for nanofiltration. Further to this, other green solvents used for membrane fabrication have included TamiSolv NxGl [95], Polarclean [96], dimethyl isosorbide [97] and Cyrene™ [98].

The use of green solvent replacements for interfacial polymerisation has also been explored and oleic acid, which is found in olives, canola and tallow was investigated by Falca *et al.* [99]. TFC membranes were prepared using oleic acid and a PAN support. The membranes exhibited an MWCO of 650 g/mol and high methanol permeance of 57 L m^{-2} h^{-1} bar^{-1}. In addition to this, decanoic acid, a medium-chain fatty acid found in coconut oil and palm kernel oil and other animal fats, has been reported as an alternative solvent for IP by Ong *et al.* [100]. TFC membranes were fabricated using a PAN support and were tested for OSN applications. The molecular weight cut-off for these membranes was around 650 g/mol. The permeance of the TFC membrane was tested against commercially available Solsep 030705 and Duramem 150 membranes and the green PA surpassed in methanol permeance at 60 L m^{-2} h^{-1} bar^{-1}, 1.4 L m^{-2} h^{-1} bar^{-1} and 0.48 L m^{-2} h^{-1} bar^{-1} respectively. The work opens up an avenue of exploration into the use of alternative solvents that can be used instead of toxic conventional solvents, as the bio-renewable solvents that were selected in the above studies do not impose any health and safety risks during membrane preparation.

2.4.3 Polymers for fabrication

In order to mitigate the environmental burden posed by membrane fabrication, a feasible strategy is to prepare biodegradable membranes from renewable materials that do not persist in the environment. One example of this is using the naturally occurring polymer Poly(lactic acid) (PLA) which is a polyester derived from renewable biomass. Le Phuong *et al.* reported the use of this polymer in combination with bamboo fibres to create a membrane derived solely from natural materials [101]. The membranes produced

in this work were tested for stability in organic solvents and although the membrane did not exhibit stability in the harsh polar aprotic solvent DMF, the membranes were able to remain intact in hexane, Cyrene™, 2-MeTHF, NMP, ethyl acetate and toluene for six months. It was found that bamboo fibre was insoluble in solvents and the dissolution in DMF was due to the PLA dissolving rather than the bamboo fibre. This work presents an interesting and innovative alternative to conventional petroleum derived polymers for applications in OSN.

Further to the use of natural materials, the recycling of polymers can also be adopted. Pulido *et al.* utilised waste water bottles to fabricate membranes from recycled poly(ethylene terephthalate) (PET) [102]. This polymer is resistant to harsh polar aprotic solvents such as DMF and therefore does not require an additional cross-linking step. The membranes were produced using NIPS utilising ethanol and methanol as the coagulant. The membrane exhibited high solvent permeances ranging from 50 to 300 L m^{-2} h^{-1} bar^{-1}, in solvents such as hexane and DMF. The membranes were also tested using DMF at 100 °C and the membrane exhibited excellent integrity in the hot polar solvent.

A study was conducted comparing PEEK, a synthetic polymer that remains stable in polar aprotic solvents, to the conventionally used polymer polyimide for OSN [65]. The fabrication procedure, amount of waste generated during fabrication and the environmental burden of fabrication using the two polymers was compared. Green metrics such as the E-factor, which is a measure of waste produced with respect to the product, and solvent intensity, which is a measure of the solvents used during fabrication with respect to the product were investigated. Further to this, the waste cost was also explored to assess the environmental impact of the fabrication of the two polymer membranes. It was found that the solvent intensity of PEEK membranes was 8.3 compared to 224 for the PI-based membranes. The total waste produced during the fabrication of the PEEK membranes was 0.21 kg m^{-2} whereas the traditional polyimide fabrication method generated 6.58 kg m^{-2} of waste. The difference in the two values can be attributed to the need for chemical-crosslinking of PI, as a greater number of solvents and reagents are required, generating

greater waste. The study highlighted that the use of PEEK a synthetic polymer possesses many environmental and economic advantages compared to conventional polyimide. The use of PEEK as a polymer alternative for OSN has also been reported by Kim *et al.* [68] and da Silva Burgal *et al.* [66].

2.4.4 Alternative fabrication methods

Another method for imbuing sustainability in membrane fabrication is modifying the fabrication process for OSN by incorporating the cross-linking solution as the coagulant during phase inversion. Vanhereck *et al.* reported the use of an aqueous-based amine cross-linker rather than the conventional isopropanol-based amine solution to produce PI membranes suitable for use in OSN [103]. The combination of using the cross-linker as the coagulant eliminated the need for an additional post-synthesis cross-linking step and also the amount of liquid waste generated during the fabrication process [103].

Park *et al.* reported the use of recycled plastic PET support which was the foundation of a hydrophobic TFC membrane. The study used the green solvent p-cymene for phase inversion and interfacial polymerisation and the TFC membrane was tested for OSN applications.[104]. Green monomers for interfacial polymerisation, tannic acid in the aqueous phase and priamine in the organic phase were also used to produce the first reported TFC membrane produced solely through green materials for OSN applications. The membranes experienced acetone permeance of 9.1 L m^{-2} h^{-1} bar^{-1}, and a molecular weight cut-off of 395 g/mol.

Herman *et al.* reported an interesting method to reduce the number of steps involved in membrane fabrication and to reduce the amount of waste produced [105]. This was done through the combination of phase inversion, crosslinking and impregnation of a polyimide support by adding amines to the aqueous coagulation bath [105]. A combination of hexamethylenediamine and MPD in the coagulation bath produced PI membranes that

had already been cross-linked and impregnated with MPD through a one-step process, and the only step required was the addition of a TMC/n-hexane solution to produce TFC membranes. The TFC membranes fabricated using this method experienced ethanol permeance of 0.17 L m^{-2} h^{-1} bar^{-1} and a Rose Bengal rejection of 97.5 %. The solvent intensity of the two methods, the traditional method and the new method used in this work, were compared. The solvent intensities were calculated to be 519 and 269 respectively, indicating that a reduction in the amount of solvent used resulted in less waste and a better environmental impact of membrane fabrication [105].

Paseta *et al.* investigated using TMC vapours for interfacial polymerisation with an aqueous MPD solution [106]. The exclusion of the organic solvent during fabrication presented an interesting, greener fabrication alternative. The use of reagents using this method was compared with the traditional method of fabrication using a TMC-hexane solution, and the use of the TMC vapours for IP reduced the TMC consumption by 92 %. The fabrication of polyamide through the TMC vapours was formed on a polyimide support and tested for OSN applications. A Rose Bengal rejection of 98 % was experienced, and water permeation reached 2.4 L m^{-2} h^{-1} bar^{-1}, compared to 1.2 L m^{-2} h^{-1} bar^{-1}, when using the traditional TMC-hexane polyamide fabrication method [106].

Many other different monomers have been used for interfacial polymerisation and these include dopamine typically sourced from mussels [51], [107]–[110], tannic acid typically sourced from seeds and galls [51], [111]–[113] vanillic alcohol commonly produced from lignin waste [51], [114], [115], quercetin [116], morin hydrate [117] and cyclodexterin [69]. A bio-inspired coating is produced, which has applications in both water purification and organic solvent nanofiltration. The use of plant-based monomers was investigated by Fei *et al.* to produce bio-inspired membrane coatings [51]. This work looked at eugenol which is extracted from cloves, morin which comes from guava leaves, and quercetin which is a common plant flavanol to produce membranes that were suitable for OSN [51]. The coatings experienced a molecular weight cut-off between 390–1550 g/mol and 0.5–40 L m^{-2} h^{-1} bar^{-1}, permeance in acetone.

Separation processes are essential in numerous industries and as the focus on climate change and water resources increases globally the use of membrane separation will increase. Membranes produced using naturally derived or recycled materials will ensure that membrane separation is a green alternative. The use of alternative solvents, monomers and fabrication methods has the potential to change the membrane research field. Next-generation membranes can be fabricated with eco-friendly, sustainable, less hazardous materials to produce membranes that have higher through-puts and require less energy. The work in this thesis will look at bio-renewable green solvents and sustainable fabrication methods to produce membranes for nanofiltration in aqueous and organic applications.

References

[1] R. W. Baker, *Membrane technology and applications*. John Wiley and Sons, 2012.

[2] R. J. Petersen, "Composite reverse osmosis and nanofiltration membranes," *Journal of membrane science*, vol. 83, no. 1, pp. 81–150, 1993.

[3] S. Loeb and S. Sourirajan, "Sea water demineralization by means of an osmotic membrane," in ACS Publications, 1962.

[4] M. Mulder, *Basic principles of membrane technology*. Springer Science and Business Media, 2012.

[5] A. Boam and A. Nozari, "Fine chemical: Osn–a lower energy alternative," *Filtration and separation*, vol. 43, no. 3, pp. 46–48, 2006.

[6] K. Scott, *Handbook of industrial membranes*. Elsevier, 1995.

[7] P. Vandezande, L. E. Gevers, and I. F. Vankelecom, "Solvent resistant nanofiltration: Separating on a molecular level," *Chemical Society Reviews*, vol. 37, no. 2, pp. 365–405, 2008.

[8] A. W. Mohammad, Y. Teow, W. Ang, Y. Chung, D. Oatley-Radcliffe, and N. Hilal, "Nanofiltration membranes review: Recent advances and future prospects," *Desalination*, vol. 356, pp. 226–254, 2015.

[9] W. Lau, A. Ismail, N. Misdan, and M. Kassim, "A recent progress in thin film composite membrane: A review," *Desalination*, vol. 287, pp. 190–199, 2012.

[10] J. Aburabie, P. Neelakanda, M. Karunakaran, and K.-V. Peinemann, "Thin-film composite crosslinked polythiosemicarbazide membranes for organic solvent nanofiltration (osn)," *Reactive and Functional Polymers*, vol. 86, pp. 225–232, 2015.

[11] P. Marchetti, M. F. Jimenez Solomon, G. Szekely, and A. G. Livingston, "Molecular separation with organic solvent nanofiltration: A critical review," *Chemical reviews*, vol. 114, no. 21, pp. 10 735–10 806, 2014.

[12] F.-f. Chang, W.-j. Liu, and X.-m. Wang, "Comparison of polyamide nanofiltration and low-pressure reverse osmosis membranes on as (iii) rejection under various operational conditions," *Desalination*, vol. 334, no. 1, pp. 10–16, 2014.

[13] W. Fang, L. Shi, and R. Wang, "Interfacially polymerized composite nanofiltration hollow fiber membranes for low-pressure water softening," *Journal of membrane science*, vol. 430, pp. 129–139, 2013.

[14] Y.-L. Lin, J.-H. Chiou, and C.-H. Lee, "Effect of silica fouling on the removal of pharmaceuticals and personal care products by nanofiltration and reverse osmosis membranes," *Journal of hazardous materials*, vol. 277, pp. 102–109, 2014.

[15] A. Akbari, S. Desclaux, J. Rouch, P. Aptel, and J. Remigy, "New uv-photografted nanofiltration membranes for the treatment of colored textile dye effluents," *Journal of membrane science*, vol. 286, no. 1-2, pp. 342–350, 2006.

[16] N. Zaghbani, A. Hafiane, and M. Dhahbi, "Removal of safranin t from wastewater using micellar enhanced ultrafiltration," *Desalination*, vol. 222, no. 1-3, pp. 348–356, 2008.

[17] I. Koyuncu, D. Topacik, and M. R. Wiesner, "Factors influencing flux decline during nanofiltration of solutions containing dyes and salts," *Water research*, vol. 38, no. 2, pp. 432–440, 2004.

[18] A. Aouni, C. Fersi, B. Cuartas-Uribe, A. Bes-Pia, M. I. Alcaina-Miranda, and M. Dhahbi, "Reactive dyes rejection and textile effluent treatment study using ultrafiltration and nanofiltration processes," *Desalination*, vol. 297, pp. 87–96, 2012.

[19] A. Akbari, S. Desclaux, J.-C. Rouch, and J.-C. Remigy, "Application of nanofiltration hollow fibre membranes, developed by photografting, to treatment of anionic dye solutions," *Journal of membrane science*, vol. 297, no. 1-2, pp. 243–252, 2007.

[20] M. Rabiller-Baudry, G. Nasser, T. Renouard, D. Delaunay, and M. Camus, "Comparison of two nanofiltration membrane reactors for a model reaction of olefin metathesis achieved in toluene," *Separation and Purification Technology*, vol. 116, pp. 46–60, 2013.

[21] D. Ormerod, B. Sledsens, G. Vercammen, *et al.*, "Demonstration of purification of a pharmaceutical intermediate via organic solvent nanofiltration in the presence of acid," *Separation and Purification Technology*, vol. 115, pp. 158–162, 2013.

[22] A. P. B. Ribeiro, J. M. de Moura, L. A. Goncalves, J. C. C. Petrus, and L. A. Viotto, "Solvent recovery from soybean oil/hexane miscella by polymeric membranes," *Journal of Membrane Science*, vol. 282, no. 1-2, pp. 328–336, 2006.

[23] E. Rundquist, C. Pink, E. Vilminot, and A. Livingston, "Facilitating the use of counter-current chromatography in pharmaceutical purification through use of organic solvent nanofiltration," *Journal of Chromatography A*, vol. 1229, pp. 156–163, 2012.

[24] G. Szekely, J. Bandarra, W. Heggie, B. Sellergren, and F. C. Ferreira, "A hybrid approach to reach stringent low genotoxic impurity contents in active pharmaceutical ingredients: Combining molecularly imprinted polymers and organic solvent nanofiltration for removal of 1, 3-diisopropylurea," *Separation and purification technology*, vol. 86, pp. 79–87, 2012.

[25] C. J. Pink, H.-t. Wong, F. C. Ferreira, and A. G. Livingston, "Organic solvent nanofiltration and adsorbents; a hybrid approach to achieve ultra low palladium contamination of post coupling reaction products," *Organic Process Research and Development*, vol. 12, no. 4, pp. 589–595, 2008.

[26] E. M. Rundquist, C. J. Pink, and A. G. Livingston, "Organic solvent nanofiltration: A potential alternative to distillation for solvent recovery from crystallisation mother liquors," *Green Chemistry*, vol. 14, no. 8, pp. 2197–2205, 2012.

[27] G. Szekely, M. F. Jimenez-Solomon, P. Marchetti, J. F. Kim, and A. G. Livingston, "Sustainability assessment of organic solvent nanofiltration: From fabrication to application," *Green Chemistry*, vol. 16, no. 10, pp. 4440–4473, 2014.

[28] J. E. Cadotte and R. J. Petersen, "Thin-film composite reverse-osmosis membranes: Origin, development, and recent advances," in ACS Publications, 1981.

[29] C. Y. Tang, Y.-N. Kwon, and J. O. Leckie, "Effect of membrane chemistry and coating layer on physiochemical properties of thin film composite polyamide ro and nf membranes: I. ftir and xps characterization of polyamide and coating layer chemistry," *Desalination*, vol. 242, no. 1-3, pp. 149–167, 2009.

[30] B. Khorshidi, T. Thundat, B. Fleck, and M. Sadrzadeh, "Thin film composite polyamide membranes: Parametric study on the influence of synthesis conditions," *RSC Advances*, vol. 5, no. 68, pp. 54 985–54 997, 2015.

[31] M. Razali, C. Didaskalou, J. F. Kim, *et al.*, "Exploring and exploiting the effect of solvent treatment in membrane separations," *ACS Applied Materials and Interfaces*, vol. 9, no. 12, pp. 11 279–11 289, 2017.

[32] A. Sagle and B. Freeman, "Fundamentals of membranes for water treatment," *The future of desalination in Texas*, vol. 2, no. 363, p. 137, 2004.

[33] M. Adamczak, G. Kaminska, and J. Bohdziewicz, "Preparation of polymer membranes by in situ interfacial polymerization," *International Journal of Polymer Science*, vol. 2019, 2019.

[34] M. K. Purkait, M. K. Sinha, P. Mondal, and R. Singh, "Introduction to membranes," in *Interface Science and Technology*, vol. 25, Elsevier, 2018, pp. 1–37.

[35] T.-D. Lu, B.-Z. Chen, J. Wang, *et al.*, "Electrospun nanofiber substrates that enhance polar solvent separation from organic compounds in thin-film composites," *Journal of Materials Chemistry A*, vol. 6, no. 31, pp. 15 047–15 056, 2018.

[36] X. Loh, M. Sairam, A. Bismarck, J. Steinke, A. Livingston, and K. Li, "Crosslinked integrally skinned asymmetric polyaniline membranes for use in organic solvents," *Journal of Membrane Science*, vol. 326, no. 2, pp. 635–642, 2009.

[37] M. F. J. Solomon, Y. Bhole, and A. G. Livingston, "High flux membranes for organic solvent nanofiltration (osn)—interfacial polymerization with solvent activation," *Journal of membrane science*, vol. 423, pp. 371–382, 2012.

[38] M. Mertens, C. Van Goethem, M. Thijs, G. Koeckelberghs, and I. F. Vankelecom, "Crosslinked pvdf-membranes for solvent resistant nanofiltration," *Journal of Membrane Science*, vol. 566, pp. 223–230, 2018.

[39] I. B. Valtcheva, S. C. Kumbharkar, J. F. Kim, Y. Bhole, and A. G. Livingston, "Beyond polyimide: Crosslinked polybenzimidazole membranes for organic solvent nanofiltration (osn) in harsh environments," *Journal of Membrane Science*, vol. 457, pp. 62–72, 2014.

[40] J. Jegal, S. G. Min, and K.-H. Lee, "Factors affecting the interfacial polymerization of polyamide active layers for the formation of polyamide composite membranes," *Journal of Applied Polymer Science*, vol. 86, no. 11, pp. 2781–2787, 2002.

[41] E. Maaskant, W. Vogel, T. J. Dingemans, and N. E. Benes, "The use of a star-shaped trifunctional acyl chloride for the preparation of polyamide thin film composite membranes," *Journal of membrane science*, vol. 567, pp. 321–328, 2018.

[42] N. Saha and S. Joshi, "Performance evaluation of thin film composite polyamide nanofiltration membrane with variation in monomer type," *Journal of Membrane Science*, vol. 342, no. 1-2, pp. 60–69, 2009.

[43] I. Roh, S. Park, J. Kim, and C. Kim, "Effects of the polyamide molecular structure on the performance of reverse osmosis membranes," *Journal of Polymer Science Part B: Polymer Physics*, vol. 36, no. 11, pp. 1821–1830, 1998.

[44] J. Cadotte, R. King, R. Majerle, and R. Petersen, "Interfacial synthesis in the preparation of reverse osmosis membranes," *Journal of Macromolecular Science—Chemistry*, vol. 15, no. 5, pp. 727–755, 1981.

[45] A. Al-Hobaib, M. Alsuhybani, K. M. Al-Sheetan, and M. R. Shaik, "Reverse osmosis membranes prepared by interfacial polymerization in n-heptane containing different co-solvents," *Desalination and Water Treatment*, vol. 57, no. 36, pp. 16 733–16 744, 2016.

[46] G.-Y. Chai and W. B. Krantz, "Formation and characterization of polyamide membranes via interfacial polymerization," *Journal of Membrane Science*, vol. 93, no. 2, pp. 175–192, 1994.

[47] L. Hu, S. Zhang, R. Han, and X. Jian, "Preparation and performance of novel thermally stable polyamide/ppenk composite nanofiltration membranes," *Applied Surface Science*, vol. 258, no. 22, pp. 9047–9053, 2012.

[48] B. Khorshidi, T. Thundat, B. A. Fleck, and M. Sadrzadeh, "A novel approach toward fabrication of high performance thin film composite polyamide membranes," *Scientific reports*, vol. 6, p. 22 069, 2016.

[49] A. Akbari and S. M. Mojallali Rostami, "Development of permeability properties of polyamide thin film composite nanofiltration membrane by using the dimethyl sulfoxide additive," *Journal of Water Reuse and Desalination*, vol. 4, no. 3, pp. 174–181, 2014.

[50] N. P. Cheremisinoff, *Condensed encyclopedia of polymer engineering terms*. Butterworth-Heinemann, 2001.

[51] F. Fei, H. A. Le Phuong, C. F. Blanford, and G. Szekely, "Tailoring the performance of organic solvent nanofiltration membranes with biophenol coatings," *ACS applied polymer materials*, vol. 1, no. 3, pp. 452–460, 2019.

[52] D. Fritsch, P. Merten, K. Heinrich, M. Lazar, and M. Priske, "High performance organic solvent nanofiltration membranes: Development and thorough testing of thin film composite membranes made of polymers of intrinsic microporosity (pims)," *Journal of Membrane Science*, vol. 401, pp. 222–231, 2012.

[53] A. V. Volkov, V. V. Parashchuk, D. F. Stamatialis, V. S. Khotimsky, V. V. Volkov, and M. Wessling, "High permeable ptmsp/pan composite membranes for solvent nanofiltration," *Journal of membrane science*, vol. 333, no. 1-2, pp. 88–93, 2009.

[54] H. M. Tham, K. Y. Wang, D. Hua, S. Japip, and T.-S. Chung, "From ultrafiltration to nanofiltration: Hydrazine cross-linked polyacrylonitrile hollow fiber membranes for organic solvent nanofiltration," *Journal of membrane science*, vol. 542, pp. 289–299, 2017.

[55] M. F. J. Solomon, Y. Bhole, and A. G. Livingston, "High flux hydrophobic membranes for organic solvent nanofiltration (osn)—interfacial polymerization, surface modification and solvent activation," *Journal of membrane science*, vol. 434, pp. 193–203, 2013.

[56] Y. C. Xu, Y. P. Tang, L. F. Liu, Z. H. Guo, and L. Shao, "Nanocomposite organic solvent nanofiltration membranes by a highly-efficient mussel-inspired co-deposition strategy," *Journal of Membrane Science*, vol. 526, pp. 32–42, 2017.

[57] I. Soroko and A. Livingston, "Impact of tio2 nanoparticles on morphology and performance of crosslinked polyimide organic solvent nanofiltration (osn) membranes," *Journal of Membrane Science*, vol. 343, no. 1-2, pp. 189–198, 2009.

[58] S. Monjezi, M. Soltanieh, A. C. Sanford, and J. Park, "Polyaniline membranes for nanofiltration of solvent from dewaxed lube oil," *Separation Science and Technology*, vol. 54, no. 5, pp. 795–802, 2019.

[59] M. Sairam, X. Loh, Y. Bhole, *et al.*, "Spiral-wound polyaniline membrane modules for organic solvent nanofiltration (osn)," *Journal of Membrane Science*, vol. 349, no. 1-2, pp. 123–129, 2010.

[60] J. Shen, S. Shahid, A. Sarihan, D. A. Patterson, and E. A. Emanuelsson, "Effect of polyacid dopants on the performance of polyaniline membranes in organic solvent nanofiltration," *Separation and Purification Technology*, vol. 204, pp. 336–344, 2018.

[61] M. Sairam, X. X. Loh, K. Li, A. Bismarck, J. H. G. Steinke, and A. G. Livingston, "Nanoporous asymmetric polyaniline films for filtration of organic solvents," *Journal of Membrane Science*, vol. 330, no. 1-2, pp. 166–174, 2009.

[62] R. A. Milescu, C. R. McElroy, T. J. Farmer, P. M. Williams, M. J. Walters, and J. H. Clark, "Fabrication of pes/pvp water filtration membranes using cyrene, a safer bio-based polar aprotic solvent," *Advances in Polymer Technology*, vol. 2019, 2019.

[63] X. Li, B. Chen, W. Cai, T. Wang, Z. Wu, and J. Li, "Highly stable pdms–ptfpms/pvdf osn membranes for hexane recovery during vegetable oil production," *RSC advances*, vol. 7, no. 19, pp. 11 381–11 388, 2017.

[64] P. Silva, S. Han, and A. G. Livingston, "Solvent transport in organic solvent nanofiltration membranes," *Journal of Membrane Science*, vol. 262, no. 1-2, pp. 49–59, 2005.

[65] J. da Silva Burgal, L. Peeva, and A. Livingston, "Towards improved membrane production: Using low-toxicity solvents for the preparation of peek nanofiltration membranes," *Green Chemistry*, vol. 18, no. 8, pp. 2374–2384, 2016.

[66] J. da Silva Burgal, L. G. Peeva, S. Kumbharkar, and A. Livingston, "Organic solvent resistant poly (ether-ether-ketone) nanofiltration membranes," *Journal of membrane science*, vol. 479, pp. 105–116, 2015.

[67] S. Karan, Z. Jiang, and A. G. Livingston, "Sub–10 nm polyamide nanofilms with ultrafast solvent transport for molecular separation," *Science*, vol. 348, no. 6241, pp. 1347–1351, 2015.

[68] J. H. Kim, S. J. Moon, S. H. Park, M. Cook, A. G. Livingston, and Y. M. Lee, "A robust thin film composite membrane incorporating thermally rearranged polymer support for organic solvent nanofiltration and pressure retarded osmosis," *Journal of Membrane Science*, vol. 550, pp. 322–331, 2018.

[69] S.-J. Xu, Q. Shen, Z.-L. Xu, and Z.-Q. Dong, "Novel designed tfc membrane based on host-guest interaction for organic solvent nanofiltration (osn)," *Journal of Membrane Science*, vol. 588, p. 117 227, 2019.

[70] A. Kulkarni, D. Mukherjee, and W. N. Gill, "Flux enhancement by hydrophilization of thin film composite reverse osmosis membranes," *Journal of Membrane Science*, vol. 114, no. 1, pp. 39–50, 1996.

[71] S. M. Aharoni, "The solubility parameters of aromatic polyamides," *Journal of applied polymer science*, vol. 45, no. 5, pp. 813–817, 1992.

[72] M. F. Jimenez-Solomon, Q. Song, K. E. Jelfs, M. Munoz-Ibanez, and A. G. Livingston, "Polymer nanofilms with enhanced microporosity by interfacial polymerization," *Nature materials*, vol. 15, no. 7, pp. 760–767, 2016.

[73] C. Li, S. Li, L. Tian, J. Zhang, B. Su, and M. Z. Hu, "Covalent organic frameworks (cofs)-incorporated thin film nanocomposite (tfn) membranes for high-flux organic solvent nanofiltration (osn)," *Journal of Membrane Science*, vol. 572, pp. 520–531, 2019.

[74] C. Li, S. Li, L. Lv, B. Su, and M. Z. Hu, "High solvent-resistant and integrally crosslinked polyimide-based composite membranes for organic solvent nanofiltration," *Journal of Membrane Science*, vol. 564, pp. 10–21, 2018.

[75] Y. Guo, S. Li, B. Su, and B. Mandal, "Fluorine incorporation for enhancing solvent resistance of organic solvent nanofiltration membrane," *Chemical Engineering Journal*, vol. 369, pp. 498–510, 2019.

[76] L. Xia, J. Ren, M. Weyd, and J. R. McCutcheon, "Ceramic-supported thin film composite membrane for organic solvent nanofiltration," *Journal of membrane science*, vol. 563, pp. 857–863, 2018.

[77] J. Zhang, Z. Qin, L. Yang, H. Guo, and S. Han, "Activation promoted ionic liquid modification of reverse osmosis membrane towards enhanced permeability for desalination," *Journal of the Taiwan Institute of Chemical Engineers*, vol. 80, pp. 25–33, 2017.

[78] M. Shi, W. Yan, C. Dong, L. Liu, S. Xie, and C. Gao, "Solvent activation before heat-treatment for improving reverse osmosis membrane performance," *Journal of Membrane Science*, vol. 595, p. 117 565, 2020.

[79] D. Prat, A. Wells, J. Hayler, *et al.*, "Chem21 selection guide of classical-and less classical-solvents," *Green Chemistry*, vol. 18, no. 1, pp. 288–296, 2015.

[80] P. Anastas and N. Eghbali, "Green chemistry: Principles and practice," *Chemical Society Reviews*, vol. 39, no. 1, pp. 301–312, 2010.

[81] F. P. Byrne, S. Jin, G. Paggiola, *et al.*, "Tools and techniques for solvent selection: Green solvent selection guides," *Sustainable Chemical Processes*, vol. 4, no. 1, p. 7, 2016.

[82] D. Prat, J. Hayler, and A. Wells, "A survey of solvent selection guides," *Green Chemistry*, vol. 16, no. 10, pp. 4546–4551, 2014.

[83] C. M. Alder, J. D. Hayler, R. K. Henderson, *et al.*, "Updating and further expanding gsk's solvent sustainability guide," *Green Chemistry*, vol. 18, no. 13, pp. 3879–3890, 2016.

[84] C. R. McElroy, A. Constantinou, L. C. Jones, L. Summerton, and J. H. Clark, "Towards a holistic approach to metrics for the 21st century pharmaceutical industry," *Green Chemistry*, vol. 17, no. 5, pp. 3111–3121, 2015.

[85] D. Prat, O. Pardigon, H.-W. Flemming, *et al.*, "Sanofi's solvent selection guide: A step toward more sustainable processes," *Organic Process Research and Development*, vol. 17, no. 12, pp. 1517–1525, 2013.

[86] K. Alfonsi, J. Colberg, P. J. Dunn, *et al.*, "Green chemistry tools to influence a medicinal chemistry and research chemistry based organisation," *Green Chemistry*, vol. 10, no. 1, pp. 31–36, 2008.

[87] C. Capello, U. Fischer, and K. Hungerbuhler, "What is a green solvent? a comprehensive framework for the environmental assessment of solvents," *Green Chemistry*, vol. 9, no. 9, pp. 927–934, 2007.

[88] L. J. Diorazio, D. R. Hose, and N. K. Adlington, "Toward a more holistic framework for solvent selection," *Organic Process Research and Development*, vol. 20, no. 4, pp. 760–773, 2016.

[89] M. Doble, K. Rollins, and A. Kumar, *Green chemistry and engineering*. Academic Press, 2010.

[90] H. Marien, L. Bellings, S. Hermans, and I. F. Vankelecom, "Sustainable process for the preparation of high-performance thin-film composite membranes using ionic liquids as the reaction medium," *ChemSusChem*, vol. 9, no. 10, pp. 1101–1111, 2016.

[91] D. Y. Xing, N. Peng, and T.-S. Chung, "Formation of cellulose acetate membranes via phase inversion using ionic liquid,[bmim] scn, as the solvent," *Industrial and Engineering Chemistry Research*, vol. 49, no. 18, pp. 8761–8769, 2010.

[92] Y. Hartanto, M. Corvilain, H. Marien, J. Janssen, and I. F. Vankelecom, "Interfacial polymerization of thin-film composite forward osmosis membranes using ionic liquids as organic reagent phase," *Journal of Membrane Science*, vol. 601, p. 117 869, 2020.

[93] I. Soroko, Y. Bhole, and A. G. Livingston, "Environmentally friendly route for the preparation of solvent resistant polyimide nanofiltration membranes," *Green Chemistry*, vol. 13, no. 1, pp. 162–168, 2011.

[94] M. A. Rasool, C. Van Goethem, and I. F. Vankelecom, "Green preparation process using methyl lactate for cellulose-acetate-based nanofiltration membranes," *Separation and Purification Technology*, vol. 232, p. 115 903, 2020.

[95] X. Jiang, W. F. Yong, J. Gao, D.-D. Shao, and S.-P. Sun, "Understanding the role of substrates on thin film composite membranes: A green solvent approach with tamisolve nxg," *Journal of Membrane Science*, p. 119 530, 2021.

[96] C. Ursino, F. Russo, R. Ferrari, *et al.*, "Polyethersulfone hollow fiber membranes prepared with polarclean as a more sustainable solvent," *Journal of Membrane Science*, vol. 608, p. 118 216, 2020.

[97] F. Russo, F. Galiano, F. Pedace, F. Aricò, and A. Figoli, "Dimethyl isosorbide as a green solvent for sustainable ultrafiltration and microfiltration membrane preparation," *ACS Sustainable Chemistry and Engineering*, vol. 8, no. 1, pp. 659–668, 2019.

[98] T. Marino, F. Galiano, A. Molino, and A. Figoli, "New frontiers in sustainable membrane preparation: Cyrene as green bioderived solvent," *Journal of membrane science*, vol. 580, pp. 224–234, 2019.

[99] G. Falca, V. E. Musteata, S. Chisca, M. N. Hedhili, C. Ong, and S. P. Nunes, "Naturally extracted hydrophobic solvent and self-assembly in interfacial polymerization," *ACS Applied Materials and Interfaces*, 2021.

[100] C. Ong, G. Falca, T. Huang, *et al.*, "Green synthesis of thin-film composite membranes for organic solvent nanofiltration," *ACS Sustainable Chemistry and Engineering*, vol. 8, no. 31, pp. 11 541–11 548, 2020.

[101] H. A. Le Phuong, N. A. Izzati Ayob, C. F. Blanford, N. F. Mohammad Rawi, and G. Szekely, "Nonwoven membrane supports from renewable resources: Bamboo fiber reinforced poly (lactic acid) composites," *ACS Sustainable Chemistry and Engineering*, vol. 7, no. 13, pp. 11 885–11 893, 2019.

[102] B. A. Pulido, O. S. Habboub, S. L. Aristizabal, G. Szekely, and S. P. Nunes, "Recycled poly (ethylene terephthalate) for high temperature solvent resistant membranes," *ACS Applied Polymer Materials*, vol. 1, no. 9, pp. 2379–2387, 2019.

[103] K. Vanherck, A. Cano-Odena, G. Koeckelberghs, T. Dedroog, and I. Vankelecom, "A simplified diamine crosslinking method for pi nanofiltration membranes," *Journal of membrane science*, vol. 353, no. 1-2, pp. 135–143, 2010.

[104] S.-H. Park, A. Alammar, Z. Fulop, B. A. Pulido, S. P. Nunes, and G. Szekely, "Hydrophobic thin film composite nanofiltration membranes derived solely from sustainable sources," *Green Chemistry*, 2021.

[105] S. Hermans, E. Dom, H. Marien, G. Koeckelberghs, and I. F. Vankelecom, "Efficient synthesis of interfacially polymerized membranes for solvent resistant nanofiltration," *Journal of Membrane Science*, vol. 476, pp. 356–363, 2015.

[106] L. Paseta, M. Navarro, J. Coronas, and C. Tellez, "Greener processes in the preparation of thin film nanocomposite membranes with diverse metal-organic frameworks for organic solvent nanofiltration," *Journal of Industrial and Engineering Chemistry*, vol. 77, pp. 344–354, 2019.

[107] G. Han, S. Zhang, X. Li, N. Widjojo, and T.-S. Chung, "Thin film composite forward osmosis membranes based on polydopamine modified polysulfone substrates with enhancements in both water flux and salt rejection," *Chemical Engineering Science*, vol. 80, pp. 219–231, 2012.

[108] Y.-L. Ji, M. B. M. Y. Ang, H.-C. Hung, *et al.*, "Bio-inspired deposition of polydopamine on pvdf followed by interfacial cross-linking with trimesoyl chloride as means of preparing composite membranes for isopropanol dehydration," *Journal of Membrane Science*, vol. 557, pp. 58–66, 2018.

[109] J. T. Arena, B. McCloskey, B. D. Freeman, and J. R. McCutcheon, "Surface modification of thin film composite membrane support layers with polydopamine: Enabling use of reverse osmosis membranes in pressure retarded osmosis," *Journal of Membrane Science*, vol. 375, no. 1-2, pp. 55–62, 2011.

[110] D. Zhao, J. F. Kim, G. Ignacz, P. Pogany, Y. M. Lee, and G. Szekely, "Bio-inspired robust membranes nanoengineered from interpenetrating polymer networks of polybenzimidazole/polydopamine," *ACS nano*, vol. 13, no. 1, pp. 125–133, 2019.

[111] Y. Zhang, Y. Su, J. Peng, *et al.*, "Composite nanofiltration membranes prepared by interfacial polymerization with natural material tannic acid and trimesoyl chloride," *Journal of Membrane Science*, vol. 429, pp. 235–242, 2013.

[112] Q. Li, Z. Liao, X. Fang, *et al.*, "Tannic acid assisted interfacial polymerization based loose thin-film composite nf membrane for dye/salt separation," *Desalination*, vol. 479, p. 114 343, 2020.

[113] T. Li, Y. Xiao, D. Guo, *et al.*, "In-situ coating tio2 surface by plant-inspired tannic acid for fabrication of thin film nanocomposite nanofiltration membranes toward enhanced separation and antibacterial performance," *Journal of colloid and interface science*, vol. 572, pp. 114–121, 2020.

[114] A. Zhou, C. Shi, X. He, *et al.*, "Polyarylester nanofiltration membrane prepared from monomers of vanillic alcohol and trimesoyl chloride," *Separation and Purification Technology*, vol. 193, pp. 58–68, 2018.

[115] A. Zhou, M. Almijbilee, J. Zheng, and L. Wang, "A thin film composite membrane prepared from monomers of vanillin and trimesoyl chloride for organic solvent nanofiltration," *Separation and Purification Technology*, p. 118 394, 2021.

[116] M. H. Abdellah, L. Perez-Manriquez, T. Puspasari, C. A. Scholes, S. E. Kentish, and K.-V. Peinemann, "Effective interfacially polymerized polyester solvent resistant nanofiltration membrane from bioderived materials," *Advanced Sustainable Systems*, vol. 2, no. 7, p. 1 800 043, 2018.

[117] L. Perez-Manriquez, P. Neelakanda, and K.-V. Peinemann, "Morin-based nanofiltration membranes for organic solvent separation processes," *Journal of Membrane Science*, vol. 554, pp. 1–5, 2018.

Chapter 3

Methods and Materials

The materials that were used in this work will be listed and the different protocols that were used for membrane fabrication will be described. Further to this, the different characterisation techniques that were used to characterise the membranes will also be presented.

3.1 Materials

The materials used for the work carried out in this thesis are listed in Table 3.1, 3.2, 3.3 as well as their sources.

Table 3.1: Materials used for Membrane Fabrication

Material	Source
Cellulose acetate (average Mn ∼ 30,000 g/mol, 39.8 wt% acetyl content)	Sigma Aldrich
Polyimide P84	HP Polymer GmbH
N-Methyl-2-pyrrolidone (NMP) (99.9 % purity)	Sigma Aldrich
Dimethylformamide (DMF) (95% purity)	Fisher Chemicals
Cyrene™ [(-)-dihydrolevoglucosenone (1S, 5R)-6, 8-dioxabicyclo[3.2.1]octan-4-one	Sigma Aldrich
Methanol (99.99% purity)	Fisher Chemicals
Acetone (99.99% purity)	Fisher Chemicals
Potassium hydroxide (KOH) pellets	Alfa Aesar
Acetic Acid	Sigma Aldrich
NF 270 membrane	FilmTEC

Table 3.2: Materials used for Interfacial Polymerisation

Material	Source
Piperazine (PIP, 99.0 %)	Sigma Aldrich
1,3,5-benzenetricarbonyl chloride (TMC, 98+ %)	Sigma Aldrich
2-Methyltetrahydrofuran (99.0 purity %)	Sigma Aldrich
n-hexane (99.0 purity %)	Fisher Chemicals

Table 3.3: Materials used for Solvent Filtration

Material	Source
Ethanol (99.99% purity)	Fisher Chemicals
Acetone (99.99% purity)	Fisher Chemicals
Toluene (99.99% purity)	Fisher Chemicals
n-hexane (99.0 purity %)	Fisher Chemicals
Chloroform (99.99% purity)	Fisher Chemicals
Dimethylformamide (DMF) (95% purity)	Fisher Chemicals
Dichloromethane (DCM) (99.99% purity)	Fisher Chemicals

Table 3.4: Materials used for Solvent Activation

Material	Source
Ethanol (99.99% purity)	Fisher Chemicals
Dimethylformamide (DMF) (95% purity)	Fisher Chemicals
Dimethyl sulfoxide (99.99% purity)	Sigma Aldrich
Cyrene™ [(-)-dihydrolevoglucosenone (1S, 5R)-6, 8-dioxabicyclo[3.2.1]octan-4-one	Sigma Aldrich

Table 3.5: Materials used for Nanofiltration Testing

	Molecular Weight (g mol^{-1})	Source
Sodium sulfate (Na_2SO_4, $\geq$ 99.0%),	142.0	Sigma Aldrich
Magnesium sulfate ($MgSO_4$, $\geq$ 99.0%),	120.3	Sigma Aldrich
Magnesium chloride ($MgCl_2$, $\geq$ 98.0%)	95.2	Sigma Aldrich
Sodium chloride (NaCl,$\geq$ 99.5%)	54.4	Sigma Aldrich
Rose Bengal (RB, 95%)	1017.6	Sigma Aldrich
Fast Green F (FGF, 99.5%)	808.0	Sigma Aldrich
Rhodamine B (Rh B, 95 %)	479.0	Alfa Aesar
Methyl Orange (MO, 85%)	327.3	Alfa Aesar
Methylene Blue (MB, 80%)	319.9	Alfa Aesar
Polyethylene glycol	200-20,000	Alfa Aesar

3.2 Experimental methodologies

3.2.1 Preparation of supports for membranes used in organic solvent nanofiltration in chapter 4

Polyimide: 12 wt.% polyimide was dissolved in NMP or Cyrene™ at 80 °C, and the solution was stirred until complete dissolution. The solution was left overnight to remove any air bubbles present. The dope solution was then cast onto a glass plate using a casting knife (Elcometer 3700) set at a thickness of 200 μm at room temperature. Immediately after casting, the support was immersed into the coagulation bath containing deionised

water for phase inversion to occur at room temperature.

Cellulose acetate: 17.5 wt.% cellulose acetate was dissolved in Cyrene™ or Cyrene™ and acetic acid (3:1) or DMF at 50 °C, and the solution was stirred until complete dissolution. The solution was left overnight to remove any air bubbles present. The dope solution was then cast onto a glass plate using a casting knife (Elcometer 3700) set at a thickness of 200 μm. Immediately after casting, the support was immersed into the coagulation bath containing the deacytalation solution (0.05 M KOH/water) where phase inversion occurred, and the membrane was left in the solution for 0, 30, 60, 90 and 120 minutes at room temperature. The supports were removed from the solution and rinsed with deionised water until a neutral pH was obtained. The supports were kept in DI water until characterisation.

3.2.2 Preparation of free-standing polyamide films in Chapter 5

PA(n-hexane): To fabricate a conventional polyamide film which will have the abbreviation "PA(n-hexane)", 0.1 wt.% TMC was first dissolved in n-hexane and the organic solution was introduced into aqueous solutions containing 2 wt.% PIP.

PA(2-MeTHF): To fabricate the bio-derived polyamide film which will have the abbreviation "PA(2-MeTHF)", 0.1 - 3 wt.% TMC was first dissolved in 2-MeTHF, and the organic solutions were introduced into aqueous solutions containing 2 wt.% PIP.

All characterisations were carried out on the PA(n-hexane) of 0.1 wt.% TMC and 2 wt.% PIP and PA(2-MeTHF) of 2 wt.% TMC and 2 wt.% PIP. Further details on the difference in the concentration of TMC used between the two polymers in this work are found in Chapter 5.

3.2.3 Fabrication of supports for membranes used in organic solvent nanofiltration in Chapter 5

Fabrication of TFC membranes PA(n-hexane): The support was taped to a glass plate, with the skin layer facing upwards, and placed in an aqueous solution of 2 wt.% PIP for 2 min. The amine-loaded support was pressed with a roller and wiped to remove excess amine solution, prior to immersion in an n-hexane solution 0.1 wt.% TMC for 1 min. The TFC membrane was then rinsed with n-hexane to remove any unreacted TMC. The membrane was left in water for 24 hours prior to testing.

Fabrication of TFC membranes PA(2-MeTHF): The support was taped to a glass plate, with the skin layer facing upwards, and placed in an aqueous solution of 3 wt.% PIP for 3 mins before immersion in 3 wt.% TMC in 2-MeTHF for 4 mins. Resultant membranes were rinsed with 2-MeTHF to remove excess TMC and stored in water for 24 hours prior to characterisation.

Solvent activation: DMF, DMSO and Cyrene™ were used as solvents for activation and were filtered through the membrane at 5 bar for 10 minutes before the feed solution was introduced.

3.2.4 Preparation of supports for membranes used in aqueous nanofiltration in Chapter 6

10 wt.% cellulose acetate was dissolved in with Cyrene™ or Cyrene™ and acetone or Cyrene™ and methanol at a 50:50 ratio at room temperature, and the solution was stirred until complete dissolution. The solution was left overnight to remove any air bubbles present. The dope solution was then cast onto a glass plate using a casting knife (Elcometer 3700) set at a thickness of 200 μm. Immediately after casting, the support

was immersed into the coagulation bath containing deionised water for phase inversion to occur at room temperature. The TFC membrane fabrication was carried out using the same methodology as highlighted in section 3.2.2.

Solvent activation: Ethanol was used as the solvent for activation and was filtered through the membrane at 5 bar for 10 minutes before the feed solution was introduced.

3.3 Physicochemical characterisation

3.3.1 Cloud point measurements/ternary phase diagram

The cloud points of the polymer solutions were determined by visual observation of a turbidity change of the transparent polymer solution, while titrating it with the non-solvent under continuous magnetic stirring and at 30 °C. All polymer solutions were weighed prior to titration experiments. Cloud point was reached when the turbidity of the polymer solutions did not disappear after stirring for more than one hour. Samples were weighed again to determine the amount of non-solvent added to the solution. The three points: polymer, solvent and non-solvent were used to plot the ternary phase diagram for each polymer solution.

3.3.2 X-ray photoelectron spectroscopy

X-ray Photoelectron Spectroscopy (XPS) of PA(n-hexane) and PA(2-MeTHF) was carried out using a Scienta 300 machine, operating at 1 x 10^{-9} bar. The X-ray source was an unmonochromated Al Ka source and the pass energy was set to 75 eV. Survey scans were collected at a dwell time of 133 msec, a step size of 200 meV and 2 scans were

added. Detailed scans were 2 scans at a dwell time of 533 msec with a 20 meV step. The polymers were dried at 120 °C prior to characterisation.

3.3.3 Solvent immersion

Solvent immersion tests were carried out in two different instances in this work. In chapter 4, supports were immersed in DMF, ethanol, acetone, toluene, chloroform, DCM and n-hexane. In chapter 5 the two polyamide layers were immersed in DMF and THF. Swelling tests were carried out using 1 cm x 1 cm sample pieces and were immersed in 5 mL of solvent. The samples were dried in a vacuum oven at 100 °C before weighing. The degree of swelling was calculated using the following equation:

$$\text{Degree of swelling} = \frac{W_f - W_i}{W_i} \tag{3.1}$$

Where:
W_i is the initial weight of the polymer after immersion
W_f is the final weight of the polymer, and all weights are in grams.

3.3.4 Porosity

The total porosity of the support samples in Chapter 4 was determined by filling the pores of a pre-weighed support sample with water. The water-loaded samples were weighed and the volume of water was obtained by the following equation:

$$Porosity = \frac{W_w - W_d}{Ad\rho} \tag{3.2}$$

where:

A is the surface area of the sample (m^2 g^{-1})

d is the average thickness of the substrate (μm),

ρ is the density of water (g cm^{-3})

W_i and W_d are the mass of the wet and dry samples (g).

3.3.5 Scanning electron microscopy

Morphology of all the synthesised materials in this work was characterised by using a JEOS JSM-IT100 Scanning Electron Microscope (SEM). Each SEM sample was sputter-coated with a 10 nm gold layer prior to analysis. For the cross-sectional morphology of membrane samples, all samples were freeze fractured in liquid nitrogen.

3.3.6 Contact angle measurements

Water contact angle measurements were carried out using a First Ten Angstroms (FTA 32) Instrument using the sessile drop method. For each membrane, five measurements were performed and averages and standard deviations were derived. Ossila contact angle software was used to determine the contact angle.

3.3.7 Thermal gravimetric analysis

Thermal gravimetric analysis (TGA) was carried out using a Mettler Toldeo TGA/DSC 3+ system. Thermal stability for the polymers and supports was studied, giving weight loss as a function of temperature. The polymers were heated from RT to 800 °C at a rate of 10 °C min^{-1}. under a flow of nitrogen (flow of 100 mL/min). Samples were dried in a vacuum oven at 120 °C overnight prior to characterisation.

3.3.8 Fourier transform infrared spectroscopy

Fourier Transform Infrared Spectroscopy (FTIR) was performed in attenuated total reflectance (ATR) mode on an IRTracer-100 Shimadzu spectrometer to characterise functional groups over a range of 600 – 4000 cm^{-1}. All samples of the polymers were dried for 12 h in a vacuum oven at 120 °C before analysis to remove any solvent present.

3.3.9 N_2 Gas adsorption isotherms

Brunauer-Emmett-Teller (BET) surface areas were determined by nitrogen adsorption-desorption isotherms for PA(n-hexane) and PA(2-MeTHF) at 77 K (Autosorb-iQ, Quantachrome). Samples were degassed under vacuum at 120 °C for 24 h before characterisation. All samples were dried for 12 h in a vacuum oven at 120 °C before degassing to remove any solvent present.

3.3.10 Solid State ^{13}C NMR spectroscopy

Solid-state NMR experiments were performed on PA(n-hexane) and PA(2-MeTHF) using Bruker Avance III spectrometers. ^{13}C NMR spectra were recorded at 14.1 T, with samples packed into 4-mm outer diameter rotors. All samples were dried for 12 h in a vacuum oven at 120 °C before characterisation to remove any solvent present.

3.3.11 Nanofiltration testing

The water and solvent permeance of the membranes produced in this work were measured using a stainless-steel dead-end pressure cell. The cell had a volume of 990 mL and a diameter of 70 mm, with a membrane area of 38.5 cm^2. The membrane was fitted at the bottom of the cell and the cell was filled with feed solution and tightly closed with clamps. The feed solution was pressurised with nitrogen gas at 5 bar at room temperature. During filtration, the feed solution was stirred at 700 rpm to avoid concentration polarisation. Permeate samples of 50 mL were collected in capped flasks as a function of time, weighed, and analysed. The permeance was calculated using the following equation:

$$Permeance = \frac{V}{At\Delta P} * 100\% \tag{3.3}$$

where:

permeance (L m^{-2} h^{-1} bar^{-1})

V is the volume of the solvent passing through the membrane (L),

A is the effective membrane area (m^2),

t is the operation time (h),

ΔP is trans-membrane pressure (bar).

The rejection of the membranes was calculated using the following equation:

$$Rejection\% = (1 - \frac{C_P}{C_F}) * 100\% \tag{3.4}$$

where:
C_p and C_f are the solute concentrations in the permeate and feed solution, respectively.

For aqueous nanofiltration experiments, a conductivity meter was used to determine the salt concentration of the feed and the permeate. For organic solvent nanofiltration experiments, the dye concentrations in the solvents were determined using UV-VIS spectrometry.

For membrane performance, at least three independent membranes were tested under identical operating conditions. The error bar on the graphs represents the standard deviation of reproducible results.

For the tests conducted with NF 270 TFC membrane, the membrane was compacted at 5 bar for 10 hours prior to characterisation. For the tests conducted with the membranes produced in this work, the membranes were compacted for 1 hour at 5 bar prior to characterisation.

3.3.12 Ultraviolet-visible spectroscopy measurements

Ultraviolet-visible spectroscopy (UV-Vis) spectra were obtained to determine dye concentrations during OSN testing using a Thermo Scientific Evolution 60 UV-Vis spectrophotometer. All sample measurements were performed in a wavelength range of 300 nm to 800 nm, with an interval of 1 nm.

3.3.13 Molecular weight cut-off measurements

Molecular Weight Cut-off (MWCO) tests were carried out using different polyethylene glycol (PEG) aqueous solutions of different molecular weights as the feed solution. These were filtered through the membrane at 5 bar and the permeate samples were collected. The concentration of organic solutes was measured with a TOC VCPH/CPN Shimadzu analyser in a non-purgeable organic carbon mode. Prior to the use of the TOC calibration standards were prepared using potassium hydrogen phthalate. Equation 3.4 was used to calculate the rejection of the different PEG solutions. A graph was plotted with the rejection of the PEG against the PEG molecular weight, and the MWCO was determined from the graph at 90 %.

Chapter 4

Comparative study on the replacement of petroleum-derived to bio-renewable solvents for membrane fabrication

4.1 Introduction

Cyrene™ is a bio-renewable solvent derived from waste cellulose and was first developed by the Circa Group in partnership with Professor James Clark, at the University of York. Cyrene™ has demonstrated the capability to substitute toxic petroleum-derived solvents such as DMF and NMP due to the similarities in density and polarity of the solvents, see Table 4.1 for the data [1], [2]. Cyrene™ is synthesised in a two-step process from waste cellulose, via a manufacturing process that is almost energy neutral and releases water to the environment [3]. Cyrene™ has very low toxicity, well below the hazard thresholds defined by the Globally Harmonized System of Classification and Labelling of Chemicals (GHS). The replacement of DMF and NMP with Cyrene™ has many environmental and health benefits, see Table 4.1 for the hazard statements associated with the three solvents [4]. As Cyrene™ is produced from renewable materials such as waste biomass and cellulose, it can be classified as a green solvent, however, despite the green origins of the solvent, Cyrene™ has a yellow ranking in many solvent selection guides [4]. This yellow ranking is due to the high boiling point it possesses of 227 °C which results in a high-temperature requirement for solvent recovery [3], [4]. Despite this classification, Cyrene™ adheres to two of the principles of Green Chemistry, 'safer solvents and auxiliaries' and 'use of renewable feedstocks' and was explored for membrane fabrication [5].

Cyrene™ has been successfully employed as a green solvent substitute in several industrially-relevant applications. The use of Cyrene™ has been investigated for graphene fabrication [6], synthesis of organic urea [7] and the fabrication of metal-organic frameworks [8]. Further to this, Cyrene™ has been used to produce the highest quality graphene inks ever produced using the green solvent instead of traditionally-used NMP [9]. Cyrene™ has also been reported to prepare polymeric membranes, and the use of Cyrene™ for membrane fabrication was first explored by Marino *et al.* [2]. The study investigated the use of Cyrene™ as a substitute for NMP and DMF in PVDF and PES support fabrication [2]. The fabrication conditions were investigated through the use of coupling vapour-induced- and non-solvent-induced phase separation. Optimal conditions were found with regard

to membrane morphology and properties such as the pure water permeation and pore size were investigated [2]. The use of Cyrene™ has also been reported by Milescu *et al.*, for the fabrication of PES membranes with the addition of the pore-forming agent polyvinylpyrrolidone (PVP) [1]. The temperature of the casting gel, coagulation time and PVP concentrations were investigated to produce PES supports with different morphologies [1]. These two studies report the proof of concept of using the solvent for the fabrication of a support. To this date, a thin film composite membrane has not been fabricated using Cyrene™ supports and further to this, the application of the supports produced using Cyrene™ have not been reported.

Table 4.1: Physico-chemical properties for Cyrene™, NMP and DMF, values taken from Marino *et al.* [2]

Properties	Cyrene™	NMP	DMF
Colour	Colourless	Colourless	Colourless
Molecular weight (g/mol)	128.13	99.13	73.09
Formula	$C_6H_8O_3$	C_5H_9NO	C_3H_7NO
Boiling point (°C)	227	202	153
Flash point (°C)	108	91	58
Density (g/cm^3)	1.25	1.02	0.93
Water miscibility	Complete	Complete	Complete
Hazard Statement	H319 Causes serious eye irritation	H315 - Causes skin irritation H319 - Causes serious eye irritation H335 - May cause respiratory irritation H360D - May damage the unborn child,	H226 - Flammable liquid and vapour H312 + H332 - Harmful when in contact with skin and toxic if inhaled H319 - Causes serious eye irritation
CHEM21 ranking	Problematic (Yellow)	Hazardous (Red)	Hazardous (Red)

In this chapter, the use of Cyrene™ for membrane fabrication was explored by producing a support suitable for organic solvent nanofiltration applications. Initially, polyimide, the most conventional polymer used for OSN, was used for fabrication; this polymer can easily be cross-linked to produce supports suitable for harsh organic solvent filtration using different methods [10]–[13]. As the fabrication of PI-Cyrene™ supports was not possible due to solvent/polymer/non-solvent incompatibility, the polymer was changed to cellulose acetate.

Cellulose acetate is a renewable polymer, and the use of this polymer coupled with Cyrene™ produced supports solely using bio-renewable materials in line with the fifth and seventh principles of Green Chemistry. A comparative study was carried out, and supports produced using DMF (the conventionally used solvent) were compared to supports produced using a combination of Cyrene™ and acetic acid (the bio-renewable alternative). The study looked at investigating the effects of using a bio-renewable solvent on the resultant support characteristics. The thermal and chemical stability, solvent filtration and morphology of the two supports were investigated to assess the suitability of exchanging a petroleum-derived solvent for an alternative bio-renewable solvent.

4.2 Hansen solubility parameters of polyimide

Hansen solubility parameters (HSP) were developed to predict the solubility of polymers in solvents based on the idea that "like dissolves like". Hansen represented materials as a substance in a 3-dimensional space called the Hansen space; the components in each dimension represent δ_D, δ_P, and δ_H attributed to dispersive forces, polar forces, and hydrogen bonding, respectively.

The Hansen solubility parameter distance between solvent and polymer, R_a is a measure of polymer-solvent affinities, see Equation 4.1. Smaller values of R_a indicate

good compatibility between the solvent and polymer to form a homogeneous solution. Good solvents have a distance from the centre of sphere R_a less than R_o (radius of Hansen solubility sphere or polymer sphere). The relative energy difference (RED) is used to describe the ability to dissolve a polymer in a solvent, as shown in Equation 4.2. Theoretically, RED < 1 the molecules are alike and will dissolve, if RED $= 1$ the system will partially dissolve and if RED > 1 the system will not dissolve.

$$R_a = \sqrt{4(\delta_{DS} - \delta_{DP})^2 + (\delta_{PS} - \delta_{PP})^2 + (\delta_{HS} - \delta_{HP})^2} \tag{4.1}$$

Where:

R_a is the distance between solvent and polymer

δ_P Hansen parameter representing polar interaction

δ_D Hansen parameter representing dispersive interaction

δ_H Hansen parameter representing hydrogen bonding parameter

S is the solvent

P is the polymer

$$RED = \frac{R_a}{R_o} \tag{4.2}$$

Where:

RED is the relative energy difference

R_a is the distance between the solvent and polymer

R_o is the experimental sphere radius for the polymer

To explore the solubility of polyimide in Cyrene™, the Hansen solubility parameters of PI, Cyrene™ and NMP which is the traditionally used solvent for PI support fabrication were compared [14]. The Hansen distance between the polymer and the two solvents R_a, NMP and Cyrene™ was calculated using Equation 4.1 and the results are listed in Table 4.2. The use of Cyrene™ presented a smaller R_a value compared to NMP at 7.1 and 7.9 respectively, indicating good polymer solvent compatibility. In addition to this, the relative energy difference was calculated using Equation 4.2. The RED value of Cyrene™ was lower than that of NMP at 0.53 and 0.59 respectively, indicating better compatibility between this polymer/solvent system.

Table 4.2: Hansen solubility parameters of PI membranes cast using Cyrene™ and NMP using the non-solvent water, values taken from Marino *et al.* [2]

	Polyimide	NMP	Cyrene™	Water
δ_D (MPa$^{1/2}$)	20.9	18.0	18.8	15.5
δ_P (MPa$^{1/2}$)	11.3	12.3	10.6	16.0
δ_H (MPa$^{1/2}$)	9.7	7.2	6.90	42.3
R_a	-	7.9	7.1	-
R_o	13.4			
RED	-	0.59	0.53	-

4.3 Casting PI and Cyrene™ dope solution

A polymer dope solution consisting of polyimide and NMP was used to fabricate a support. A coagulation bath containing water at room temperature (23 °C) was used, and phase inversion proceeded to produce smooth supports, see Figure 4.1a. A dope solution consisting of PI and Cyrene™ was cast using similar conditions and the resultant support was produced with wrinkles and ridges on the surface, see Figure 4.1b. To overcome the ridges and wrinkles, different polymer concentrations ranging from 10-25 wt.% were explored, however, ridges and wrinkles were still produced on all the supports.

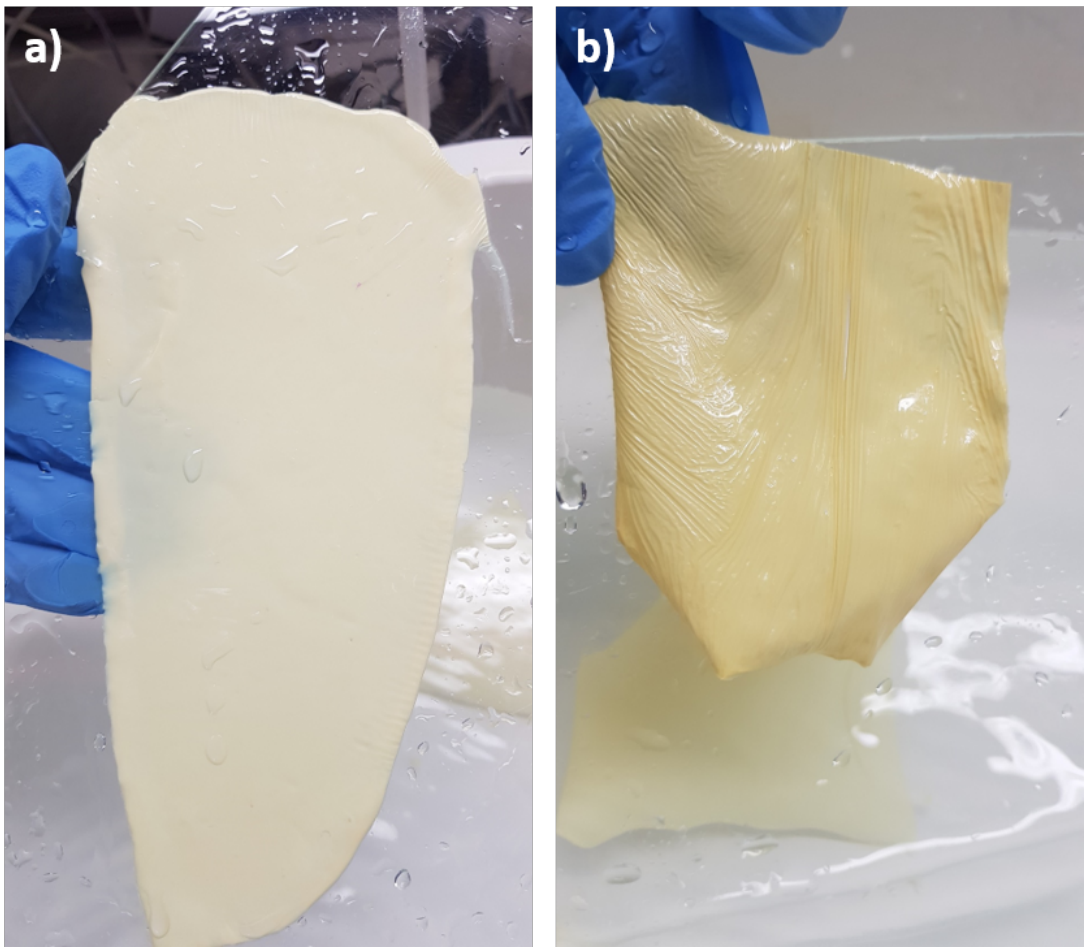

Figure 4.1: a) Support cast using a PI-NMP dope solution, b) Support cast using a PI-Cyrene™ dope solution. The casting temperature and the coagulation bath were both at room temperature, 23 °C. The non-solvent used was DI water.

To further investigate the suitability of PI and Cyrene™ support fabrication, the temperature of the coagulation bath was heated to different temperatures ranging from 30 -70°C. A change in temperature for the coagulation bath was investigated to see if higher temperatures would relax the support during fabrication and eradicate the wrinkles. For all the supports produced here the temperature of the coagulation bath matched the temperature of the dope solution. Figure 4.2a shows the support that was produced using a dope solution and coagulation bath at 60 °C and the holes and ridges are more prominent than when using a dope solution and coagulation bath at room temperature (see Figure 4.1b for the support image). In addition to the ridges and holes, the support was non-uniform with varying thickness, which is evident in Figure 4.2a. The change in thickness of the NMP and Cyrene™ supports was further investigated by measuring the thickness of the cast wet support straight after phase inversion and comparing it to the initial 200 μm setting that was used on the casting knife. The supports produced using the solvent NMP were able to retain the thickness in both the room temperature and 60 °C coagulation bath. On the other hand, the support cast using Cyrene™ experienced a thickness loss of 56 % during phase inversion at room temperature and 60 % when the coagulation bath was at 60 °C, see Table 4.3 for the data. This change in thickness suggests that the PI/Cyrene™/water system is unable to produce support suitable for filtration applications.

Table 4.3: Phase inversion parameters of the PI membranes cast using NMP and Cyrene™ and all measurements are of the wet films after phase inversion has occurred

Dope solution	Temperature of water (°C)	Phase inversion time (s)	Reduction in thickness(%)
10% PI Cyrene™	23	663	56
10% PI Cyrene™	60	501	62
10% PI NMP	23	53	0
10% PI NMP	60	25	0

The phase inversion time was investigated to see if a difference in phase inversion time was experienced when using the two solvents. The time taken for phase inversion to

complete was recorded when the support detached itself from the glass plate. A substantial increase in phase inversion time was experienced when using the Cyrene™ dope solution compared to the NMP dope solution at 663 s and 53 s respectively when using a room temperature dope solution and coagulation bath. The change in time could be attributed to the viscosity of the solvent, as the viscosity of Cyrene™ is considerably higher at 14.5 cP compared to 1.67 cP for NMP. The increased viscosity of the Cyrene™-based dope solution required more non-solvent for phase inversion to occur resulting in a slower demixing process [15]. The change in the phase inversion time generally does not alter the support surface structure and the ridges, wrinkles and holes are not a result of this as a slower demixing process results in less porosity in the support with smaller pore sizes [15].

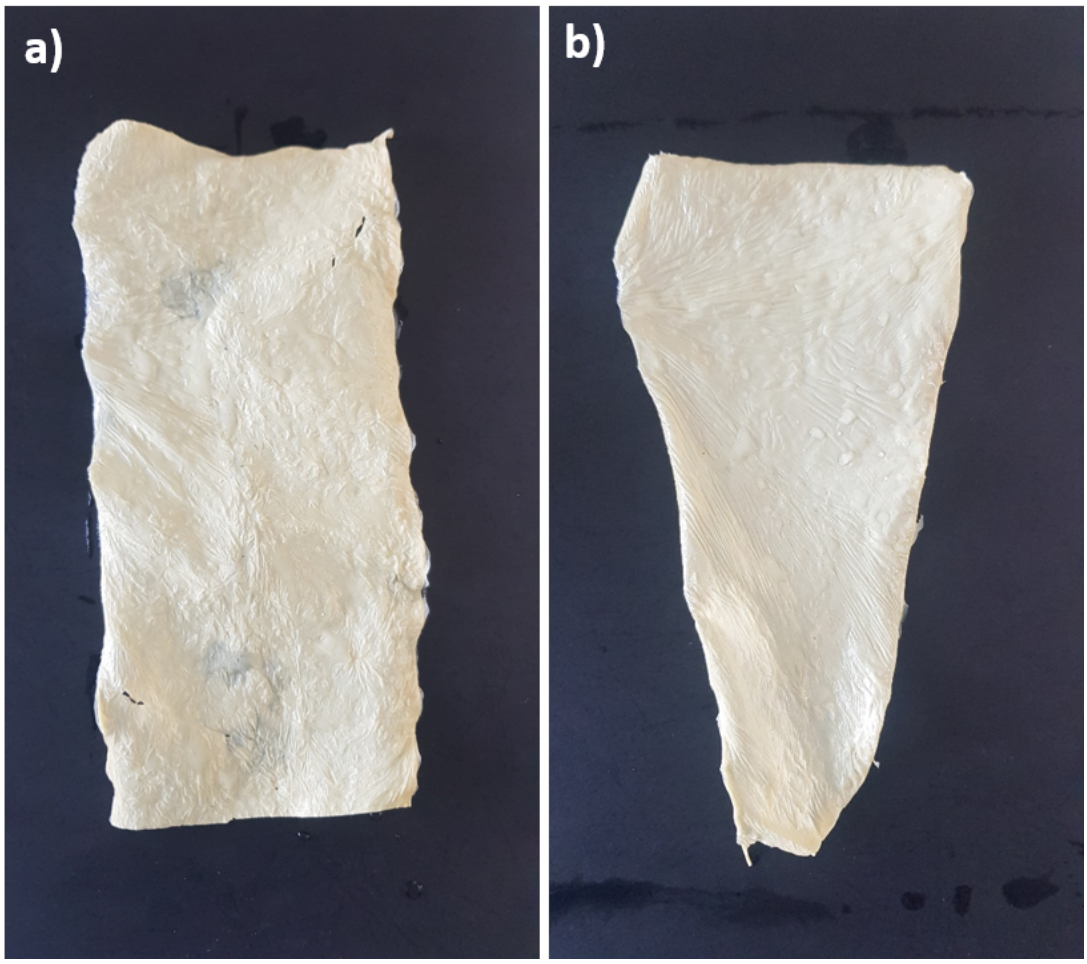

Figure 4.2: a) Support cast using a PI-Cyrene™ dope solution and coagulation bath temperature of 60 °C b) Support cast using a PI-Cyrene™ dope solution with a polymer dope solution at 60 °C and a room temperature coagulation bath. The non-solvent used was DI water for both supports.

Figure 4.2b shows the Cyrene™ based support produced using a hot casting dope solution at 60 °C with a room temperature coagulation bath. The resultant support had ridges but no holes formed. The support was less stable compared to the supports produced using a room temperature dope solution, as a higher thickness reduction was experienced.

To further investigate the feasibility of a PI-Cyrene™ polymer solution, a solvent mixture solution consisting of NMP and Cyrene™ (50:50) was used to produce a support. The resultant support was smoother and phase inversion was able to proceed quicker in water due to the addition of NMP which lowered the viscosity of the dope solution, however, ridges and wrinkles were still formed, see Figure 4.3 thus deeming the solvent mixture also unsuitable for support fabrication.

Figure 4.3: Support cast using a PI and 50:50 NMP and Cyrene™ dope solution using DI water as the non-solvent, the casting and coagulation took place at room temperature

4.3. Casting PI and Cyrene™ dope solution

A PI-NMP dope solution with a water coagulation bath is a common fabrication method, and further to this different PI-solvent dope solutions have been successfully reported with a water coagulation bath such as PI-DMF [16] and a PI-DMSO solution [10]. The two polymers, PES and PVDF, have been successfully reported by Marino *et al.* to produce a support with Cyrene™ and a water coagulation bath [2]. From the results that were obtained in this experiment, it is clear that there are interactions between the polymer PI/solvent Cyrene™/non-solvent water system and that this system in particular is incompatible [17], [18]. Experimentally, the work explored many possible solutions to produce a support using a PI and Cyrene™ polymer solution: different concentrations of PI were used in Cyrene™ to form a solution, and they all formed ridges. The use of heating the solution and the coagulation bath was used to mitigate any temperature changes that may be causing the ridges, however they were all unsuccessful as a smooth support was not produced.

Another method that was explored to investigate the feasibility of a PI-Cyrene™ polymer dope solution was to change the non-solvent from DI water to different alcohols such as ethanol, isopropanol and methanol. Phase inversion did not proceed in any of the alcohols and Table 4.4 summarises the findings produced in this work. From the different methods used in this work to produce a support using a PI-Cyrene™ polymer dope solution it can be concluded that although Cyrene™ was able to dissolve polyimide and the Hansen solubility parameters were better compared to NMP, it was not possible to produce a support for filtration applications with the polymer-solvent system. The polymer was changed from polyimide to cellulose acetate to produce a support suitable for OSN applications.

Table 4.4: Summary of different solvents used for PI support fabrication including the work conducted with Cyrene™ and different solvents used for fabrication

Polymer	Solvent	Non-solvent	Outcome	Reference
PI	NMP	Water	✓	[14]
PI	DMF	Water	✓	[16]
PI	DMSO	Water	✓	[10]
PI	Cyrene™	Water	**X**	this work
PI	Cyrene™	Ethanol	**X**	this work
PI	Cyrene™	Methanol	**X**	this work
PI	Cyrene™	Isopropanol	**X**	this work
PI	Cyrene™/NMP	Water	**X**	this work

4.4 Hansen solubility parameters of cellulose acetate

To explore the solubility of cellulose acetate in Cyrene™, the Hansen solubility parameters of CA, Cyrene™ and 'undesirable' solvents NMP and DMF which are common solvents used to fabricate CA supports were compared. The Hansen solubility parameters for Cyrene™ were comparable to those of DMF and NMP, see Table 4.5 and the RED values for the CA Cyrene™, NMP and DMF dope solutions were 1.05, 0.87 and 0.36, respectively. Hansen states that with a RED value >1, the two materials do not dissolve, but despite the high RED value for CA and Cyrene™, CA was soluble in Cyrene™ and a homogenous solution was formed when the polymer dope solution was heated to 80 °C [19]. As DMF had the lowest RED value and is commonly used to produce CA supports,

this solvent was chosen to fabricate supports that would be used as a benchmark to which the CA-Cyrene™ supports would be compared to [20]–[23].

Table 4.5: Hansen solubility parameters of CA and Cyrene™ and DMF and the solvent mixture Cyrene™/acetic acid, values taken from [2], [24]

	Cellulose Acetate	DMF	Cyrene™	Acetic Acid	solvent mixture
δ_D (MPa$^{1/2}$)	18.6	17.4	18.8	14.5	17.7
δ_P (MPa$^{1/2}$)	12.7	13.7	10.6	8.0	9.9
δ_H (MPa$^{1/2}$)	11.0	11.3	6.9	13.5	8.3
RED	-	0.4	1.1	1.5	0.9
R_o	8.8				

4.5 Cellulose acetate and Cyrene™ based supports for water filtration

A CA-Cyrene™ based support was fabricated to investigate how this green solvent compared to other green solvents reported in literature. Rasool *et al.,* conducted a study using organic carbonates as a substitute for NMP in support fabrication and the water permeance of the CA support produced using a mixture of propylene carbonate and styrene carbonate (PC/SC) was less than 1.0 L m^{-2} h^{-1} bar^{-1} [24]. In addition to this to this, Rasool *et al.,* also explored glycerol derivatives, namely triacetin, diacetin and glycerol-formal as solvents for support fabrication [25]. The CA supports fabricated in this study were produced using a solvent mixture system using the glycerol derivatives and 2-MeTHF. A water permeance of 5.7 L m^{-2} h^{-1} bar^{-1} was experienced from the CA-diacetin/2-

MeTHF support and 1.0 L m^{-2} h^{-1} bar^{-1} for the CA-triacetin/2-MeTHF support and 1.1 L m^{-2} h^{-1} bar^{-1} for the CA-glycerol formal/2-MeTHF support [25]. Further to this, several other works have been reported for the fabrication of CA membrane and are listed in Table 4.6 and Figure 4.4. Cyrene™ produced the most permeable CA supports that have been reported in literature at 98 L m^{-2} h^{-1} bar^{-1}. In some cases, the support fabricated with Cyrene™ was 98 times higher than other reported supports produced through green solvents [19], [24], [26].

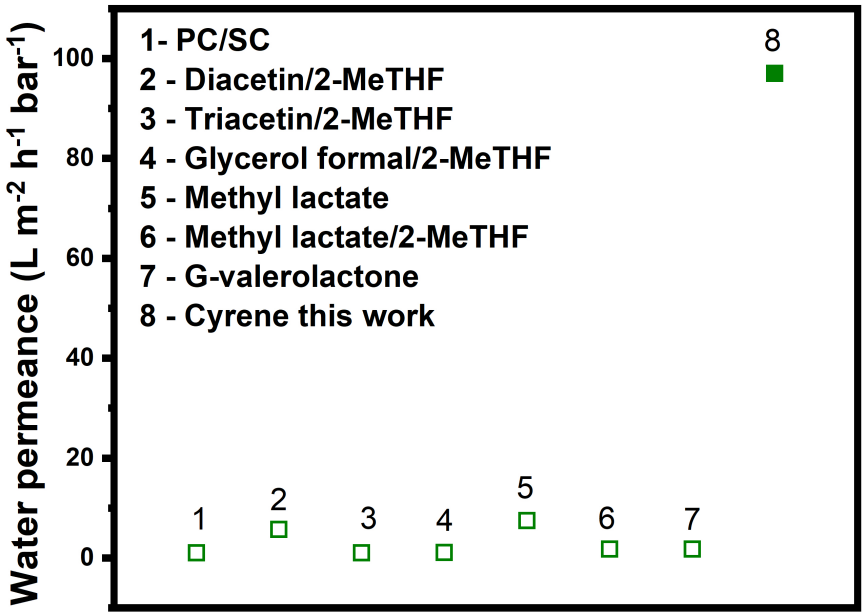

Figure 4.4: Comparison of the green solvents reported in the literature and the work done in this work

Table 4.6: Performance comparison of the cellulose acetate membranes produced using bio-renewable solvents

Polymer	Solvent system	Water permeance L m^{-2} h^{-1} bar^{-1}	Ref
CA	PC/SC	1.0	[24]
CA	Diacetin/2-MeTHF	5.7	[25]
CA	Triacetin/2-MeTHF	1.0	[25]
CA	glycerol formal/2-MeTHF	1.1	[25]
CA	Methyl lactate	7.5	[19]
CA	Methyl lactate/2-MeTHF	1.8	[19]
CA	G-valerolactone	1.8	[26]
CA	Cyrene™	98.0	this work

4.6 Deacetylation of cellulose acetate support

Deacetylation is a technique commonly used to hydrolyse the acetyl group from cellulose acetate to produce regenerated cellulose (RC) which is stable in organic solvents [27]. Many procedures have been employed for deacetylation such as the use of a benzene and acetic acid solution [28] and sodium hydroxide (NaOH) or potassium hydroxide (KOH) solutions in either ethanol or water [29]–[31]. Increasing the concentration of these solutions can reduce reaction times, which typically last for 30 hours at room temperature [29]. Ahmed *et al.* used a combination of sonication and a NaOH/ethanol solution for deacetylation [29]. Son *et al.* reported the use of a KOH/ethanol solution for 24 hours to hydrolyse the acetyl group [31]. Wittamar *et al.,* investigated the use of KOH of different molarities

(0.05 - 0.5 M) in a mixture of ethanol and water [32]. This study found that CA was able to transform into RC under different conditions; 260 min if immersed in 0.05 M aqueous KOH and 90 min if immersed in 0.1 M aqueous KOH solutions [32].

In line with the third and fifth principal of Green Chemistry, the alkalinity of the solution was kept as low as possible to keep the reagents as green as possible [5]. This also minimised the use of organic solvents during membrane fabrication and also allowed for lower amounts of hazardous waste to be produced. An aqueous KOH solution was employed for deacetylation at a low concentration of 0.05 M. The deacetylation reaction scheme for the transition from cellulose acetate to regenerated cellulose used in this work is shown in Figure 4.5.

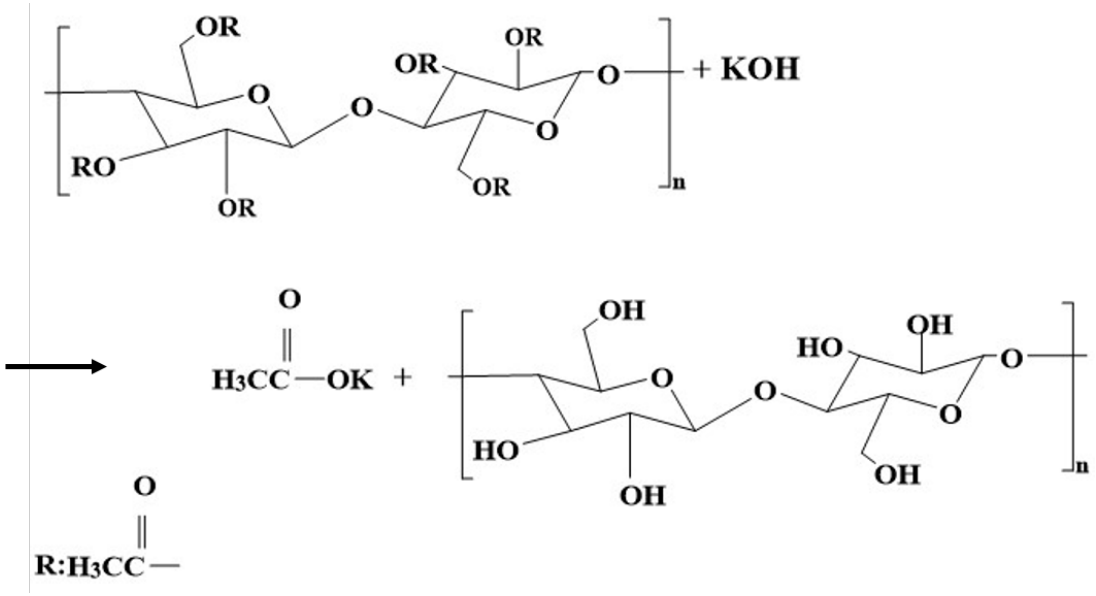

Figure 4.5: Reaction scheme of the transition from cellulose acetate to regenerated cellulose using an aqueous KOH solution. Potassium acetate is produced during the reaction

A CA-Cyrene™ dope solution was prepared and cast to form a smooth support. The CA support produced using the Cyrene™-based polymer dope solution was not able to retain the structure during deacetylation and upon contact with the aqueous KOH solution, the support crumpled into a ball. The collapsed structure of the support after contact

with the 0.05 M KOH solution is shown in Figure 4.6a.

To enhance the stability of the support, acetic acid was added to the CA-Cyrene™ polymer dope solution to produce a Cyrene™/acetic acid (3:1) solvent system. Acetic acid was selected as the solvent as it is a precursor in cellulose acetate synthesis and also has a yellow ranking on the CHEM21 solvent selection guide [33], [34]. Additionally, acetic acid reduced the RED value from 1.05 to 0.89, improving the CA solubility in the Cyrene™ based system, (see Table 4.5, Section 4.4 for the data). The temperature of dissolution for the polymer dope solution was reduced from 80 °C to 50 °C, as the polymer had better solubility in the solvent mixture system, lowering the energy consumption associated with the fabrication of these supports. In line with using non-toxic solvents, this solvent mixture and CA dope solution was tested and upon contact with the deacetylation medium, the support was able to retain the structure to produce a support suitable for filtration applications, see Figure 4.6b.

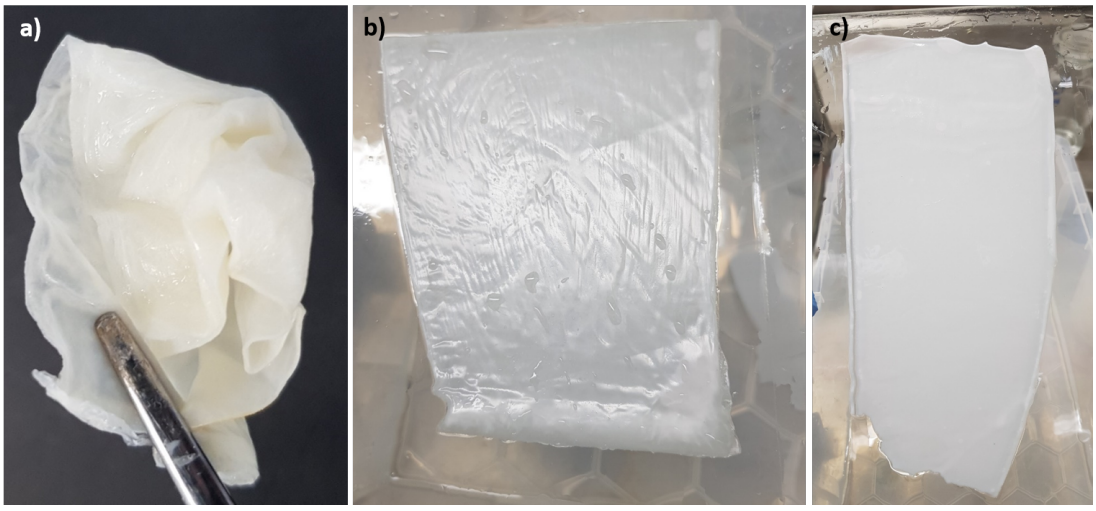

Figure 4.6: a) Support cast using a CA-Cyrene™ dope solution - structure collapse that occurred upon contact with the deacetylation medium b) Support cast using a CA-Cyrene™/AA dope solution with a water coagulation bath with a 90 mins deacetylation c) Support cast using a CA-Cyrene™/AA dope solution and using the deacetylation medium as the coagulation bath to produce regenerated cellulose supports. The deacetylation medium in all experiments was an aqueous 0.05 M KOH solution.

4.6. Deacetylation of cellulose acetate support

In line with principles of Green Chemistry to reduce the amount of waste produced in processes and to reduce the number of steps required in fabrication as highlighted by Szekely *et al.* [35], the deacetylation medium (0.05 M KOH in water) was used as the non-solvent/coagulant medium for producing the regenerated cellulose porous supports, (see Figure 4.6c for the support). The combination of using the deacetylation medium as the coagulant in phase inversion to produce supports suitable for organic solvent filtration applications through a one-step process allowed for a significant reduction in the amount of liquid waste generated during the fabrication process.

The conventional method used for fabrication is where phase inversion takes place and subsequently the support is immersed into the deacetylation medium. To produce one support, approximately 4 L of water for phase inversion is required and another 2 L of water for deacetylation to occur. The waste generated from this process during phase inversion will contain Cyrene™ and acetic acid. During the deacetylation process any residual Cyrene™ and acetic acid that was present in the support will be leached out and a potassium acetate salt, which is the by-product of the deacetylation reaction of cellulose acetate with potassium hydroxide, will be produced [31]. The combination of the 6 L of waste produced through both processes would require targeted disposal. The combination of using the deacetylation medium as the coagulant in phase inversion to produce supports in a one-step process eliminates the extra 2 L of waste generated and as a result offers a sustainable protocol for producing quick porous supports that are stable in organic solvents.

The optimal time for deacetylation to occur with the CA-Cyrene™/AA polymer dope solution was 90 min, and this was tested with FTIR to confirm the change from cellulose acetate to regenerated cellulose. Figure 4.7 shows the change in FTIR peaks as the deacetylation time increased from 0 to 120 mins at room temperature. The disappearance of the C=O (1745 cm^{-1}), C-CH_3 (1375 cm^{-1}) and C-O-C (1235 cm^{-1}) peaks correspond to the hydrolysis of the acetate groups from cellulose acetate, producing regenerated cellulose. Figure 4.8 shows the FTIR spectra between 500-200 cm^{-1} of the supports cast

using a CA-DMF and CA-Cyrene™/AA dope solutions, at 90 minutes both supports have undergone deacetylation irrespective of the solvent used for fabrication.

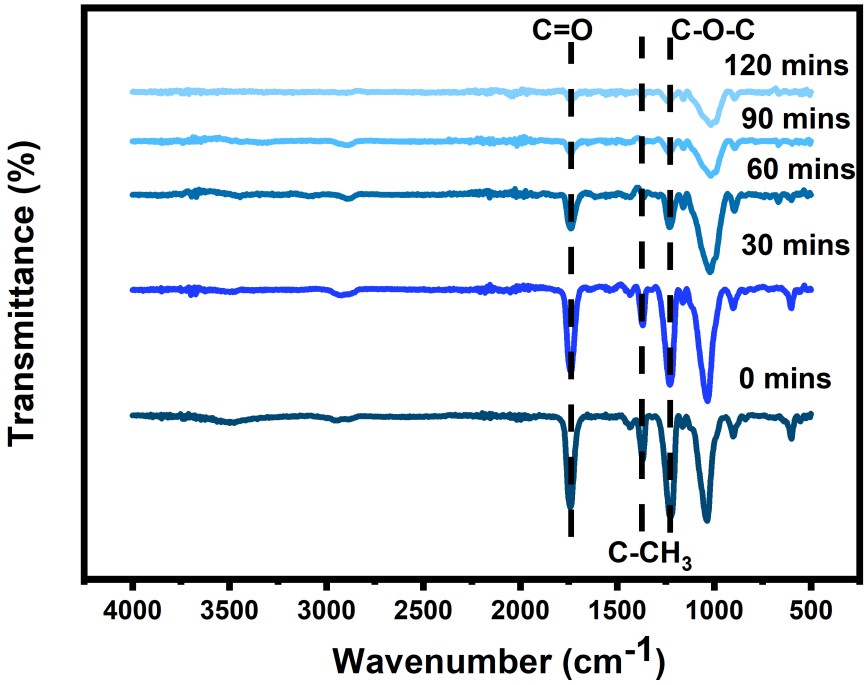

Figure 4.7: FTIR spectra analysis showing the transformation of CA into regenerated cellulose under different deacetylation durations for the CA- Cyrene™/AA dope solution. All tests were carried out at room temperature and the deacetylation medium used was a 0.05 KOH aqueous solution

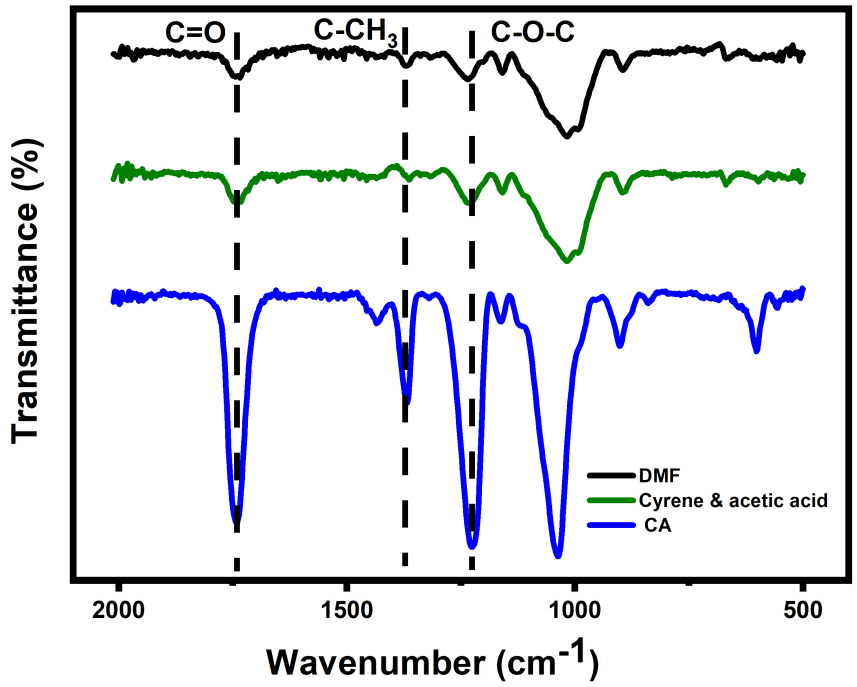

Figure 4.8: FTIR spectra analysis between 500-2000 cm^{-1} showing the transformation of CA into regenerated cellulose using CA-DMF and CA-Cyrene™/AA dope solutions at 90 min deacetylation time. All tests were carried out at room temperature and the deacetylation medium used was a 0.05 KOH aqueous solution

4.7 Thermal and chemical stability

Thermogravimetric analysis was performed on the two supports produced from the two solvents, (see Figure 4.9). Nanofiltration tests occur at room temperature, and the thermal stability of the membrane is not a characterisation that is not required for filtration experiments for both aqueous or organic solutions. However, TGA was carried out to investigate how a change of solvent during fabrication affects the material's thermal stability. In both supports, the polymer decomposition occurred at different temperature ranges, undergoing a three-step mass loss at (1) 100 - 200 °C (2) 220 - 400 °C and (3) 500 - 800 °C. The initial mass loss for the two supports was due to the removal of water

and any solvents that the support may have retained (boiling point Cyrene™: 220 °C and boiling point DMF: 153 degree C). The mass loss between 220 - 400 °C was ascribed to the thermal decomposition of cellulose, and the mass loss at 400 - 800 °C represented the complete carbonisation of the two supports [36]–[38].

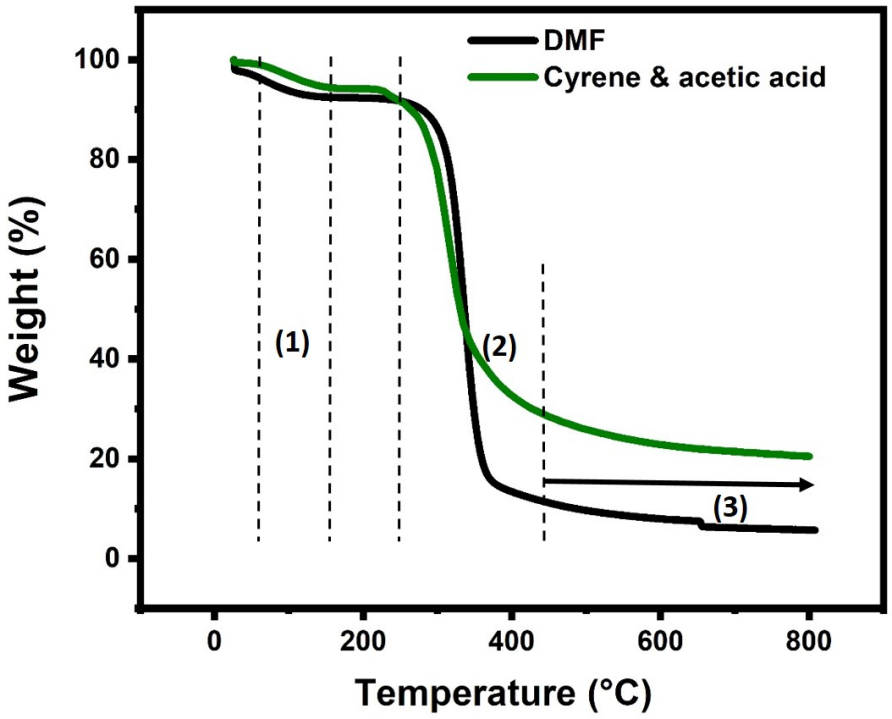

Figure 4.9: TGA of the two RC supports produced using DMF (black) and Cyrene™/AA (green). The polymers were heated from RT to 800 °C at a rate of 10 °C min^{-1} under a flow of nitrogen at 100 mL/min

The RC-Cyrene™/AA support experienced better stability at higher temperatures than the RC-DMF support as the mass loss at 800 °C is 80 % and 95 % respectively. This is in agreement with previous studies carried out with Cyrene™ based supports. Milescue *et al.* reported that Cyrene™ based supports experienced higher thermal stability compared to NMP supports [1].

4.7. Thermal and chemical stability

The solvent stability of the two support layers was determined using a wide range of solvents: polar aprotic - DMF, alcohol - ethanol, ketone - acetone, alkane - hexane, aromatic - toluene, chlorinated- chloroform. All tests were carried out for 48 hours at room temperature unless stated otherwise, see Table 4.7 for the data. The weight loss of the RC-Cyrene™/AA support was consistently higher than the RC-DMF support. On average, an increase of 30 % in weight loss was experienced for the RC-Cyrene™/AA supports. As the weight loss in different solvents was consistent, at approx 30 %, it was concluded that no interactions between the solvent and support occurred to cause dissolution. The increased weight loss of RC-Cyrene™/AA supports was attributed to the porosity of the support, as the RC-Cyrene™/AA supports experienced a more porous structure compared to the RC-DMF support. This increased porosity led to a higher surface area, resulting in the solvents being able to seep into the pores of the support to speed up degradation [39].

A wide range of solvents were tested for solvent immersion, and a weight loss of 9.1 % was experienced for the RC-Cyrene™/AA support, compared to 1.9 % for the DMF-based support in chloroform. From this result, it was hypothesised that the RC-Cyrene™/AA support was unstable in chlorinated environments and this was further investigated with DCM immersion, another chlorinated solvent. The RC-Cyrene™/AA support experienced a weight loss of 8.1 % compared to 1.9 % for the DMF-based support in DCM. The instability of the two RC-Cyrene™/AA supports in chlorinated solvents suggests that there could be possible interactions that take place with the RC-Cyrene™/AA support and a chlorinated environment that leads to instability and quicker dissolution of the support. Further work into the interactions between chlorinated solvents and the RC-Cyrene™/AA support would be required to investigate this phenomenon.

The two supports were able to retain structural integrity after being immersed in DMF and heated at 100 °C for 48 hours, see Table 4.7 for the weight loss data. Figure 4.10 shows the structure of the two supports after being heated for 48 hours in DMF at 100 °C, and no structural damage is shown. The support was also immersed in DMF for three months to investigate the long-term stability of the support in the harsh environment. The

RC-Cyrene™/AA support experienced a weight loss of 22.4 % and the RC-DMF support lost 17.8 %. The retention of the weight of the two supports in the harsh organic system demonstrated that the quick (90 mins) low alkali (0.05 M KOH) deacetylation process produced robust support layers that could be applied in harsh organic conditions.

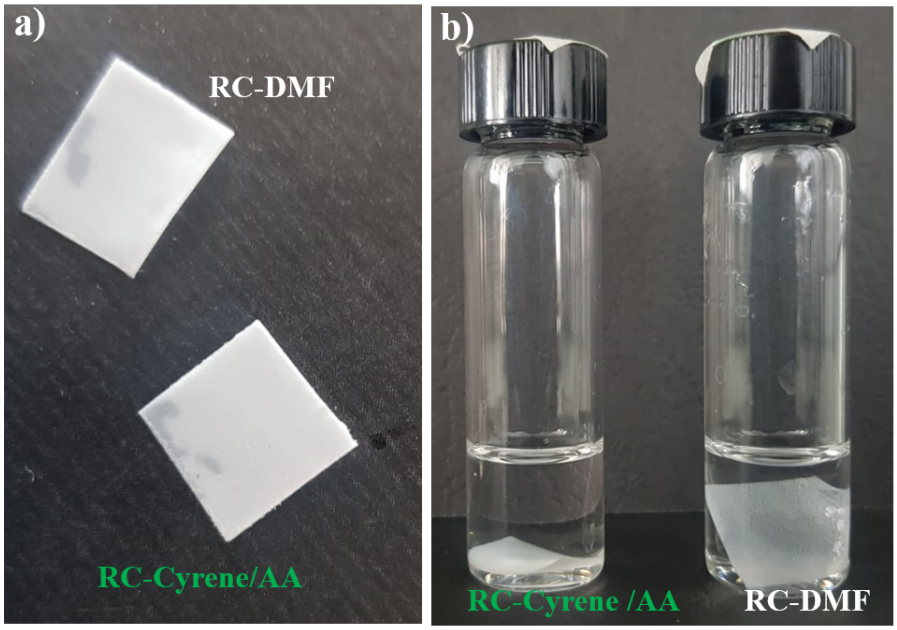

Figure 4.10: Solvent stability test using in DMF a) support after DMF immersion at 100° C and b) supports in DMF after 3 months

Table 4.7: Weight loss for the CA-DMF and CA-Cyrene™/AA support when immersed in different solvents for different durations to test the supports for solvent resistance. All tests were carried out at room temperature unless stated.

Time	DMF based support			Cyrene™/AA based support			Percentage difference (%)
	Initial weight (g)	Final weight (g)	Weight loss (%)	Initial weight (g)	Final weight (g)	Weight loss (%)	
Ethanol	0.0160	0.0159	0.62	0.0215	0.0213	0.9	33
Toluene	0.0158	0.0155	1.9	0.0218	0.0212	2.7	29
Chloroform	0.0202	0.0198	1.9	0.0128	0.0116	9.4	79
Acetone	0.0160	0.0158	1.2	0.0222	0.0218	1.8	33
DCM	0.0156	0.0154	1.3	0.0220	0.0202	8.1	83
n-hexane	0.0154	0.0150	1.6	0.0217	0.0212	2.3	30
DMF	0.0160	0.0153	3.1	0.0251	0.0238	4.6	30
DMF 100° C	0.0156	0.0145	4.1	0.0252	0.0236	5.8	29
DMF - 3 months RT	0.0161	0.0130	17.8	0.0247	0.0190	22.4	20

4.8 Permeation and solute rejection

The molecular weight cut-off for the two supports was investigated using PEG molecular markers of different molecular weights ranging from 200-20,000 g/mol in an aqueous solution. The SEM images (Figure 4.11) show that the RC-Cyrene™/AA supports are considerably more porous with surface pores of 780 nm, compared to the RC-DMF supports which had surface pores of 12 nm, see Figure 4.11a and b respectively. This suggests that the DMF-based support is in the ultrafiltration range and the Cyrene™/AA-based support is in the microfiltration range [15], [40] As expected based on the pore sizes, the MWCO for the RC-Cyrene™/AA support was considerably higher than the RC-DMF support at 10,500 g/mol (Figure 4.12a) and 590 g/mol (Figure 4.12b) respectively.

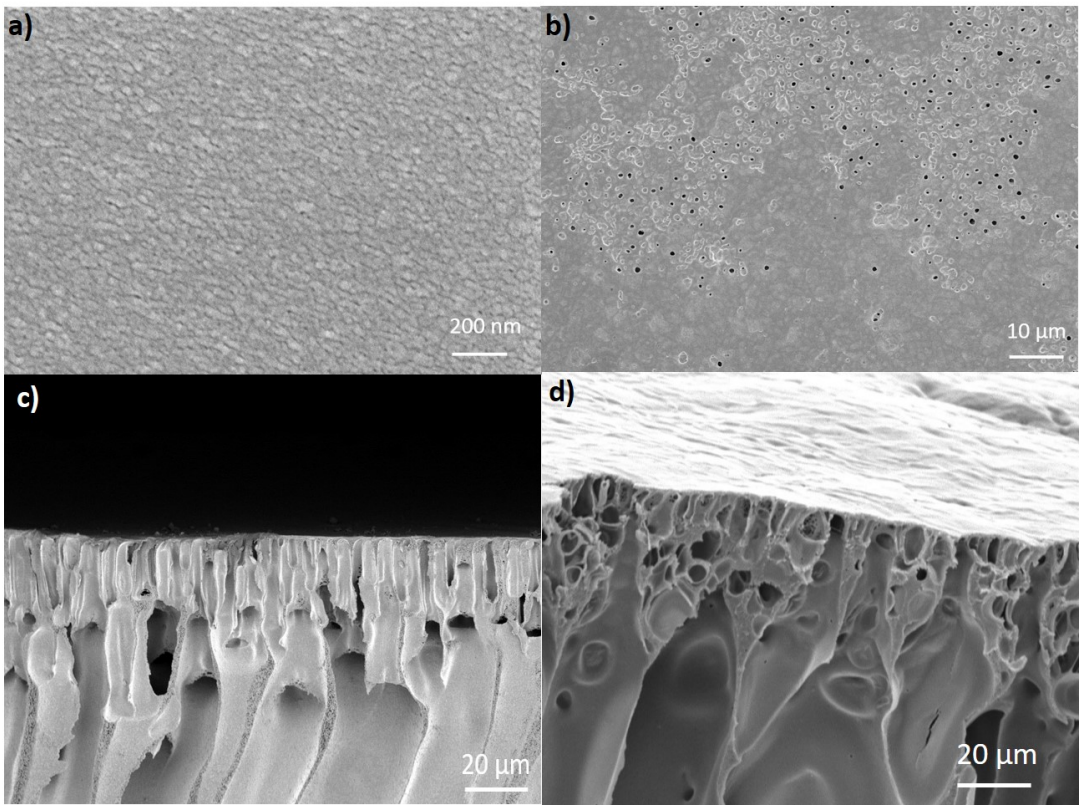

Figure 4.11: Top surface and cross-section SEM images of the two support produced using a CA dope solution of DMF (a and c) and Cyrene™/AA (b and d)

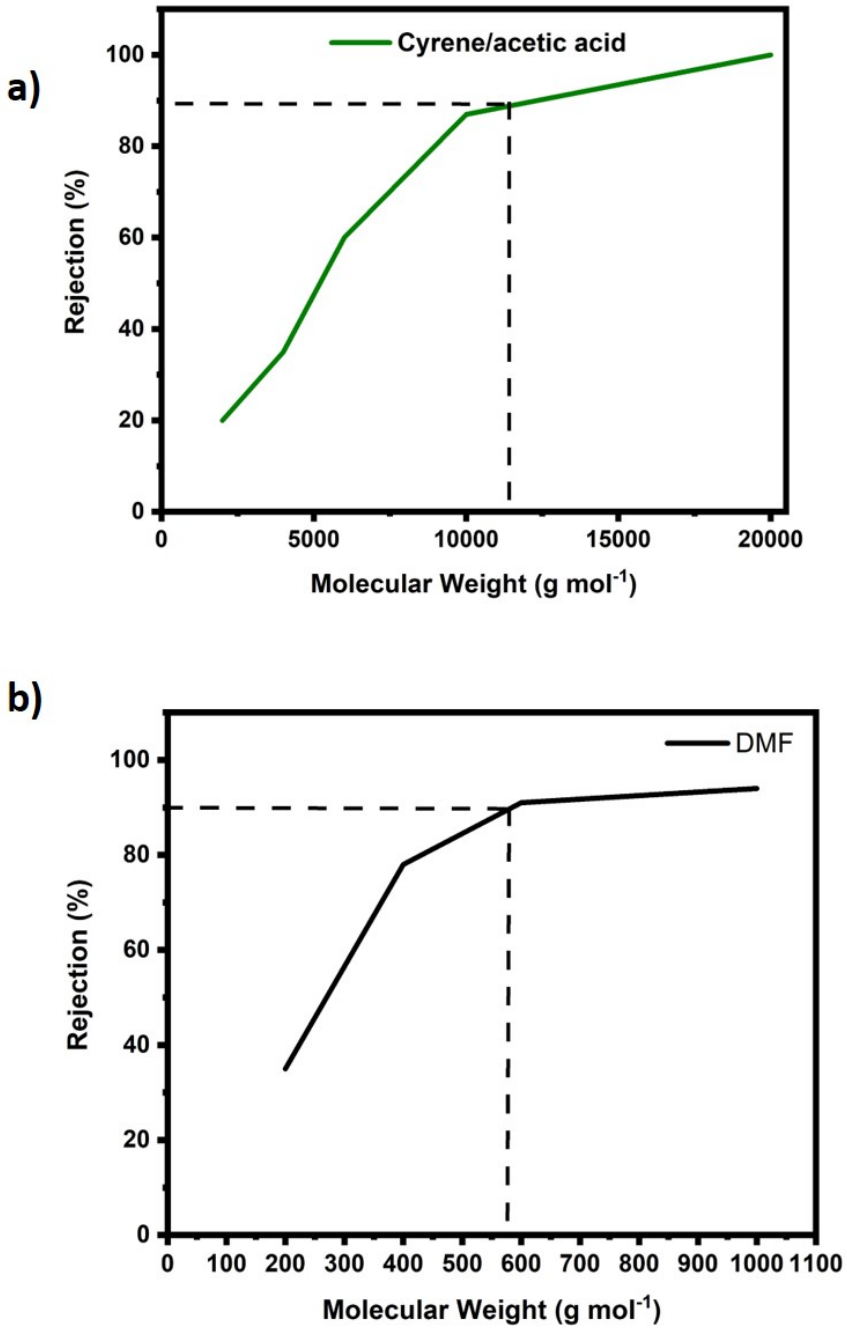

Figure 4.12: Determination of molecular weight cut off for the two supports a) RC-Cyrene™/AA support with MWCO 10,500 g/mol b) RC-DMF support with MWCO 590 g/mol

4.9 Solvent filtration

To investigate the pure solvent transport properties across the two supports, various solvents were used for the filtration test: polar aprotic - DMF, alcohol - ethanol, ketone - acetone, alkane - hexane, aromatic - toluene, chlorinated- chloroform, DCM, all tests were conducted at room temperature and at 5 bar. Further tests were conducted using chloroform and DCM to validate the conclusion of possible interactions of the RC-Cyrene™/AA support with chlorinated solvents.

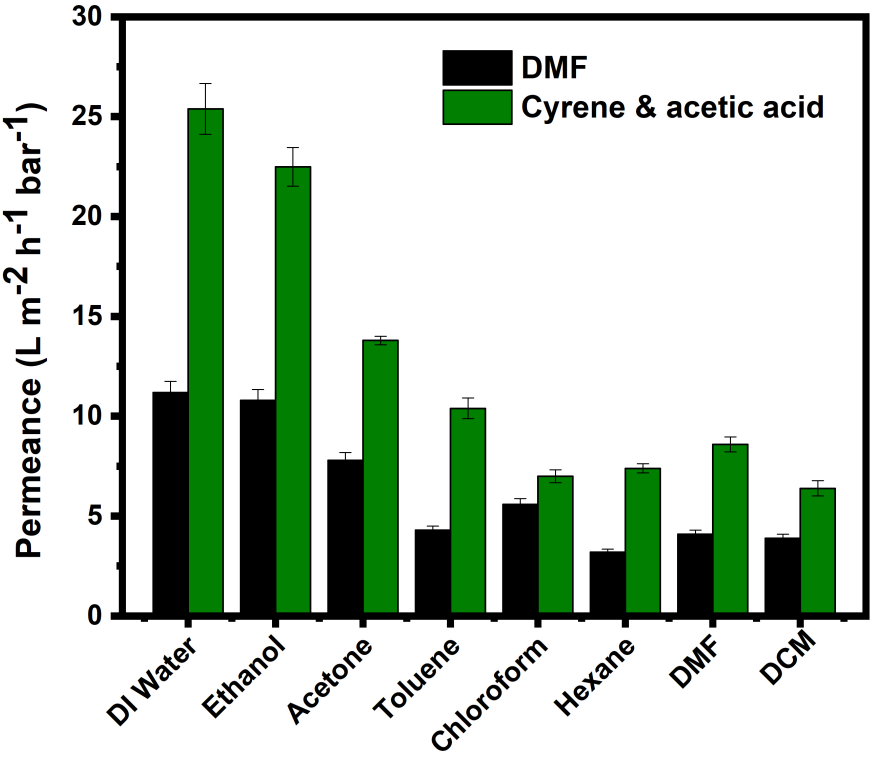

Figure 4.13: Pure solvent permeance of different solvents in RC-Cyrene™/AA (green) and RC-DMF (black) supports.All filtrations were conducted at 5 bar, room temperature and for 500 mins

The filtration of solvents in the RC-Cyrene™/AA support was higher than that of the RC-DMF support, and in some solvents over a 100 % increase in solvent permeance was experienced. The water permeance of the RC-Cyrene™/AA support was 25.4 L m^{-2} h^{-1}

bar^{-1} 114 % higher than that of the RC-DMF at 11.2 L m^{-2} h^{-1} bar^{-1}, as shown in Figure 4.13. This increase in solvent permeation can be attributed to the higher pore size of the RC-Cyrene™/AA support, as the surface pores of the RC-Cyrene™/AA support were bigger at 780 nm compared to 12 nm for the RC-DMF support, see Figure 4.11. Further to this, the MWCO of the RC-Cyrene™/AA support was considerably higher at 10,500 g/mol compared to 590 g/mol for the RC-DMF support which also further facilitated solvent permeance, see Figure 4.12 in Section 4.8.

The surface hydrophilicity was assessed by contact angle measurements, (see Figure 4.14). A contact angle less than 90 ° indicates a hydrophilic surface, and a hydrophilic surface in a membrane enhances solvent transport through the membrane [41]. The contact angle for the RC-DMF support was 50.0 ° and 35.5 ° for the RC-Cyrene™/AA support. A 48% increase in hydrophilicity was experienced when using the green solvent system. This increase in hydrophilicity also contributed to the greater water permeance experienced through the support [41].

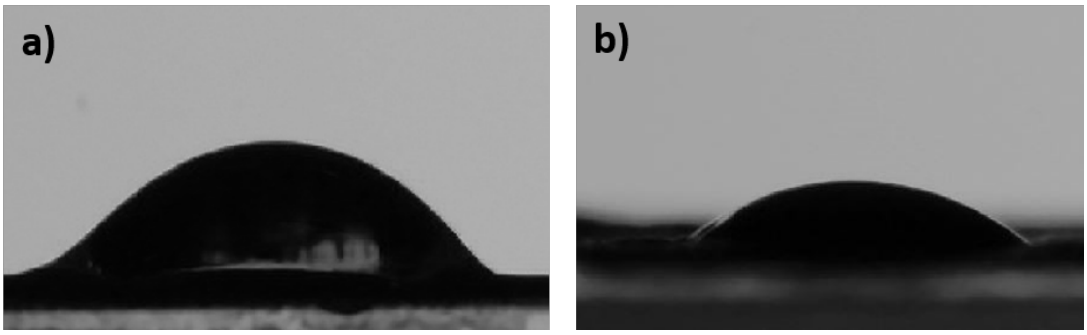

Figure 4.14: Water contact angle measurements for a) RC-DMF 50.0 ° and b) RC-Cyrene™/AA 35.3 °

The pure solvent permeances of the Cyrene™/AA support follows the order of: water> ethanol> acetone> toluene> DMF> n-hexane> chloroform> DCM. The pure solvent permeances of the DMF support follows the order of: water> ethanol > acetone> chloroform> toluene>DMF> DCM> n-hexane. With some exceptions, the order of the solvent filtration for both supports follows a similar pattern, however, the Cyrene™/AA support

experienced lower chloroform and DCM permeation compared to the DMF support. The lower permeance of the chlorinated solvents in the Cyrene™/AA support (7 L m^{-2} h^{-1} bar^{-1} and 5.6 L m^{-2} h^{-1} bar^{-1} for the DMF based support in chloroform) and the data from the solvent immersion tests (see Table 4.7) suggest that the support has lower stability in chlorinated environments. The Cyrene™/AA support could experience dissolution while the filtration is taking place resulting in low permeances. However, additional work would be required to investigate this further.

Water had the highest permeance among all the solvents in the two supports (RC-Cyrene™/AA support: 25.4 L m^{-2} h^{-1} bar^{-1} and RC-DMF: 11.2 L m^{-2} h^{-1} bar^{-1}) due to the small molecular volume, size, and viscosity, allowing for low transport resistance when crossing the membrane pores [42], [43]. The permeance of n-hexane and toluene, which are two non-polar solvents, suggests that the two supports are stable in both polar and non-polar solvents with a range of molecular weights and viscosities [42], [43].

Solvent-membrane interaction plays an important factor in determining the solvent permeances in the membrane system. To further investigate the permeation of solvents, the correlation between the solubility parameter $\delta_P MV_s^{-1}\eta_s^{-1}$ where δ_{PS} is the solvent's Hansen solubility parameter for the polarity of a solvent, MV_s is the solvent molar volume, and η_s is the solvent's dynamic viscosity was determined, (see Figure 4.15). The physical properties of these solvents are shown in Table 4.8. The permeance of solvents with varying polarity demonstrated a linear correlation with the solubility parameter, demonstrating that a solvent with higher polarity and smaller molecular volume results in higher permeance in both membranes.

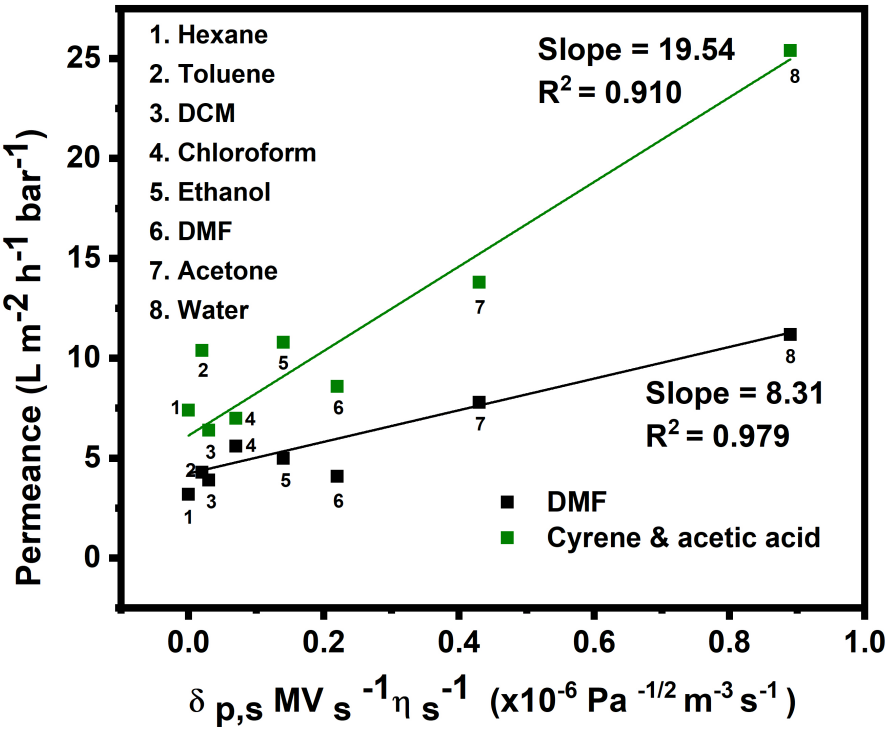

Figure 4.15: Pure solvent permeance as a function of solubility parameter in $\delta_P MV_s^{-1}\eta_s^{-1}$

Table 4.8: Physical properties of solvents used in the filtration experiments, and solvent permeances through the supports (values taken from [43])

Solvent	Viscosity η_s	Hansen solubility coefficient δ_{PS} $(MPa^{1/2})$	Molecular volume MV_s $(10^{-3}$ $nm^3)$	$\delta_P MV_s^{-1} \eta_s^{-1}$ $(10^6 Pa^{1/2} m^3 s^{-1})$	Permeance DMF support L m^{-2} h^{-1} bar^{-1}	Permeance Cyrene™& acetic acid support L m^{-2} h^{-1} bar^{-1}
Water	1	16	18	0.89	11.2	25.4
Ethanol	1.08	8.8	58.8	0.14	10.8	22.5
DMF	0.8	13.7	77	0.22	4.1	8.6
n-hexane	0.33	0	131.4	0	3.2	7.4
Acetone	0.32	10.4	75.1	0.43	7.8	13.8
Toluene	0.7	1.4	106.3	0.02	4.3	10.4
Cyrene	14.5	10.6	102.61	0.007	4.9	1.1
Chloroform	0.53	3.1	80.2	0.07	5.6	7

A long-term filtration test of both supports was undertaken, with DMF at room temperature with an operating pressure of 5 bar for 500 minutes, Figure 4.16 shows the stability of the support during this time. The drop in DMF permeance for the RC-Cyrene™/AA support from 8.2 L m^{-2} h^{-1} bar^{-1} to 7 L m^{-2} h^{-1} bar^{-1} can be attributed to the more porous support requiring a longer time to reach a steady state, once this had been reached at 7.5 L m^{-2} h^{-1} bar^{-1}, the flux was steady. Both supports experienced a drop in permeance of 0.5 L m^{-2} h^{-1} bar^{-1} over the 500 minutes. Figure 4.17 shows the RC-Cyrene™/AA support after filtration for 500 minutes. The support is intact, and no physical defects are experienced, indicating that the support can be used in harsh organic systems.

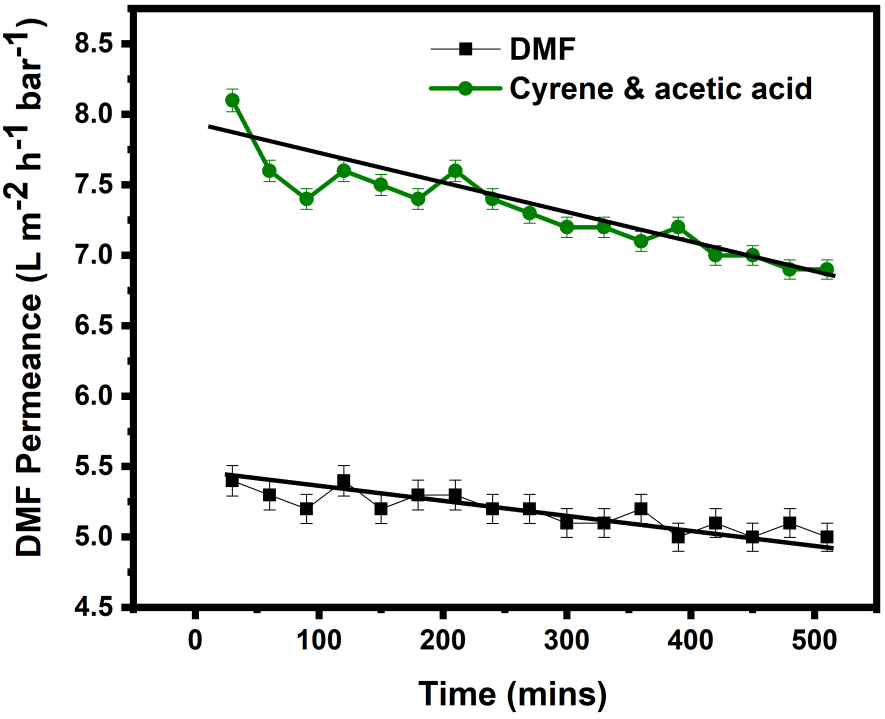

Figure 4.16: DMF permeance over 500 mins for RC-Cyrene™/AA (green) and RC-DMF (black)

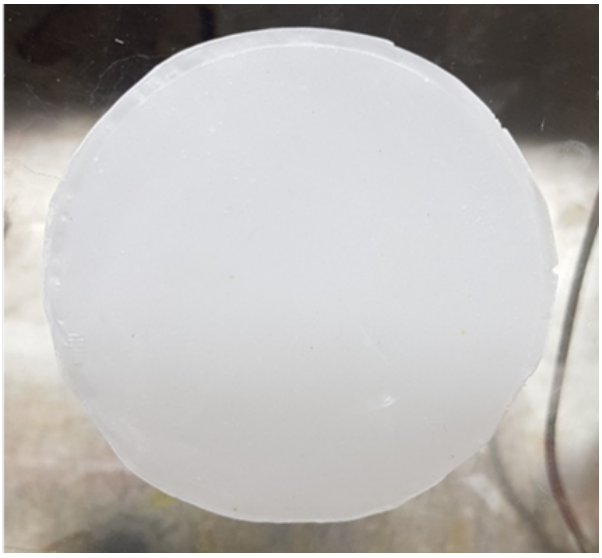

Figure 4.17: Visual aspect of the RC-Cyrene™/AA support after DMF filtration over 500 mins at room temperature with an operating pressure of 5 bar

4.10 Conclusion

The work carried out in this chapter successfully produced a support using several (third, fifth, sixth and seventh) principles of Green Chemistry. Cellulose acetate, a bio-polymer and a greener alternative to polyimide, the typical petroleum-derived polymer used for OSN, was used to produce supports. These supports underwent deacetylation to hydrolyse the acetate group to produce regenerated cellulose, which was stable in harsh organic solvents. The protocol used for the deacetylation method was quick (90 mins) and no harsh chemicals were required, and work was carried out at room temperature.

The study showed that Cyrene™, a bio-renewable solvent, can be used as an alternative for petroleum-derived DMF to successfully produce a support. The Cyrene™/AA supports exhibited excellent permeance of solvents, and a 115% increase was experienced for water permeation compared to RC-DMF (RC-Cyrene™/AA support: 25.4 L m^{-2} h^{-1} bar^{-1} and RC-DMF: 11.2 L m^{-2} h^{-1} bar^{-1}. The excellent solvent permeation in the RC-Cyrene™/AA

could be attributed to the MWCO of the support, as it was considerably higher at 10,500 g/mol compared to 590 g/mol for the RC-DMF support. Further to this, the green solvent system produced a more hydrophilic support, which further facilitated solvent permeance at 35.3 ° compared to 50.0 ° for the RC-DMF support. The RC-Cyrene™/AA support exhibited better thermal stability compared to RC-DMF at high temperatures. The benign deacetylation protocol produced supports that maintained structural integrity and excellent stability in DMF immersion at 100 °C, the supports were stable in harsh organic solvents and performed well in different solvent environments. Further to the performance of the support, the health and safety and environmental benefits of changing the solvents are also highly advantageous, as the hazards and risks associated with the use of Cyrene™ are lower compared to DMF.

The study also showed that changing petroleum-derived solvents for green alternatives is not a like-for-like swap, different parameters need to be optimised to achieve this. For example, a PI-Cyrene™ dope solution was not able to successfully produce a support for filtration applications whereas PI-NMP a commonly used polymer/solvent system was successful. Water is the most commonly used non-solvent for fabrication, however, was volatile for the PI-Cyrene™ system [15]. The fine-tuning of parameters can be advantageous as the design of fabrication, materials and methods can be reinvented to greener alternatives, changing the way membranes are fabricated. The RC-Cyrene™/AA support will be used in Chapter 5 as the foundation for a thin film composite membrane and will be explored for organic solvent filtration applications.

References

[1] R. A. Milescu, C. R. McElroy, T. J. Farmer, P. M. Williams, M. J. Walters, and J. H. Clark, "Fabrication of pes/pvp water filtration membranes using cyrene, a safer bio-based polar aprotic solvent," *Advances in Polymer Technology*, vol. 2019, 2019.

[2] T. Marino, F. Galiano, A. Molino, and A. Figoli, "New frontiers in sustainable membrane preparation: Cyrene as green bioderived solvent," *Journal of membrane science*, vol. 580, pp. 224–234, 2019.

[3] I. C. Adaka and P. F. Uzor, "Cyrene as a green solvent in the pharmaceutical industry," in *Green Sustainable Process for Chemical and Environmental Engineering and Science*, Elsevier, 2021, pp. 243–248.

[4] D. Prat, A. Wells, J. Hayler, *et al.*, "Chem21 selection guide of classical-and less classical-solvents," *Green Chemistry*, vol. 18, no. 1, pp. 288–296, 2015.

[5] P. Anastas and N. Eghbali, "Green chemistry: Principles and practice," *Chemical Society Reviews*, vol. 39, no. 1, pp. 301–312, 2010.

[6] H. J. Salavagione, J. Sherwood, V. Budarin, G. Ellis, J. Clark, P. Shuttleworth, *et al.*, "Identification of high performance solvents for the sustainable processing of graphene," *Green Chemistry*, vol. 19, no. 11, pp. 2550–2560, 2017.

[7] L. Mistry, K. Mapesa, T. W. Bousfield, and J. E. Camp, "Synthesis of ureas in the bio-alternative solvent cyrene," *Green Chemistry*, vol. 19, no. 9, pp. 2123–2128, 2017.

[8] J. Zhang, G. B. White, M. D. Ryan, A. J. Hunt, and M. J. Katz, "Dihydrolevoglucosenone (cyrene) as a green alternative to n, n-dimethylformamide (dmf) in mof synthesis," *ACS Sustainable Chemistry and Engineering*, vol. 4, no. 12, pp. 7186–7192, 2016.

[9] K. Pan, Y. Fan, T. Leng, *et al.*, "Sustainable production of highly conductive multilayer graphene ink for wireless connectivity and iot applications," *Nature communications*, vol. 9, no. 1, pp. 1–10, 2018.

[10] M. F. J. Solomon, Y. Bhole, and A. G. Livingston, "High flux membranes for organic solvent nanofiltration (osn)—interfacial polymerization with solvent activation," *Journal of membrane science*, vol. 423, pp. 371–382, 2012.

[11] M. F. J. Solomon, Y. Bhole, and A. G. Livingston, "High flux hydrophobic membranes for organic solvent nanofiltration (osn)—interfacial polymerization, surface modification and solvent activation," *Journal of membrane science*, vol. 434, pp. 193–203, 2013.

[12] K. Vanherck, A. Cano-Odena, G. Koeckelberghs, T. Dedroog, and I. Vankelecom, "A simplified diamine crosslinking method for pi nanofiltration membranes," *Journal of membrane science*, vol. 353, no. 1-2, pp. 135–143, 2010.

[13] Y. Thiermeyer, S. Blumenschein, and M. Skiborowski, "Fundamental insights into the rejection behavior of polyimide-based osn membranes," *Separation and Purification Technology*, vol. 265, p. 118 492, 2021.

[14] Y. C. Xu, Y. P. Tang, L. F. Liu, Z. H. Guo, and L. Shao, "Nanocomposite organic solvent nanofiltration membranes by a highly-efficient mussel-inspired co-deposition strategy," *Journal of Membrane Science*, vol. 526, pp. 32–42, 2017.

[15] R. W. Baker, *Membrane technology and applications*. John Wiley and Sons, 2012.

[16] S. Li, C. Li, X. Song, *et al.*, "Graphene quantum dots-doped thin film nanocomposite polyimide membranes with enhanced solvent resistance for solvent-resistant nanofiltration," *ACS applied materials and interfaces*, vol. 11, no. 6, pp. 6527–6540, 2019.

[17] A. K. Holda and I. F. Vankelecom, "Understanding and guiding the phase inversion process for synthesis of solvent resistant nanofiltration membranes," *Journal of Applied Polymer Science*, vol. 132, no. 27, 2015.

[18] A. K. Holda, B. Aernouts, W. Saeys, and I. F. Vankelecom, "Study of polymer concentration and evaporation time as phase inversion parameters for polysulfone-based srnf membranes," *Journal of membrane science*, vol. 442, pp. 196–205, 2013.

[19] M. A. Rasool, C. Van Goethem, and I. F. Vankelecom, "Green preparation process using methyl lactate for cellulose-acetate-based nanofiltration membranes," *Separation and Purification Technology*, vol. 232, p. 115 903, 2020.

[20] J. Caloca, L. Z. Flores-Lopez, H. Espinoza-Gomez, E. L. Sotelo-Barrera, A. Nunez-Rivera, and R. D. Cadena-Nava, "Silver nanoparticles supported on polyethylene glycol/cellulose acetate ultrafiltration membranes: Preparation and characterization of composite," *Cellulose*, vol. 24, no. 11, pp. 4997–5012, 2017.

[21] H. Kaur, V. K. Bulasara, and R. K. Gupta, "Influence of ph and temperature of dip-coating solution on the properties of cellulose acetate-ceramic composite membrane for ultrafiltration," *Carbohydrate polymers*, vol. 195, pp. 613–621, 2018.

[22] B. Tarus, N. Fadel, A. Al-Oufy, and M. El-Messiry, "Effect of polymer concentration on the morphology and mechanical characteristics of electrospun cellulose acetate and poly (vinyl chloride) nanofiber mats," *Alexandria Engineering Journal*, vol. 55, no. 3, pp. 2975–2984, 2016.

[23] H. Idress, S. Zaidi, A. Sabir, *et al.*, "Cellulose acetate based complexation-nf membranes for the removal of pb (ii) from waste water," *Scientific Reports*, vol. 11, no. 1, pp. 1–14, 2021.

[24] M. A. Rasool, P. P. Pescarmona, and I. F. Vankelecom, "Applicability of organic carbonates as green solvents for membrane preparation," *ACS Sustainable Chemistry and Engineering*, vol. 7, no. 16, pp. 13 774–13 785, 2019.

[25] M. A. Rasool and I. F. Vankelecom, "Preparation of full-bio-based nanofiltration membranes," *Journal of Membrane Science*, vol. 618, p. 118 674, 2021.

[26] M. A. Rasool and I. Vankelecom, "Use of γ-valerolactone and glycerol derivatives as bio-based renewable solvents for membrane preparation," *Green chemistry*, vol. 21, no. 5, pp. 1054–1064, 2019.

[27] M. I. Kim and Y.-S. Lee, "Deacetylation of cellulose acetate nanofibers by fluorination for carbon nanofibers," *Materials Letters*, vol. 181, pp. 236–239, 2016.

[28] N. Olaru and L. Olaru, "Cellulose acetate deacetylation in benzene/acetic acid/water systems," *Journal of applied polymer science*, vol. 94, no. 5, pp. 1965–1968, 2004.

[29] F. Ahmed, A. A. Arbab, A. W. Jatoi, *et al.*, "Ultrasonic-assisted deacetylation of cellulose acetate nanofibers: A rapid method to produce cellulose nanofibers," *Ultrasonics sonochemistry*, vol. 36, pp. 319–325, 2017.

[30] X. He, "Optimization of deacetylation process for regenerated cellulose hollow fiber membranes," *International Journal of Polymer Science*, vol. 2017, 2017.

[31] W. K. Son, J. H. Youk, T. S. Lee, and W. H. Park, "Electrospinning of ultrafine cellulose acetate fibers: Studies of a new solvent system and deacetylation of ultrafine cellulose acetate fibers," *Journal of Polymer Science Part B: Polymer Physics*, vol. 42, no. 1, pp. 5–11, 2004.

[32] A. Wittmar, D. Vorat, and M. Ulbricht, "Two step and one step preparation of porous nanocomposite cellulose membranes doped with tio 2," *RSC advances*, vol. 5, no. 107, pp. 88 070–88 078, 2015.

[33] B. Caballero, L. C. Trugo, and P. M. Finglas, *Encyclopedia of food sciences and nutrition*. Academic, 2003.

[34] M. Paul and S. D. Jons, "Chemistry and fabrication of polymeric nanofiltration membranes: A review," *Polymer*, vol. 103, pp. 417–456, 2016.

[35] G. Szekely, M. F. Jimenez-Solomon, P. Marchetti, J. F. Kim, and A. G. Livingston, "Sustainability assessment of organic solvent nanofiltration: From fabrication to application," *Green Chemistry*, vol. 16, no. 10, pp. 4440–4473, 2014.

[36] R. Candido, G. Godoy, and A. R. Goncalves, "Characterization and application of cellulose acetate synthesized from sugarcane bagasse," *Carbohydrate polymers*, vol. 167, pp. 280–289, 2017.

[37] H. Kamal, F. Abd-Elrahim, and S. Lotfy, "Characterization and some properties of cellulose acetate-co-polyethylene oxide blends prepared by the use of gamma irradiation," *Journal of Radiation Research and Applied Sciences*, vol. 7, no. 2, pp. 146–153, 2014.

[38] G. F. Leal, L. A. Ramos, D. H. Barrett, A. A. S. Curvelo, and C. B. Rodella, "A thermogravimetric analysis (tga) method to determine the catalytic conversion of cellulose from carbon-supported hydrogenolysis process," *Thermochimica Acta*, vol. 616, pp. 9–13, 2015.

[39] K. Odelius, A. Höglund, S. Kumar, *et al.*, "Porosity and pore size regulate the degradation product profile of polylactide," *Biomacromolecules*, vol. 12, no. 4, pp. 1250–1258, 2011.

[40] R. J. Petersen, "Composite reverse osmosis and nanofiltration membranes," *Journal of membrane science*, vol. 83, no. 1, pp. 81–150, 1993.

[41] Y. C. Xu, X. Q. Cheng, J. Long, and L. Shao, "A novel monoamine modification strategy toward high-performance organic solvent nanofiltration (osn) membrane for sustainable molecular separations," *Journal of Membrane Science*, vol. 497, pp. 77–89, 2016.

[42] T.-D. Lu, L.-L. Zhao, W. F. Yong, Q. Wang, L. Duan, and S.-P. Sun, "Highly solvent-durable thin-film molecular sieve membranes with insoluble polyimide nanofibrous substrate," *Chemical Engineering Journal*, vol. 409, p. 128 206, 2021.

[43] S.-H. Park, A. Alammar, Z. Fulop, B. A. Pulido, S. P. Nunes, and G. Szekely, "Hydrophobic thin film composite nanofiltration membranes derived solely from sustainable sources," *Green Chemistry*, 2021.

Chapter 5

Thin film composite membranes fabricated using bio-renewable solvents for applications in organic solvent nanofiltration

Interfacial polymerization (IP) is a technique extensively utilised in the polymer production industry to manufacture polymers such as polyamide with unique topological and chemical properties [1]. Polyamide is the selective layer that is commonly employed for the fabrication of thin film composite membranes [2]. Key for IP is the interface between two immiscible solvents – water and an organic solvent that is typically a hydrocarbon such as hexane, cyclohexane or heptane [3]–[5]. Monomers that are only soluble in each phase diffuse towards the interface and polymerise in this region of significant chemical potential difference to form a polyamide film with a thickness of a few tens of nanometres [6].

The use of hazardous and reprotoxic solvents during IP is no longer a viable option for polymer synthesis as these solvents not only carry great health and safety risks but also are a major generator of toxic waste in chemical processes [7]. Recent legislation directives have driven the development of biomass-derived solvents as direct replacements for traditional petroleum-based organic solvents in industrial processes, underpinning the seventh principle of Green Chemistry [7], [8]. As mentioned earlier, the immiscibility with water of the organic solvent is a prerequisite for IP which reduces the number of possible solvents that could be utilised. The exploration of alternative green solvents has been conducted extensively with ionic liquids. Ionic liquids are a class of solvents that are categorised as green solvents due to the low vapour pressure they experience [9]. The successful use of ionic liquids has been widely reported for the use as the organic phase in interfacial polymerisation [6], [9]–[13]. Further to this, the use of bio-renewable solvents such as oleic acid [14] and deconoic acid [15] have also been reported as solvents for interfacial polymerisation.

Recently, 2-methyltetrahydrofuran (2-MeTHF) a bio-renewable solvent produced from agricultural waste and corncobs has arisen as an alternative for tetrahydrofuran (THF) in organometallic chemistry and biocatalysis [16], [17]. The use of this solvent has also been explored as the replacement for n-hexane for the extraction of carotenoids and aromas, and the properties of the two solvents are listed in Table 5.1 [16], [17]. Due to the immiscibility

of 2-MeTHF in water, the fabrication of polyamide was investigated using this solvent.

Table 5.1: Solvent physical properties for n-hexane and 2-MeTHF

Properties	n-hexane	2-MeTHF
Colour	Colourless	Colourless
Molecular weight (g/mol)	86.18	86.13
Formula	$C_6\ H_{14}$	$C_5\ H_{10}\ O$
Boiling point (°C)	69	80
Density (kg/m^3)	655	854
Water miscibility	low	low
CHEM21 ranking	Hazardous (Red)	Problematic (Yellow)
Hazard Statement	H225 - Flammable liquids H315 - Skin irritation H361f - Reproductive toxicity H336 - Specific target organ toxicity - single exposure central nervous system	H225 - Flammable liquids H302 - Acute toxicity, Oral H315- Skin irritation H318- Serious eye damage

The characteristics of the organic solvent, employed in interfacial polymerisation, is one of the most important factors affecting the polymer film [3]. The organic solution contains organic soluble monomers which forms an interface with the water phase, in which water-soluble monomers are dissolved. The reaction zone for polyamide formation is located in the organic phase due to the low solubility of TMC in water [6], [18]. As a result of this, the solubility of the polymers being polymerised into the organic solution is important - the higher the solubility, the higher the molecular weight [6]. Further to

this, the degree of crosslinking and thickness of the resultant film are all influenced by the organic solvent [3]. A good solvent for IP will improve the polymerisation efficiency for the formation of the PA films, whilst increasing the degree of crosslinking and thickness [3].

This chapter is split into two sections, firstly, two polyamides were fabricated, one from the conventionally used solvent n-hexane and one from 2-MeTHF, the bio-renewable alternative solvent. The two polymers were characterised using different methods to investigate the effect 2-MeTHF had on the resultant polymer film. In the second part of this chapter, the two polymer films were deployed as a selective layer to produce a TFC membrane using the support fabricated in Chapter 4. A comparison study was carried out using the two films, to investigate the performance of the two TFC membranes. Using the protocols already established in Chapter 4, the addition of the PA(2-MeTHF) selective layer to the RC-Cyrene™/AA support produced a TFC membrane solely through the use of bio-renewable solvents and using the third, fifth and seventh principles of Green Chemistry. The TFC membrane was tested for organic solvent nanofiltration applications, with dyes of different charges and molecular weights in ethanol was used as a feed solution.

5.1 Alternative fabrication of polyamide through interfacial polymerisation

5.1.1 Polymerisation kinetics

The organic phase containing the two organic solvents with different concentrations of trimesoyl chloride (TMC) was introduced to the aqueous phase containing piperazine (PIP). The polymerisation kinetics for the two polyamides fabricated in 2-MeTHF and n-hexane were comparable, regardless of the solvent deployed in the organic phase, polyamide was formed instantly upon contact with the aqueous PIP solutions. Higher concentrations

of TMC were required when using 2-MeTHF as the organic phase to form a polymer compared to when using the n-hexane solution - at low concentrations of 0.5 wt.% TMC, no polymer was formed, see Figure 5.1.

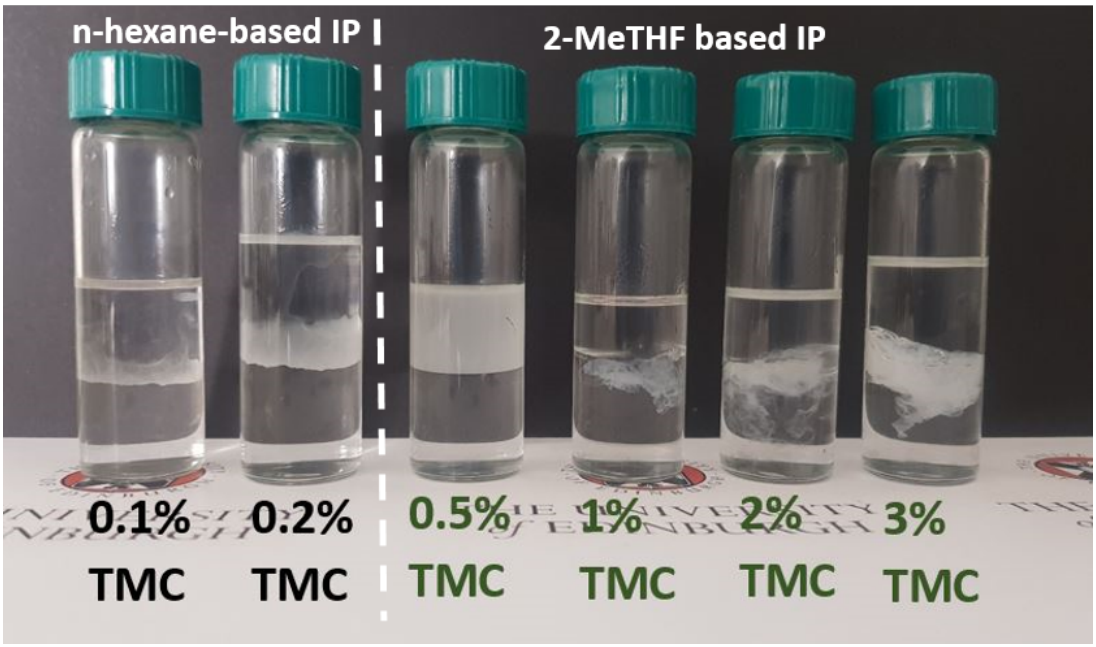

Figure 5.1: Thin PA films formed between the interface of n-hexane and water (black) and 2-MeTHF and water (green). The aqueous phase contained 2 wt.% PIP

Figure 5.1 shows the visual representation of the reaction between the polyamide produced with the two solvents. The PA(n-hexane) was produced as a film; a thin layer of the polyamide was produced in the vials, and at a higher TMC concentration (0.2 wt.%) the film was more prominent. A clear distinction between the two phases was visible, and the remnants of the film were in the organic phase, suggesting that the reaction took part in the organic phase [3]. In comparison to this, the polyamide produced with 2-MeTHF was of a bubble configuration and regardless of the TMC concentration used, a thin film was not formed. The remnants of PA(2-MeTHF) were in the aqueous phase rather than the organic phase, possibly suggesting that the reaction took place in the aqueous phase, opposite to what was experienced with the PA(n-hexane) film.

The yields of the two different polymers were vastly different, the percentage yield of

PA(n-hexane) was 87.5 %, approximately 22x more than the yield of the PA(2-MeTHF) polyamide at 3.9 %. The percentage yield of the polymers was calculated through weight measurements of the reactants and the resultant polymer. The thin-film structure in n-hexane allowed for a greater yield compared to the microspheres filled with solvent, which were produced via 2-MeTHF. Upon drying, the thin film was able to retain the shape, however, the polyamide produced from 2-MeTHF shrivelled and compacted resulting in lower yields.

5.1.2 Structure of polyamide films

The FTIR spectrum of semi-aromatic polyamide typically contains the characteristic Amide I peak, which is centered at 1630 cm^{-1} [19]. This characteristic peak was observed in the FTIR spectra of both PA(n-hexane) and PA(2-MeTHF) films, as well as a broad O-H band at 3200 – 3600 cm^{-1} that could be ascribed to the presence of carboxylic acid groups demonstrating that polyamide had been formed. The spectrum can be seen in Figure 5.2.

The Amide I band peak (at 1630 cm^{-1}) of the PA(2-MeTHF) film was less intense than that of PA(n-hexane) film and this could be attributed to the incomplete reactions between hydrolysed acyl chlorides in TMC and secondary amines of PIP [20]. The hydrolysis of TMC to trimesic acid in the presence of water yields COOH functional groups that cannot further react with amines in PIP [20]. This was shown in the spectra as a strong peak at 1750 cm^{-1} which can be ascribed to the C=O stretching of carboxylic acid groups which was not present in the PA(n-hexane) film. The absence of this peak in the PA(n-hexane) spectra indicates that the reaction between PIP and TMC completed forming PA(n-hexane) and that the PA(2-MeTHF) film had a greater amount of COOH functional groups present than the PA(n-hexane) film.

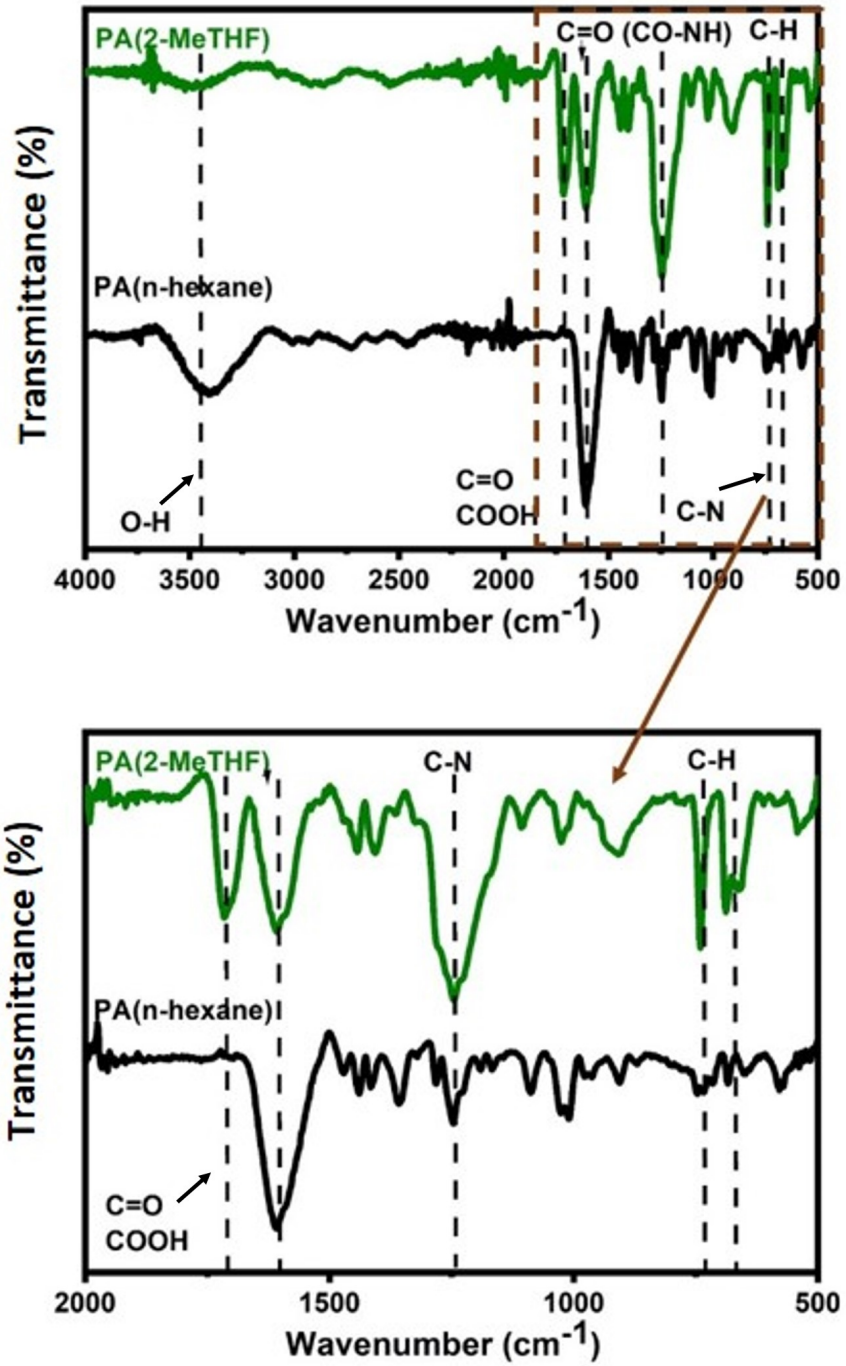

Figure 5.2: FTIR analyses of PA films produced from IP using n-hexane (black) and 2-MeTHF (green) as the organic solvent

In the FTIR spectrum of PA(2-MeTHF), Figure 5.2, it was observed that the intensity of peaks between 600 – 750 cm^{-1} which were ascribed to alkyl halides C-Cl and at 1250 cm^{-1} which were ascribed to C-N group of PIP was significantly stronger [21], [22]. The intensification of these peaks (600 – 750 cm^{-1}, 1250 cm^{-1} and 1750 cm^{-1}) corresponded to a decrease in the intensity of the Amide I band peak (1630 cm^{-1}) suggesting that less PA is formed. The amount of TMC that was used to produce PA(2-MeTHF) was 2 w/v%. twenty-fold more than the amount of TMC used to fabricate PA(n-hexane) at 0.1 w/v%. This TMC concentration for the PA(2-MeTHF) is also higher than those reported in literature and despite the higher quantities of TMC, the resultant PA(2-MeTHF) film produced less polyamide [23]–[27].

The additional COOH functional groups present in PA(2-MeTHF) were further validated with XPS analysis, see Figure 5.3 for the spectra. The O/N ratio of PA is a good indicator of the crosslinking degree of the polymer, where O/N = 1 correlates to a fully cross-linked PA where O atoms are bonded to N atoms within CONH (amide) groups [19]. Polyamide where O/N = 2 is typically a linear polymer with additional O atoms ascribing to free carboxylic acid groups [19], [28]. The O/N ratio of PA(n-hexane) was 1.07 – close to a fully cross-linked polymer, while the O/N ratio of PA(2-MeTHF) was 1.43 – indicative of PA with more COOH groups. The elemental composition of the two films can be seen in Table 5.2. The full deconvoluted spectra of the XPS analysis can be found in Appendix A.

XPS analysis also indicated that there was 80 % more Cl in PA(2-MeTHF) film than PA(n-hexane), see Table 5.2 for the elemental composition of the two polymer films. An increased Cl content was also present in the FTIR spectra for the PA(2-MeTHF) film, as the peaks were of a greater intensity compared to the PA(n-hexane) film (Figure 5.2). The higher Cl content in PA(2-MeTHF) film could be attributed to the reversible chlorine substitution of unreacted PIP amines [23]. In addition to this, hydrochloric acid (HCl) is a by-product of the reaction between amines and TMC during interfacial polymerisation, the additional chlorine present in the polymer could be attributed to HCl being encapsulated

in the film [23], [24].

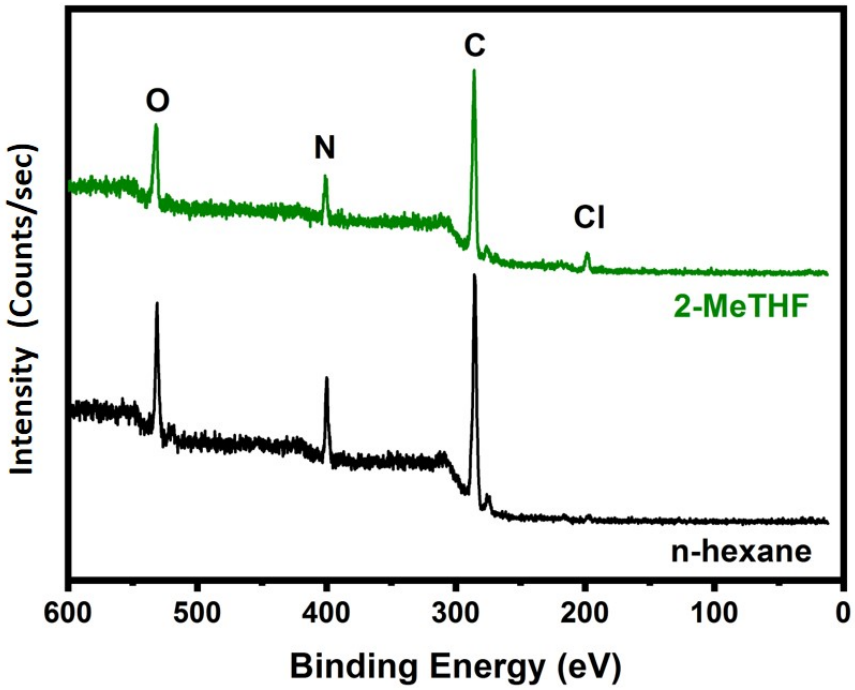

Figure 5.3: XPS analyses of PA films produced from IP using n-hexane (black) and 2-MeTHF (green) as the organic solvent

Table 5.2: Elemental composition of PA films produced using n-hexane and 2-MeTHF as the organic solvent during IP.

Solvent used in PA synthesis	C 1s %	O 1s %	N 1s %	Cl 2p %	O/N ratio
n-hexane	75.2	12.5	11.7	0.58	1.07
2 - MeTHF	75.2	12.9	8.9	2.83	1.43

The difference in crosslinking degree in the PA films as a function of solvent type was further validated using gas adsorption analysis. Crosslinking typically induces microporosity in polymers and the Brunauer-Emmett-Teller specific surface areas of PA samples produced using n-hexane and 2-MeTHF were 325 m^2 g^{-1} and 10 m^2 g^{-1}, respectively, see Figure 5.4. The lower BET surface area of the PA(2-MeTHF) is indicative of a lower crosslinking

degree in the polymer, which further corroborated the O/N ratio data obtained via XPS analysis.

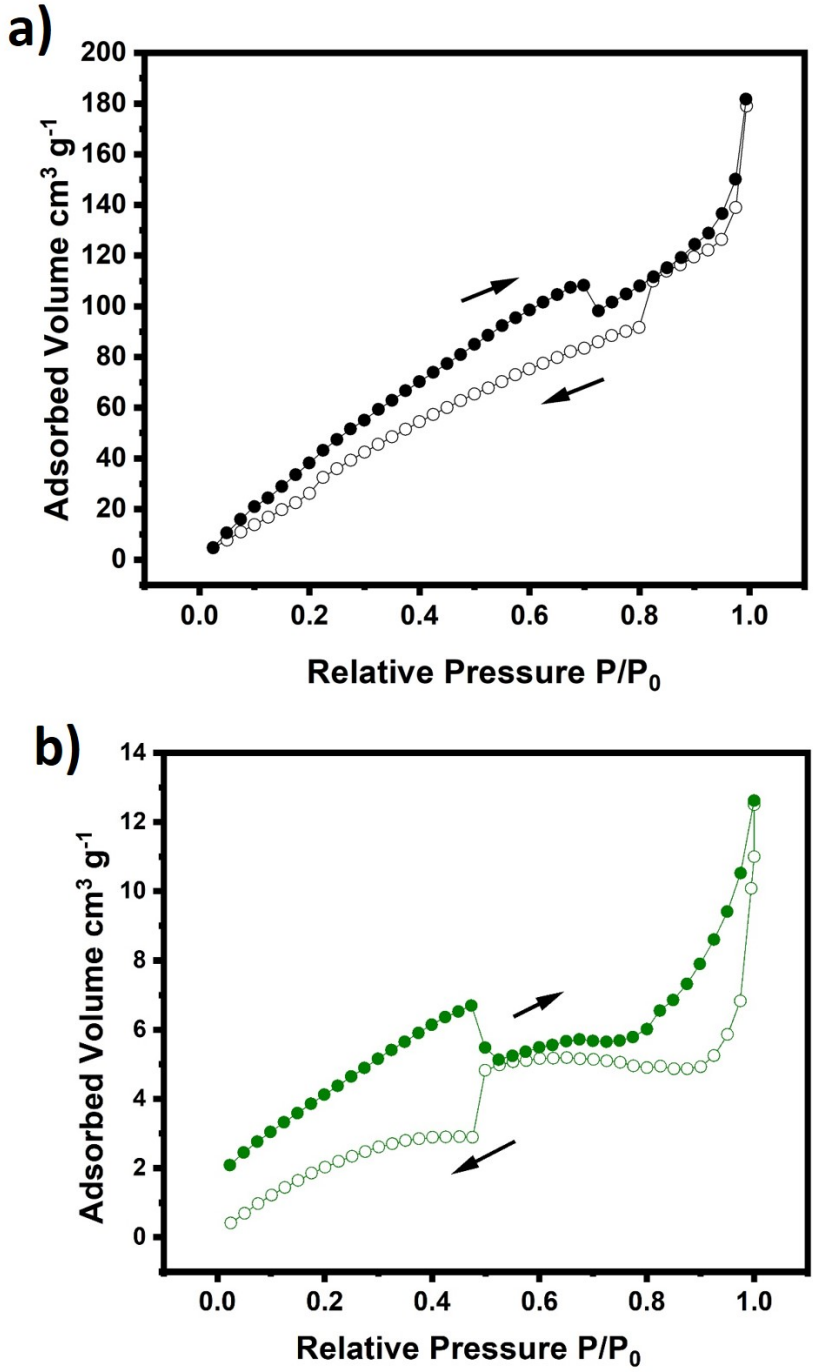

Figure 5.4: N_2 sorption isotherms at 77 K of a) polyamide produced with n-hexane (surface area: 325 m^2 g^{-1}) b) polyamide produced with 2-MeTHF (surface area: 10 m^2 g^{-1})

The morphology of the two polymer films was investigated to see if the structure of the two polyamides changed when the organic solvent changed during fabrication. It can be seen in Figure 5.5 that the structure and the pore size of the two polymers is comparable, and no physical changes have taken place.

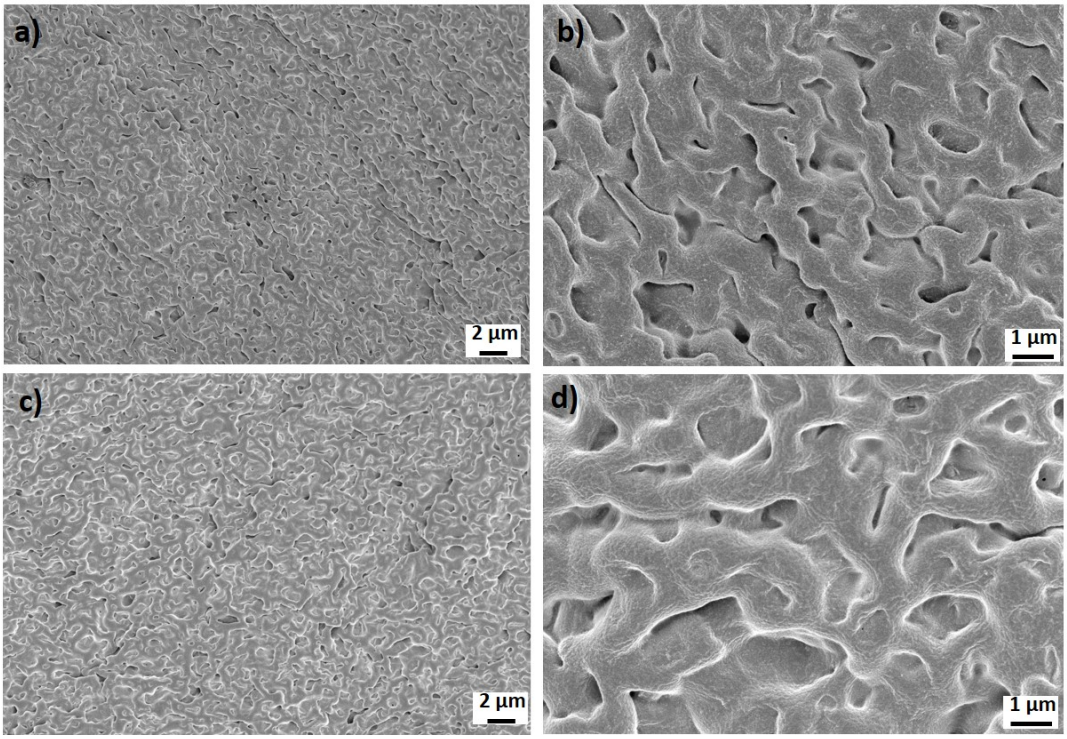

Figure 5.5: SEM images of the polyamide selective layers produced using n-hexane (a and b) and 2-MeTHF (c and d) as the organic phase

The structure of the polyamide film produced through the use of 2-MeTHF was elucidated with solid state ^{13}C NMR spectroscopy,(see Figure 5.6 for the spectra). The ^{13}C NMR depicts five signals that correspond to the expected carbons of the polymer backbone [29]–[32]. There are peaks at δ169.2 ppm (a) representing the carbonyl carbon of acids, δ131-136 ppm (b,c) representing the aromatic carbon as well as CH at 42- 62 ppm covalently bound to nitrogen as indicated by d', e, f. The d' peak in PA(2-MeTHF) suggested that there was more CHN present compared to PA(n-hexane), which was also seen in the FTIR spectra, Figure 5.2 [29], [31].

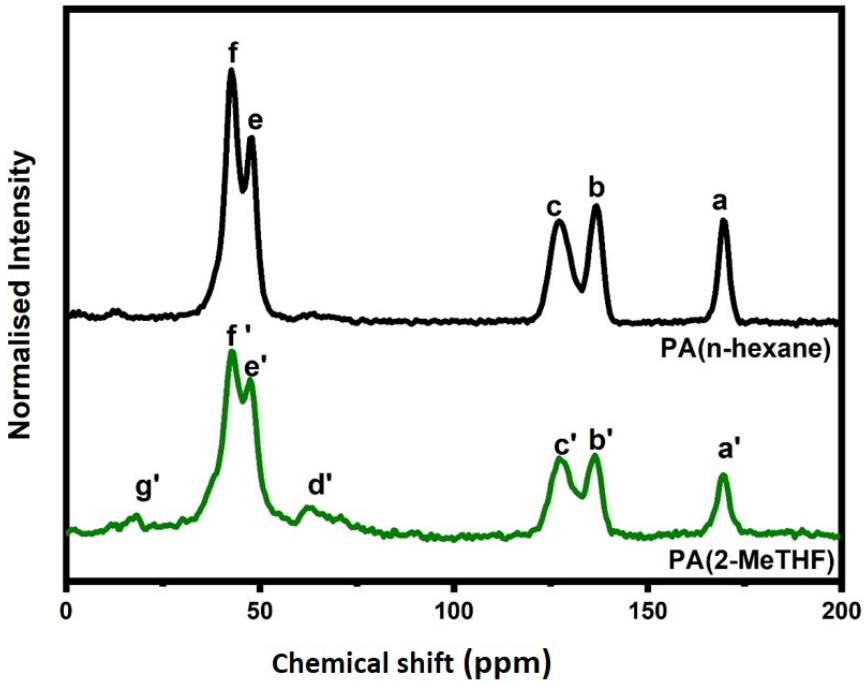

Figure 5.6: ^{13}C NMR spectra of PA(2-MeTHF) and PA(n-hexane)

From the different characterisation techniques carried out, the proposed structure of the two polyamide films are shown in Figure 5.7. XPS and FTIR analyses indicated that PA samples fabricated using the bio-renewable solvent 2-MeTHF had a higher amount of chlorine present in the polymer. This increase in chlorine content could be attributed to the unreacted acyl chlorides and this is represented in the scheme with a COCl group present. The PA(2-MeTHF) had a greater amount of the repeating unit Z present in the polymer compared to the PA(n-hexane).

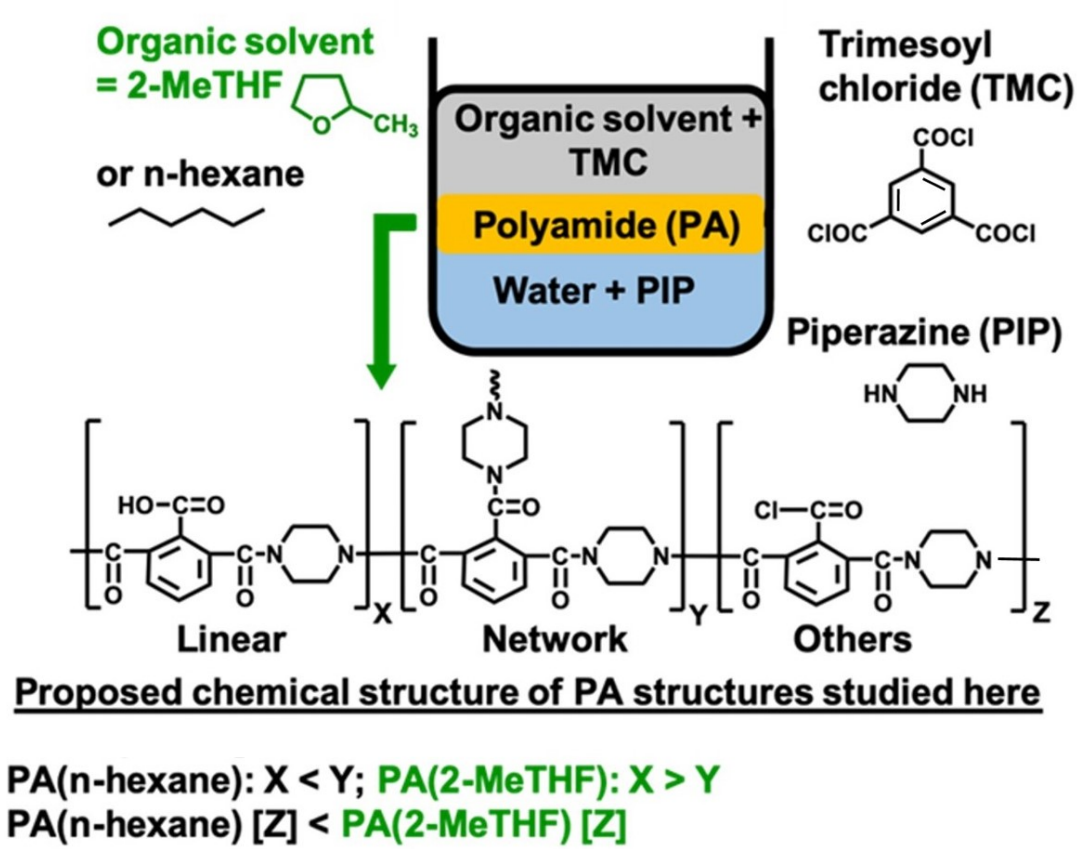

Figure 5.7: The proposed chemical structure of the semi-aromatic PA fabricated from PIP and TMC using n-hexane and 2-MeTHF

5.1.3 Thermal and chemical stability of PA films

Thermogravimetric analysis was performed on the two polyamide films produced from the two solvents, to investigate how a change of solvent during fabrication affects the material's thermal stability, (see Figure 5.8). In both the traditionally synthesised and green polyamide, polymer decomposition occurred at different temperature ranges, undergoing a two-step mass loss at (a) 100 - 200°C and (b) 400 - 600°C. The initial mass loss for the two polymers was due to the removal of water and excess organic materials present from the polymerisation reaction. The mass loss between 400 - 600°C was ascribed to the decomposition of the polymer backbone [33].

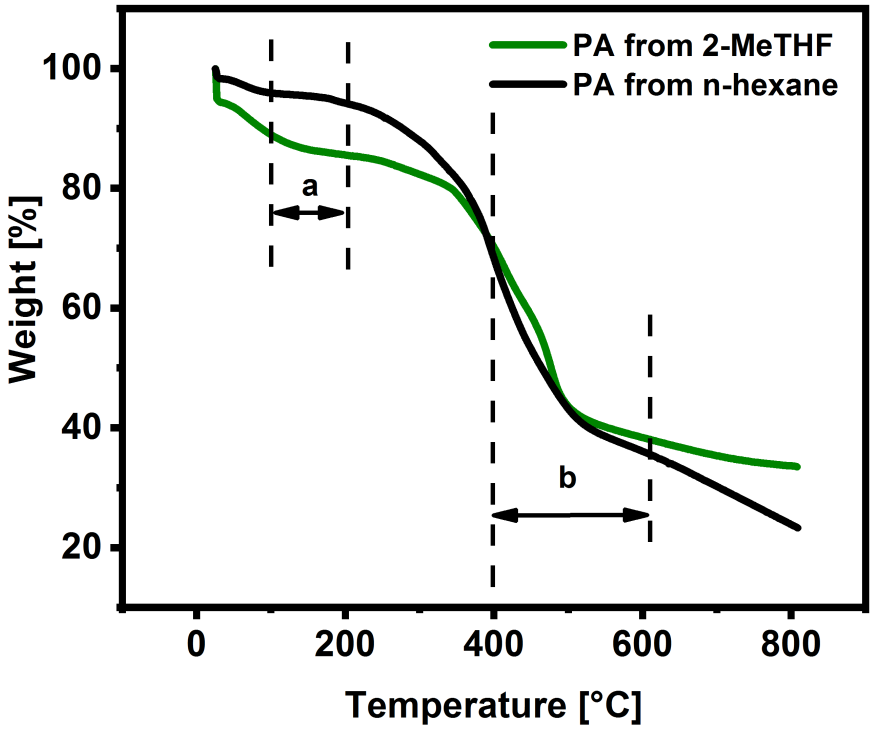

Figure 5.8: TGA curves of the two polyamide polymers produced from n-hexane (black) and 2-MeTHF (green). The polymers were heated from RT to 800 °C at a rate of 10 °C min^{-1} under a flow of nitrogen (flow of 100 mL/min).

The PA film produced via 2-MeTHF decomposed at a higher rate than the PA(n-hexane) polymer up until 200 °C. This can be ascribed to the cross-linking of the two polymers, XPS and the BET analysis indicated that the PA(2-MeTHF) polymer was less cross-linked than the PA(n-hexane) and had a looser structure. The total weight loss for the PA(2-MeTHF) between 0 -200 °C was 73 % compared to 97 % for the PA(n-hexane). The structure of the PA(2-MeTHF) had more alkyl halides, C-Cl present, which was found in the FTIR spectra see Figure 5.2 and XPS analysis in Table 5.2 in Section 5.2.1. The alkyl halide, C-Cl bonds decomposed at around 170 °C, and this decay accounts for the higher weight loss that was experienced in the PA(2-MeTHF) film [34].

At 400 - 500°C the polymer backbone decomposed and at 500 °C and carbonisation of the PA(2-MeTHF) polymer began. The weight loss of the PA(2-MeTHF) film surpassed the PA(n-hexane) film and became more stable. At 600 °C the decomposition plateaued indicating complete carbonisation of the polymer and the final weight loss of the polymer film was 55 %. The looser structure of the PA(2-MeTHF) polymer decomposed at a higher rate than the PA(n-hexane), and at 800 °C the PA(n-hexane) started to carbonise but did not reach complete carbonisation. The decomposition of the PA(n-hexane) is indicative of a more cross-linked network structure in the polymer as it was able to withstand high temperatures [33].

Interfacial polymerisation typically produces network polymers that do not dissolve in most organic solvents, as they experience a high degree of interchain hydrogen bonding and exhibit great crosslinking [35], [36]. The solubility of the polyamide films synthesised using both n-hexane and 2-MeTHF with harsh polar aprotic solvents DMF and THF was investigated by immersing the films into the solvents for 24 hours, see Figure 5.9 for the results.

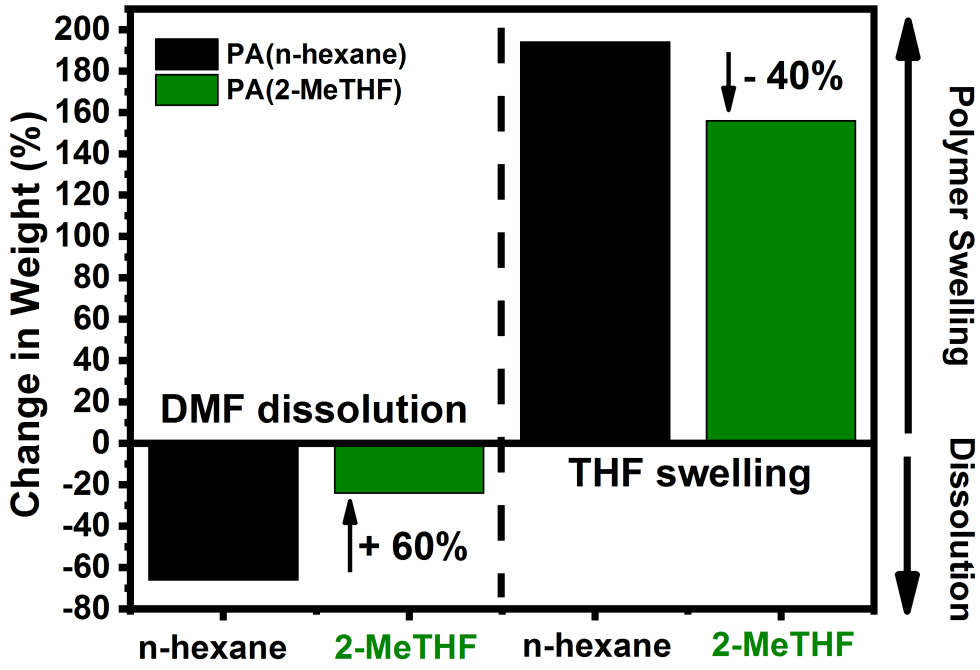

Figure 5.9: The solubility and swelling of PA(n-hexane) (black) and PA(2-MeTHF) (green) in DMF and THF, respectively.

The PA(2-MeTHF) films displayed enhanced chemical resistance at room temperature as only 20 % of PA(2-MeTHF) dissolved in DMF, three times less compared to PA(n-hexane). From the XPS and BET characterisation carried out, (Figure 5.3 and 5.4 and Table 5.2 in Section 5.2.1) it was concluded that the PA(n-hexane) experienced greater microporosity and cross-linking in the structure compared to the PA(2-MeTHF) as the O/N ratio was higher in the former film. From the cross-linking results obtained through the different characterisation techniques, it was expected that the PA(n-hexane) film would experience less dissolution in DMF compared to PA(2-MeTHF), however, this was not experienced.

After immersion in DMF, PA(n-hexane) had a thin film configuration similar to prior to immersion and the structure of the film was the same, no visible difference could be seen.

However, after immersion in DMF, the structure of the PA(2-MeTHF) polymer changed, prior to immersion the structure was soft, flat and light. After immersion, the structure was rigid and brittle and would break when touched with a spatula. Further to this, the weight of the structure increased and the weight of the polymers before and after DMF immersion is given in Table 5.3 and Figure 5.10 shows the difference in structure between the PA(2-MeTHF) films. The change in the structure of the PA(2-MeTHF) suggested that the structure was more cross-linked as a change had taken place as the rigidity increased. This could possibly be due to the leaching of unreacted monomers and small molecular weight polymers in the polymer into the solvent which would increase the weight of the PA(2-MeTHF) film.

Table 5.3: Weight loss for PA(n-hexane) and PA(2-MeTHF) when immersed in DMF and THF for 24 hours at room temperature to test the polymers for solvent resistance.

	PA(n-hexane)			PA(2-MeTHF)		
	Initial weight (g)	Final weight (g)	Weight change (%)	Initial weight (g)	Final weight (g)	Weight change(%)
DMF	0.009	0.007	-66	0.0042	0.0045	-20
THF	0.007	0.011	+160	0.0044	0.008	+160

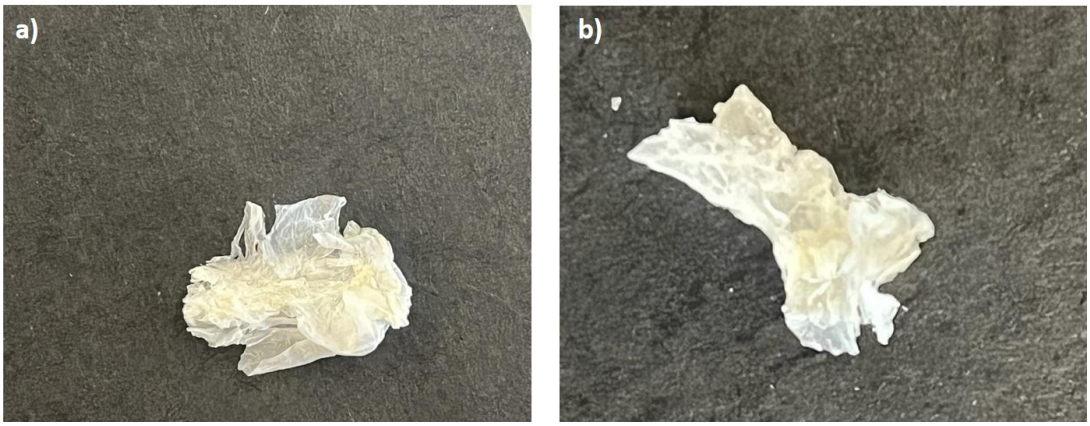

Figure 5.10: The structural change in the PA(2-MeTHF) polymer a) before and b) after DMF immersion

XPS analysis was carried out on the two polyamide films after DMF immersion to investigate the results. The O/N ratio of the two polymers had changed, and the O/N ratio before and after DMF immersion are given in Table 5.4. The O/N ratio for the PA(n-hexane) increased from 1.07 to 1.10 indicating a less cross-linked structure was produced after DMF immersion as the structure had undergone dissolution in the solvent [19]. However, the PA(2-MeTHF) experienced a decrease in the O/N ratio from 1.43 to 1.33 indicating that the polymer became more cross-linked after DMF immersion and was able to retain the structure better [19]. The increase in cross-linking could possibly be ascribed to the pendant COOH group in the structure of the PA(2-MeTHF), which formed a hydrogen bond with DMF and strengthened the PA(2-MeTHF) film [37]. However, as the ratio of the PA(2-MeTHF) after DMF immersion is less than the PA(n-hexane) prior to DMF dissolution, it was expected that the polymer would dissolve more. Further analysis would be required to investigate this phenomenon in more depth.

Table 5.4: Elemental composition of PA films produced using n-hexane and 2-MeTHF as the organic solvent during IP before and after DMF immersion

Solvent used in PA synthesis	C 1s %	O 1s %	N 1s %	Cl 1p %	O/N ratio
PA(n-hexane) before immersion	75.2	12.5	11.7	0.6	1.1
PA(2-MeTHF) before immersion	75.2	12.9	8.9	2.8	1.4
PA(n-hexane) after immersion	71.4	14.2	12.8	1.7	1.1
PA(2-MeTHF) after immersion	70.6	16.1	11.9	1.3	1.3

The difference in rigidity of the PA samples was validated with THF. The swelling of PA(2-MeTHF) samples was more subtle, evidenced by a 40 % lower THF uptake than those of PA(n-hexane) films. The data for Figure 5.9 can be found in Table 5.3. The lower swelling in THF for the PA(2-MeTHF) could possibly be attributed to the leaching of

the unreacted monomers and small molecular weight polymers that are entrapped in the PA(2-MeTHF) into the THF solvent which decreases the swelling effect of this polymer in the solvent. Further analysis would be required to investigate this phenomenon in more depth.

In line with the fifth and seventh principles of Green Chemistry, the solvent for interfacial polymerisation was changed from n-hexane, a hazardous petroleum-derived solvent to a benign bio-renewable solvent, 2-MeTHF. Greater amounts of TMC were required to produce the PA(2-MeTHF) film, and despite the higher concentrations of TMC used in fabrication, lower yields were experienced with the PA(2-MeTHF) film compared to the PA(n-hexane) film at 3.9 % and 87.5 % respectively.

The PA(2-MeTHF) had more COOH groups in the structure, which arose from the hydrolysis of TMC to trimesic acid. This increased the number of COOH groups in the produced films that were less cross-linked in structure, as the O/N ratio which was determined through XPS analysis was 1.43 for the PA(2-MeTHF) film and 1.07 for the PA(n-hexane) film. This finding was in line with the microporosity results which were carried out using BET measurements, which were 10 m^2 g^{-1} and 325 m^2 g^{-1} respectively. From the different characterisation methods carried out, it can be concluded that n-hexane is a better solvent for polyamide synthesis compared to 2-MeTHF, as the yield and the crosslinking degree of the polymer were higher than the PA(2-MeTHF) film. However, despite the low crosslinking of the PA(2-MeTHF), the polymer exhibited promising results, with the polymer being able to retain the structure better in harsh organic systems. The increased COOH groups in the polymer could be advantageous for membrane fabrication, as membranes with additional COOH groups tend to be more hydrophilic and exhibit higher permeances [38]. The two films were then deposited onto the RC-Cyrene/AA support to produce a TFC membrane, where the nanofiltration capabilities of the PA(2-MeTHF) film were examined.

5.2 Molecular separation performance

5.2.1 Effect of the Interfacial polymerisation parameters on membrane performance

The optimum reagent concentrations were explored for the PA(2-MeTHF) to find a trade-off between rejection and permeability. The selective layer structure of polyamide TFC membranes is an important factor in determining the permeation and rejection characteristics [6]. In particular, the MWCO and permeation rate are dependent on the physical and chemical structure of the selective layer [3]. Different PIP concentrations, TMC concentrations and reaction times for interfacial polymerisation were tested, see Figure 5.11. The feed solution of these filtration tests comprised ethanol and 50 ppm Rose Bengal (RB, molecular weight: 1028 g/mol) dye solution and all tests were carried out at room temperature with an operating pressure of 5 bar.

As lower concentrations of TMC in 2-MeTHF were not able to form polyamide with enough yield (0.5 - 1 wt.%, see Figure 5.1 in Section 5.1.1), a higher concentration of 2 wt.% TMC was used as the starting point and different PIP concentrations were used, ranging from 2 to 3.2 wt.%. Firstly, the time for IP was set at 2 min for the aqueous PIP solution and 2 min for the organic TMC solution, see Figure 5.11a for the results of this TFC membrane. As the concentration of the PIP monomer increased, the rejection of the membrane increased and the permeance experienced a slight decline. The membrane at 3.2 wt.% PIP experienced a RB rejection of 22 % and an ethanol permeance of 42 L m^{-2} h^{-1} bar^{-1} compared to a RB rejection of 10 % and ethanol permeance of 45 L m^{-2} h^{-1} bar^{-1} at 2 wt.% PIP. This protocol of increasing the monomer concentration has been reported by Chen *et al.,* where an increase in monomer concentration reduced the water permeation through the membrane but increased the salt rejection capability of the TFC membrane [39]. Further to this, in a study conducted by Khorshidi *et al.*, it was found that increasing the MPD concentration from 1 % to 2 % increased the salt rejection from

95 % to 97 % and decreased the water flux from 45 L m^{-2} h^{-1} bar^{-1} to 15 L m^{-2} h^{-1} bar^{-1} [4]. The rejection of 22 % was too low, and further iterations were made to increase the rejection of the polyamide selective layer.

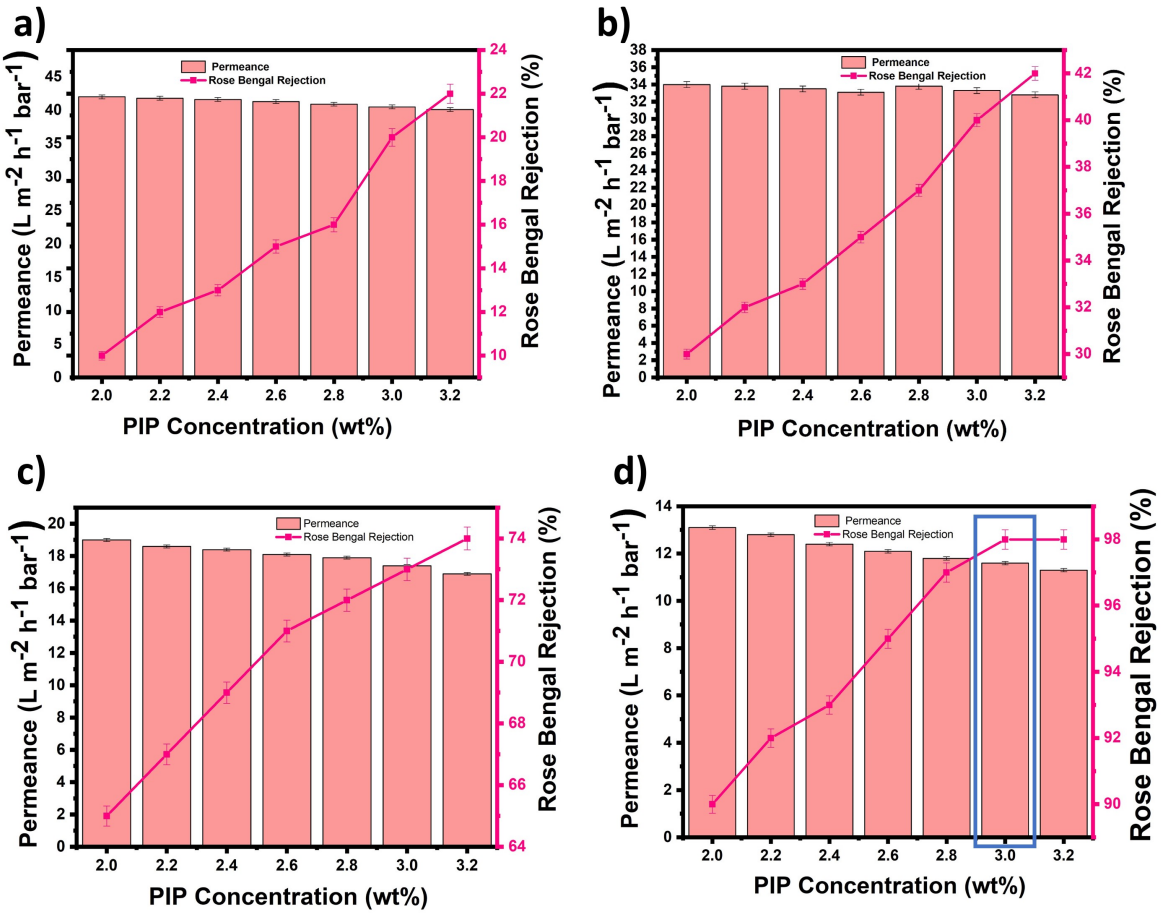

Figure 5.11: Ethanol permeance and Rose Bengal rejection at different PIP and TMC concentrations a) 2 wt.% TMC concentration with IP timings: PIP 2 min and TMC 2 min, b) 3 wt.% TMC concentration with IP timings: PIP 2 min and TMC 2 min, c) 3 wt.% TMC concentration with IP timings: PIP 3 min and TMC 3 min, d) 3 wt.% TMC concentration with IP timings: PIP 3 min and TMC 4 min

The TMC concentration was changed to 3 wt.% and the same reaction time of 2 min each for the aqueous and organic phase was used. At 3.2 wt.% PIP the TFC membrane experienced a RB rejection of 42 % and an ethanol permeance of 36 L m^{-2} h^{-1} bar^{-1} see Figure 5.11b. As expected and following other reported studies, the RB rejection increased, and ethanol permeance decreased owing to a denser film being produced [4],

[39], [40]. However, the rejection was still too low and further iterations were made to increase the rejection of the polyamide selective layer.

To keep the concentration of reagents as low as possible in line with principles of Green Chemistry, the reaction time was increased to see what effect this would have on the rejection and permeance of the TFC membrane. The TMC concentration remained at 3 wt.% and the reaction time was increased from 2 min each for the aqueous and organic phase to 3 min each. This increase in reaction time had a positive effect on the rejection of RB, as rejection increased from 42 % previously to 74 % and the permeance reached 19 L m^{-2} h^{-1} bar^{-1} for the 3.2 wt.% PIP and 3 wt.% TMC membrane, see Figure 5.11c.

To further increase the rejection and permeance, the reaction time for the organic phase was increased to 4 min and the reaction time for the aqueous phase remained at 3 min. At 3.2 wt.% the TFC membrane experienced a 98 % rejection of RB dye and an ethanol permeance of 11 L m^{-2} h^{-1} bar^{-1}, see Figure 5.11d. The membrane produced using 3 wt.% PIP experienced the same rejection and slightly higher permeance of 11.2 L m^{-2} h^{-1} bar^{-1} and as the difference between the two PIP concentrations was minimal, the most suitable conditions were set as 3 wt.% PIP and 3 wt.% TMC in 2-MeTHF for 3 min and 4 min respectively. These conditions were then used to produce a TFC using only bio-renewable solvents.

5.2.2 Membrane performance

OSN Membrane testing for membranes varies depending on the solvent and solute, and to date, no fixed OSN testing protocol has been established [41]. Different solutes are currently used by OSN researchers to characterise the separation performance of membranes and to determine the MWCO. The most popular solutes tested are different commercially available dyes within the nanofiltration range [41]. Characterising the rejection of the membrane using dyes is simple as each dye has a distinct absorption spectra and UV-

spectrophotometry can be employed to determine the dye concentration in the feed and permeate streams. In addition to dyes, styrene oligomers and ethylene glycol oligomers are also widely used as markers, as these markers are commercially available in the NF MWCO range [41].

The MWCO of a membrane can differ according to the solute and solvent used and interactions between solutes and solvents can occur, which leads to a difference in rejection in different solvents in the same membrane [42]. The affinity between the solute-solvent and solute–membrane influences the rejection of the membrane, as the effective pore size is influenced. Furthermore, different solvents also experience different permeabilities as the affinity between the solvent and membrane varies, for example, methanol experiences higher permeabilities than ethanol in polymer membranes [43]. Solvents widely used for OSN testing include: alcohols, ketones, aromatics, polar aprotic and hydrocarbons [41], [42].

Two TFC membranes with the two different selective layers PA(n-hexane) and PA(2-MeTHF) were fabricated using the RC-Cyrene™/AA support and these membranes were tested at room temperature for OSN applications. Firstly, an ethanol and methanol feed solution consisting of 50 ppm Rose Bengal dye was used for filtration. The two different solvents were used to investigate how solvent permeation and dye rejection differs in the membrane with the two different alcohols. The PA(n-hexane)/RC TFC membrane demonstrated RB rejection rates of 94 % and 95 % in ethanol and methanol, with permeances of 2.8 L m^{-2} h^{-1} bar^{-1} and 4 L m^{-2} h^{-1} bar^{-1} respectively, (see Figure 5.12).

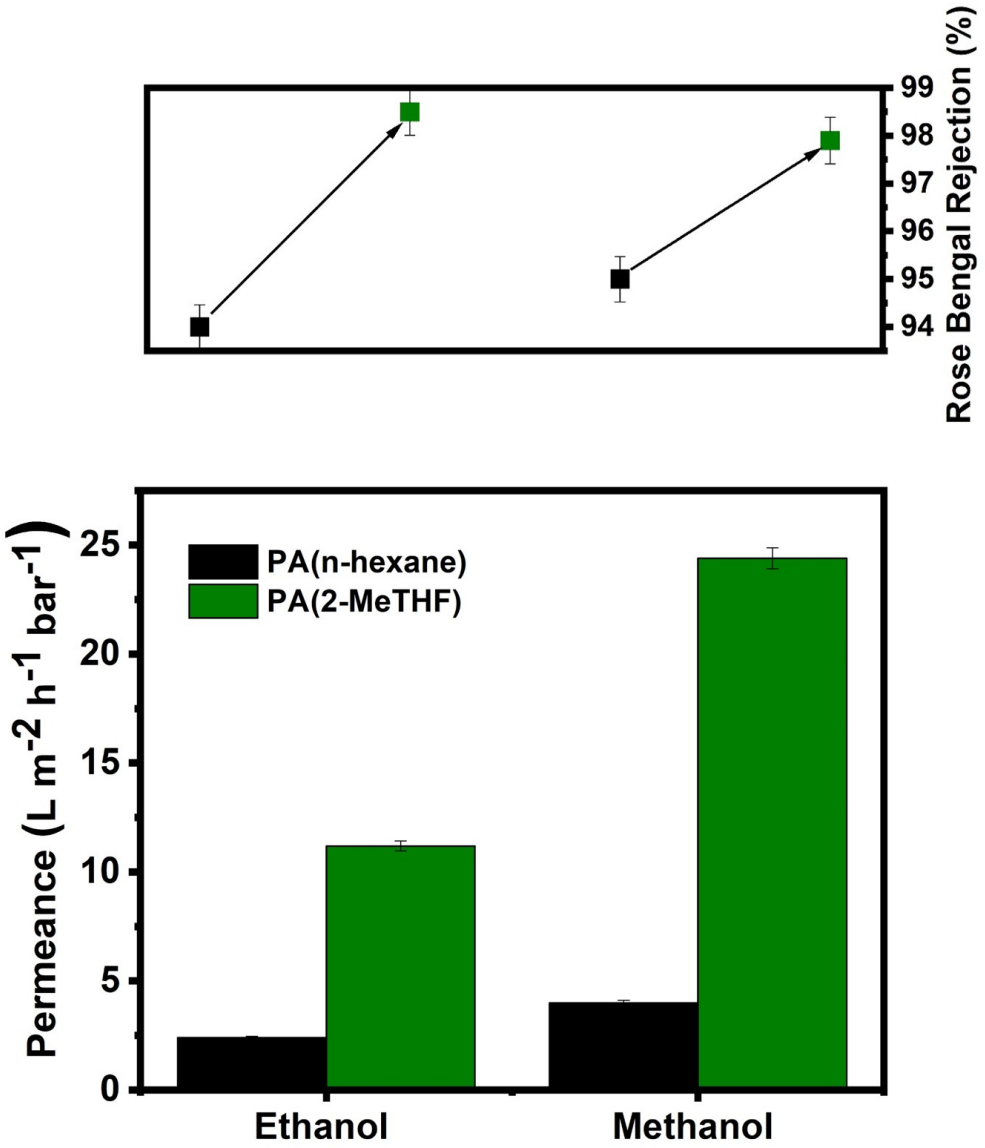

Figure 5.12: Comparison of permeance and Rose Bengal rejection of the two selective layers deposited on the RC-Cyrene/AA and RC-DMF support

The PA(2-MeTHF)/RC TFC membrane was more permeable and a 10-fold increment in methanol permeance was experienced which reached 24.8 L m^{-2} h^{-1} bar^{-1}. Further to this, the ethanol permeance experienced a 250 % increase, reaching 11.2 L m^{-2} h^{-1} bar^{-1}. The separation performance of the PA(2-MeTHF)/RC TFC membrane also increased in methanol and ethanol from 94 % to 97.9 % and from 95 % to 98.5 % respectively. The increase in permeance and rejection in a methanol feed solution compared to ethanol is a common phenomenon [42].

A feed solution consisting of a range of dyes with different charges and molecular weights was employed for tests to investigate the rejection of the two TFC membranes and the properties of the dyes are listed in Table 5.5. All tests were carried out in ethanol at room temperature with a 50 ppm dye concentration and an operating pressure of 5 bar. The feed solution was constantly stirred at 700 rpm to avoid concentration polarisation. Figure 5.13 shows the membrane rejection for different dye/ethanol feed solutions and Figure 5.14 shows the UV-VIS spectra for the feed and permeate stream for the two TFC membranes tested with the various dyes.

Table 5.5: Properties of dyes used in this work

	Molecular Weight (g mol^{-1})	Charge
Rose Bengal (RB)	1028.6	Positive
Fast Green F (FGF)	808.0	Negative
Rhodamine B (Rh B)	479.0	Positive
Methyl Orange (MO)	327.3	Negative
Methylene Blue (MB)	319.9	Positive

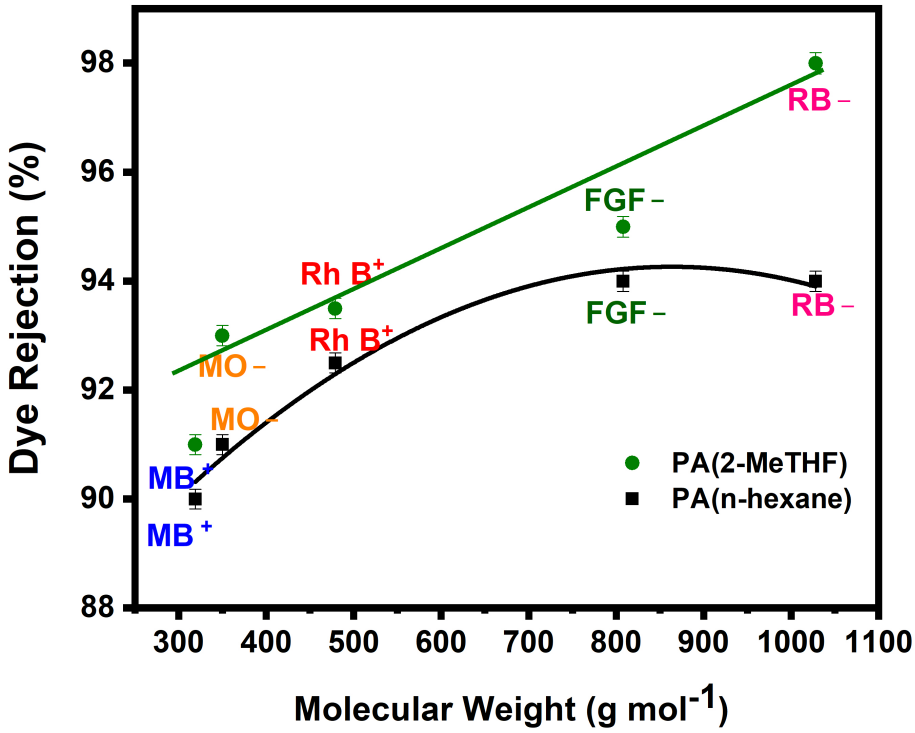

Figure 5.13: OSN separation performance of the two membranes consisting of PA(n-hexane) and PA(2-MeTHF) selective layers (feed: 50 ppm dyes in ethanol; pressure: 5bar)

The rejection of the dyes increased in both TFC membranes as the molecular weight increased indicating that the governing factor for rejection was size exclusion and all the dye rejections were above 90 %, (see Figure 5.13). The PA(2-MeTHF)/RC TFC membrane experienced higher rejections for all dyes compared to the PA(n-hexane)/RC TFC membrane. The FTIR spectra of the two polymers (see Figure 5.2) showed a sharp C=O peak present in the PA(2-MeTHF) polymer which is not present in the PA(n-hexane) polymer and the number of C=O bonds present in the two selective layers were quantified through XPS analysis in Section 5.1.2 to be 12.4 % for the PA(2-MeTHF) and 3.4 % for the PA(n-hexane) polymer film. The additional C=O in the PA(2-MeTHF) created further negativity in the charge of the selective layer, which created greater electrostatic interactions from the negatively charged PA surface to the charged dyes in the PA(2-

MeTHF)/RC TFC membrane, resulting in higher rejections with the charged dyes [44], [45].

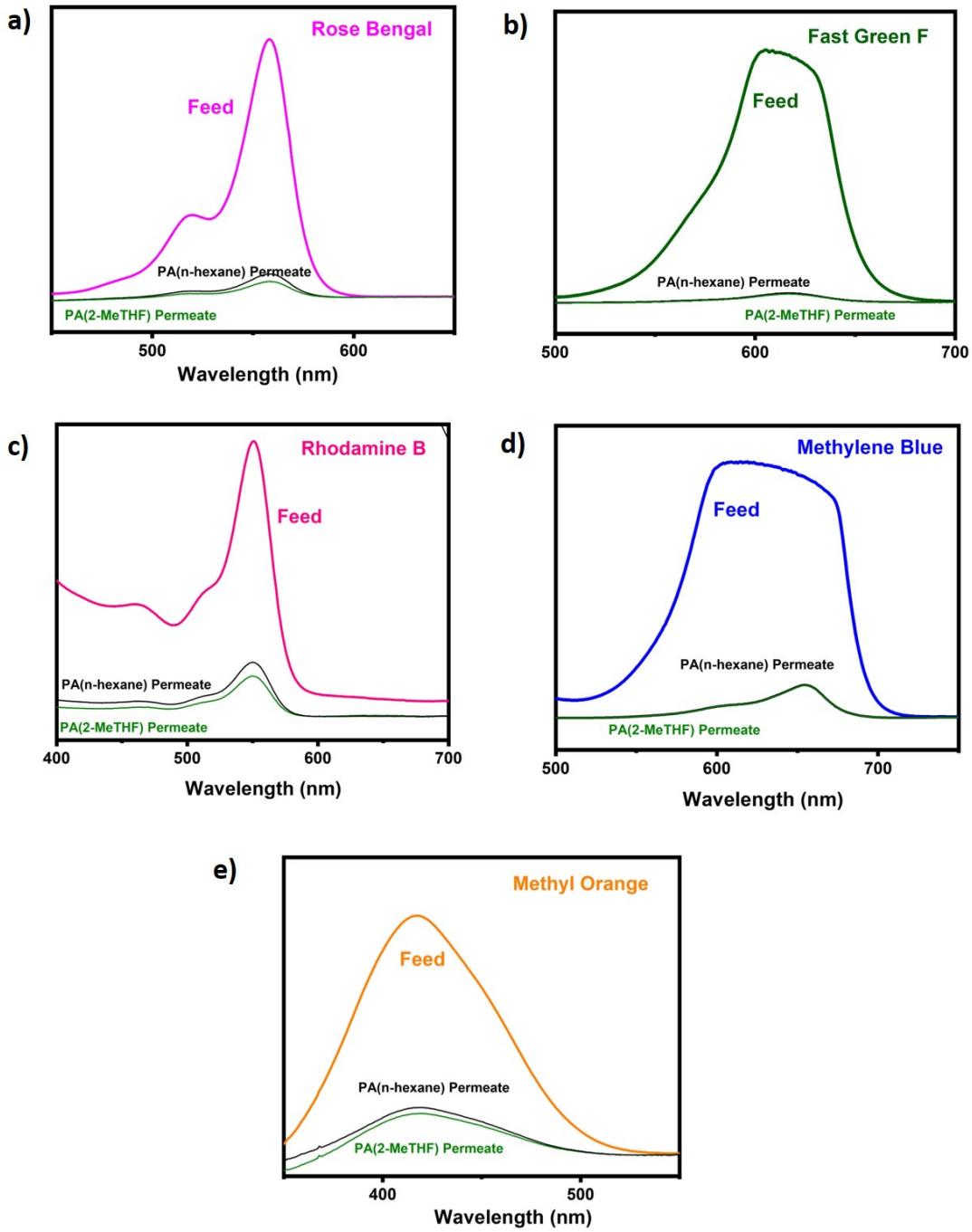

Figure 5.14: UV-VIS spectra of the two TFC membranes comprising of PA(n-hexane) and PA(2-MeTHF) selective layers, feed: 50 ppm dyes in ethanol a) Rose Bengal, b) Fast Green F, c) Rhodamine B, d) Methylene Blue, e) Methyl Orange

The PA(2-MeTHF)/RC TFC membrane experienced greater ethanol permeance compared to the PA(n-hexane)/RC TFC membrane at 11.2 L m^{-2} h^{-1} bar^{-1} and 2.8 L m^{-2} h^{-1} bar^{-1} respectively. Water contact angle measurements were carried out to investigate the difference in hydrophilicity of the two TFC membranes see Figure 5.15.

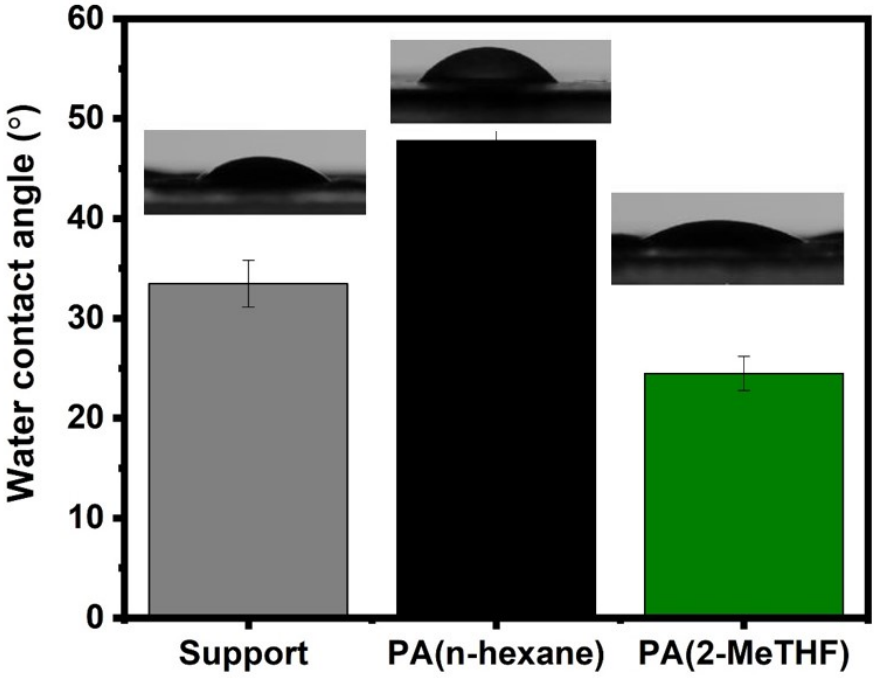

Figure 5.15: Water contact angle of the RC-Cyrene/AA support 35.5°, PA(n-hexane)/RC 47.8° and PA(2-MeTHF) 24.5°

The addition of the two selective layers onto the RC support altered the hydrophilicity of the support. The water contact angle of the support was 35.5 ° and the addition of the PA(n-hexane) layer onto the support created hydrophobicity in the TFC membrane with a water contact angle of 47.8 °. The water contact angle for the PA(2-MeTHF)/RC TFC membranes was 24.5 ° and this selective layer increased the hydrophilicity of the support, (see Figure 5.15 for the contact angle). The increase in C=O bonds in the PA(2-MeTHF) selective layer accounted for the increase in hydrophilicity for the TFC membrane, resulting in increased ethanol permeance in this TFC membrane [27]. [27]. Further to the

hydrophilicity effect of the TFC membrane, the lower O/N ratio for the PA(2-MeTHF) created a more open structure compared to PA(n-hexane) a more cross-linked structure, resulting in higher ethanol permeance. The thicknesses of the PA(n-hexane) and PA(2-MeTHF) selective layers on RC supports were comparable, at ca. 155 nm, see Figure 5.16 for the SEM image of the two TFC membranes. As the thickness of the two selective layers was the same, this could not have influenced the permeance of ethanol through the membrane.

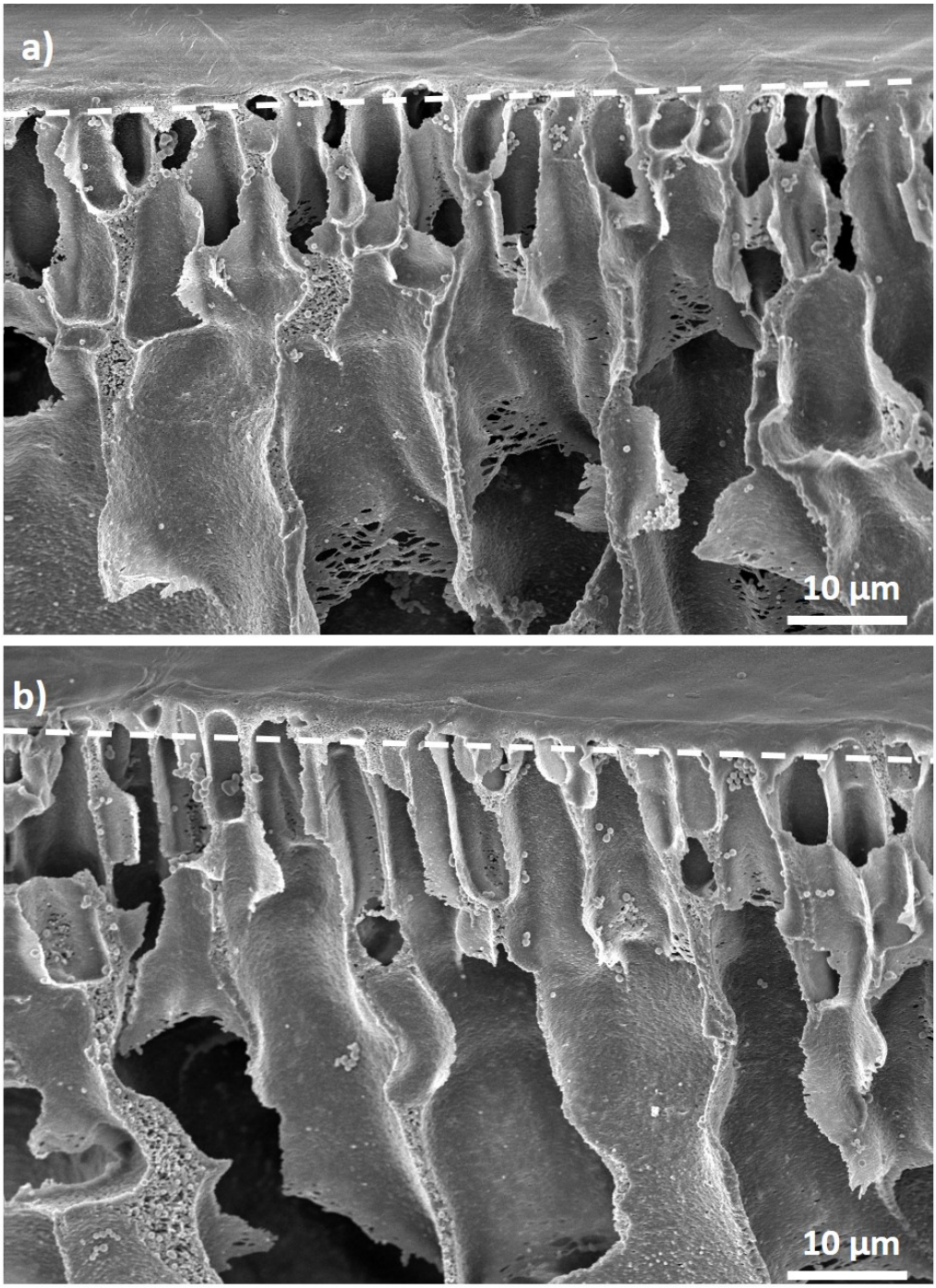

Figure 5.16: SEM images of the two TFC membranes: a) PA(n-hexane)/RC and b) PA(2-MeTHF)/RC. The white dotted line represents the selective layer which is 155 nm thick

As the support used in the work had not been used before as the foundation of a TFC membrane, the role of the support in solvent permeance and dye rejection was investigated. The two selective layers were deposited on the RC-DMF support fabricated in Chapter 4 and Figure 5.17 shows the results for the rejection and permeance comparison between the TFC membranes using the two supports.

A 50 ppm ethanol and Rose Bengal dye feed solution was used for filtration and the permeance of the membrane for the PA(n-hexane)/RC-DMF was 1.9 L m^{-2} h^{-1} bar^{-1} compared to 2.8 L m^{-2} h^{-1} bar^{-1} for the PA(n-hexane)/RC-Cyrene™/AA TFC membrane. The permeance for the PA(2-MeTHF)/RC-DMF TFC membrane was 10.5 L m^{-2} h^{-1} bar^{-1} compared to 11.2 L m^{-2} h^{-1} bar^{-1} for the PA(2-MeTHF)/RC-Cyrene™/AA TFC membrane. The RC-DMF support experienced slightly lower permeances than the RC-Cyrene™/AA support, indicating that the more porous RC-Cyrene™/AA support facilitated the permeance of the membrane. The RB rejection remained constant for both TFC membranes when changing the support indicating that the selective layer was the only contributing factor to the increase in rejection for the PA(2-MeTHF) selective layer.

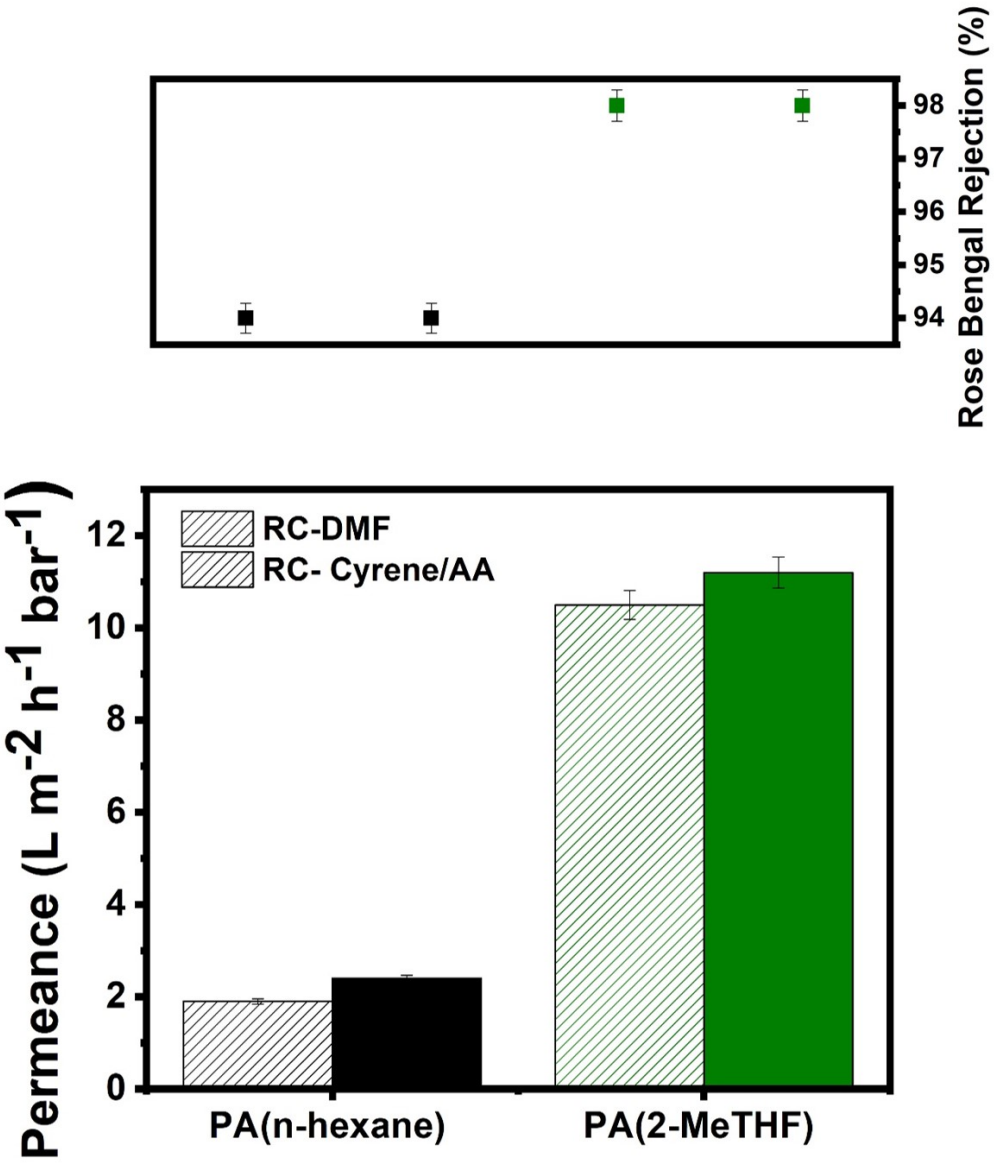

Figure 5.17: Comparison of permeance and rejection of the two selective layers deposited on the RC-Cyrene/AA and RC-DMF supports

5.2.3 Solvent activation

Solvent activation was employed to remove any contaminants or oligomers present within the membranes [26]. DMF was passed through the membrane for 10 min at 5 bar, and this is a common protocol used for membrane activation for OSN membranes [25], [46]. After solvent activation, a feed solution consisting of 50 ppm Rose Bengal and ethanol was used for permeation tests, filtrations occurred at 5 bar and work was carried out at room temperature. Both membranes experienced an increase in ethanol permeance from 2.8 L m^{-2} h^{-1} bar^{-1} to 5 L m^{-2} h^{-1} bar^{-1} and 11.2 L m^{-2} h^{-1} bar^{-1} to 25 L m^{-2} h^{-1} bar^{-1} for the PA(n-hexane)/RC and PA(2-MeTHF)/RC TFC membranes respectively, (see Figure 5.18). This increase in solvent permeance is a common phenomenon that occurs after solvent activation that can be attributed to the opening of membrane pores that may have been blocked. Further to this, solvent activation is used to possibly remove any uncrosslinked polymer fragments that may be present in the PA layer before activation, which creates additional free volume in the polymer which enhances permeances [25], [47].

Solvent activation generally increases the rejection of TFC membranes as the polyamide layer swells in DMF, which reduces or eliminates any imperfections in the polymer [25], [46]. This trend was experienced for the PA(n-hexane)/RC TFC membrane as rejection increased from 94 % to 98 %, however, this trend was not experienced with the PA(2-MeTHF) layer, as rejection slightly decreased from 98 % to 97.5 %. The dissolution of the PA(2-MeTHF) in DMF is less than the PA(n-hexane), as seen in Figure 5.9 Section 5.1.3 resulting in the difference in the solvent activation effect as the polymer was not able to swell to the same extent as PA(n-hexane).

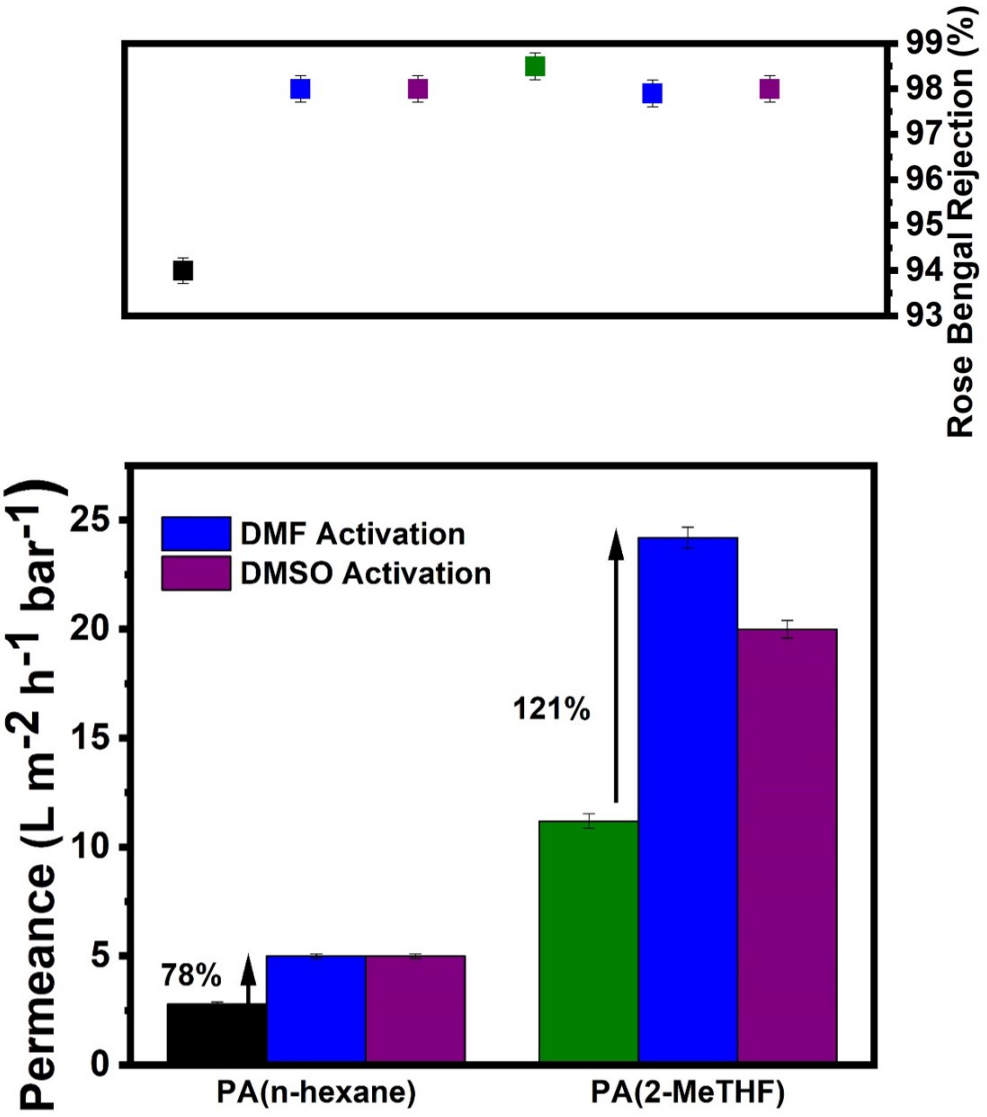

Figure 5.18: Solvent activation using DMF and DMSO for the PA(n-hexane)/RC and PA(2-MeTHF)/RC membrane. The green and black bar represent pure solvent filtration prior to activation

DMSO was used as a benign alternative to DMF for solvent activation, and this has been previously reported before by Lu *et al.*, Paseta *et al.*, Solomon *et al.*, and Hermans *et al.*, [25], [26], [46]–[48]. The DMF and DMSO permeance and rejection trends in the PA(n-hexane)/RC TFC membrane were identical, and this has been previously reported by Solomon *et al.* [25]. DMSO activation for the PA(2-MeTHF)/RC TFC membrane had

a similar effect to that of DMF activation, ethanol permeance increased but was lower than the permeance experienced with DMF activation at 20 L m^{-2} h^{-1} bar^{-1} and 25 L m^{-2} h^{-1} bar^{-1} respectively. The rejection of RB also decreased to 97.5 % the same value as after DMF activation. This trend in the difference of permeability and rejection after DMF and DMSO activation is common and has previously been reported by Hai *et al.*, Xia *et al.*, Karan *et al.*, and Lu *et al.*,[26], [49]–[51]. Figure 5.19 shows the SEM images for the PA(2-MeTHF)/RC TFC membrane before and after DMF and DMSO activation, and it can be seen that the polyamide layer was intact and that some swelling had occurred after activation.

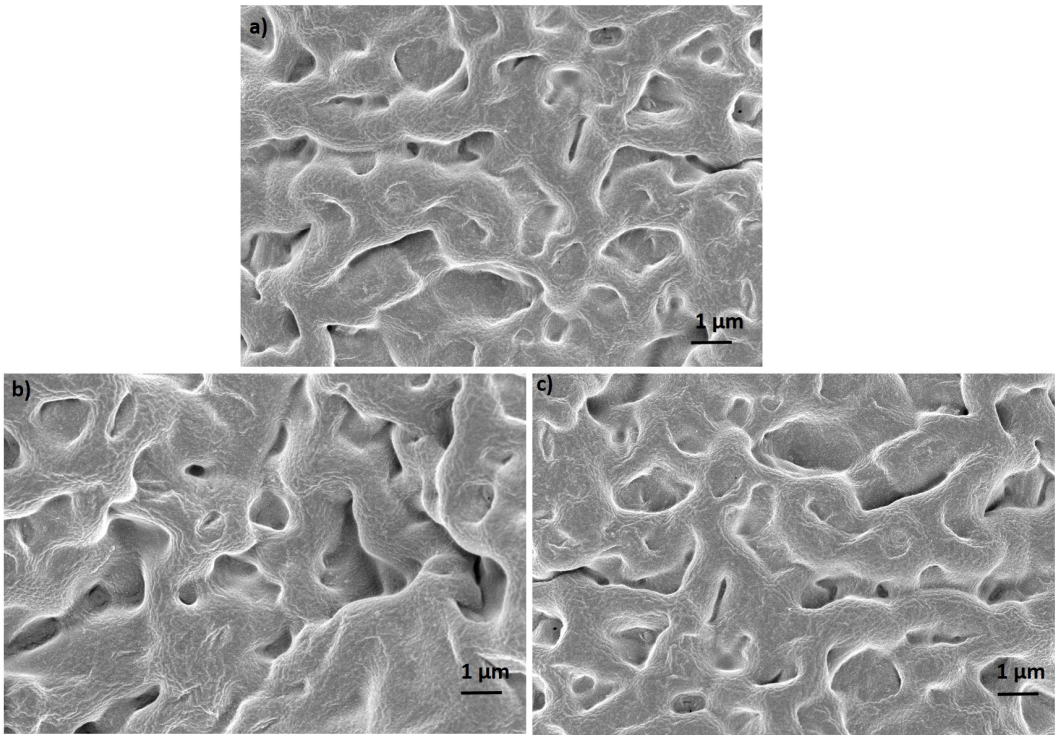

Figure 5.19: PA(2-MeTHF) surface SEM: a) before activation b) after DMF activation and c) after DMSO activation

Further to activation with DMF and DMSO, Cyrene™ was used as a solvent for activation. Cyrene™ is a green alternative for DMF and the exploration of this solvent as an alternative for activation has many environmental, health and safety benefits [52]. The same activation protocol was used and Cyrene™ was filtered through each membrane

for 10 min at 5 bar. After activation, an ethanol and RB solution was filtered through the membrane and in both membranes irrespective of the selective layer, the permeate was pink, and no dye rejection had taken place. The permeance was also measured to be 0.08 L m^{-2} h^{-1} bar^{-1} for the PA(n-hexane)/RC TFC membrane and 0.2 L m^{-2} h^{-1} bar^{-1} for the PA(2-MeTHF)/RC TFC membrane. The Hildebrand solubility parameter for Cyrene™ is 22.7 $MPa^{1/2}$ which is close to DMF and DMSO at 24.4 $MPa^{1/2}$ and 26.6 $MPa^{1/2}$ respectively, indicating that Cyrene™ should have experienced a similar trend to DMF and DMSO. This drop in permeance and rejection can be attributed to the viscosity of the solvents as the viscosity of Cyrene™ is considerably higher than DMF and DMSO at 14.5 cP, 0.92 cP and 2.0 cP respectively. The filtration of Cyrene™ could have blocked the polyamide pores, interacted with the membrane, and caused fouling resulting in the decline of permeance and rejection [53]. However, further detailed analysis into Cyrene™ activation is required to investigate this phenomenon.

5.2.4 Performance comparison

The separation performances of TFC membranes were comparable to other TFC membranes reported in literature, see Table 5.6 and Figure 5.20. The feed solution comprised of 35 ppm Rose Bengal in ethanol, and experiments were carried out at room temperature with an operating pressure ranging from 5 to 20 bar. The permeabilities of TFC membranes fabricated using bio-renewable solvents in this work surpassed membranes produced using traditional solvents (Table 5.6 and Figure 5.20). Li *et al.,* reported the use of a mixed matrix membrane containing ZIF-8, the ethanol permeance of this membrane was L m^{-2} h^{-1} bar^{-1} and RB rejection was 86 %, in comparison to the bio-renewable membrane produced using PA(2-MeTHF) and regenerated cellulose support experienced permeance three times higher at 11.2 L m^{-2} h^{-1} bar^{-1} and a higher RB rejection of 98 % [54]. The results from this work suggest that the protocols and the solvents used here could possibly replace existing methods for membrane fabrication to produce more sustainable, safer membranes that have higher through-puts.

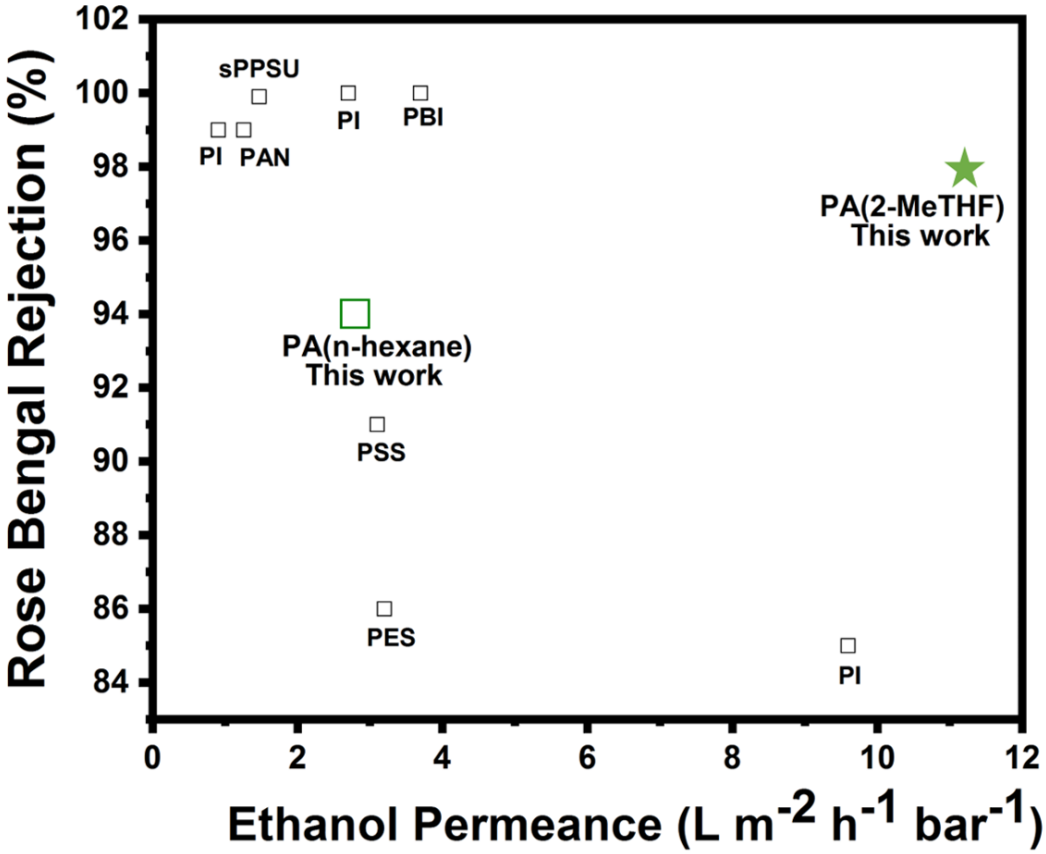

Figure 5.20: Performance comparison of current state-of-the-art membranes as reported in literature, the data for this graph can be found in Table 5.6

Table 5.6: Performance comparison of different polymer membranes tested with Ethanol and Rose Bengal for OSN.

Membrane	Operating Pressure (bar)	Permeance L m^{-2} h^{-1} bar^{-1}	Rejection (%)	Reference
PI	20	2.7	100	[47]
PES	-	3.2	86	[54]
PI	5	0.9	99	[55]
PAN	5	1.2	99	[56]
sPPSU	10	1.5	99	[57]
PSS	5	3.1	91	[58]
P84	-	9.6	85	[59]
PBI	5	3.7	100	[60]
PA(n-hexane)/RC	5	2.8	94	This work
PA(2-MeTHF)/RC	5	11.2	98	This work

5.3 Conclusion

In line with the fifth and seventh principles of Green Chemistry, the solvent for interfacial polymerisation was changed from n-hexane, a hazardous petroleum-derived solvent to a benign bio-renewable solvent, 2-MeTHF. The resultant film produced using 2-MeTHF exhibited greater chemical resistance in DMF and THF compared to the n-hexane-derived film. However, the 2-MeTHF derived polymer had less microporosity, the yields of the films were 22 times less than the conventional films and the O/N ratio indicated that the film was less cross-linked compared to the n-hexane derived film indicating that n-hexane is a better solvent for interfacial polymerisation [3].

The addition of these films onto the regenerated cellulose support produced in Chapter 4 created a thin film composite membrane produced solely from green solvents. Optimal IP parameters were explored for the 2-MeTHF polymer to find a trade-off between rejection and permeability. The PA(2-MeTHF)/RC and PA(n-hexane)/RC TFC membranes were tested for OSN applications. The PA(2-MeTHF)/RC TFC membrane exhibited increased hydrophilicity due to additional carboxylic acid groups that were present in the film, allowing for greater ethanol permeance at 11.2 L m^{-2} h^{-1} bar^{-1} compared to 2.5 L m^{-2} h^{-1} bar^{-1} experienced with PA(n-hexane)/RC TFC membrane. The permeance further increased to reach 25 L m^{-2} h^{-1} bar^{-1} after DMF activation and 20 L m^{-2} h^{-1} bar^{-1} after DMSO activation. The bio-renewable membrane experienced higher dye rejections compared to PA(n-hexane) over a molecular weight range from 300 to 1000 g/mol and all rejections were above 90 %. The membrane produced solely from bio-renewable solvent outperformed current state-of-the-art membranes and mixed matrix membranes that incorporate fillers into the membrane for enhanced separation performance.

References

[1] Y. Song, J.-B. Fan, and S. Wang, "Recent progress in interfacial polymerization," *Materials Chemistry Frontiers*, vol. 1, no. 6, pp. 1028–1040, 2017.

[2] R. W. Baker, *Membrane technology and applications*. John Wiley and Sons, 2012.

[3] J. Jegal, S. G. Min, and K.-H. Lee, "Factors affecting the interfacial polymerization of polyamide active layers for the formation of polyamide composite membranes," *Journal of Applied Polymer Science*, vol. 86, no. 11, pp. 2781–2787, 2002.

[4] B. Khorshidi, T. Thundat, B. Fleck, and M. Sadrzadeh, "Thin film composite polyamide membranes: Parametric study on the influence of synthesis conditions," *RSC Advances*, vol. 5, no. 68, pp. 54 985–54 997, 2015.

[5] A. Al-Hobaib, M. Alsuhybani, K. M. Al-Sheetan, and M. R. Shaik, "Reverse osmosis membranes prepared by interfacial polymerization in n-heptane containing different co-solvents," *Desalination and Water Treatment*, vol. 57, no. 36, pp. 16 733–16 744, 2016.

[6] H. Marien, L. Bellings, S. Hermans, and I. F. Vankelecom, "Sustainable process for the preparation of high-performance thin-film composite membranes using ionic liquids as the reaction medium," *ChemSusChem*, vol. 9, no. 10, pp. 1101–1111, 2016.

[7] G. Szekely, M. F. Jimenez-Solomon, P. Marchetti, J. F. Kim, and A. G. Livingston, "Sustainability assessment of organic solvent nanofiltration: From fabrication to application," *Green Chemistry*, vol. 16, no. 10, pp. 4440–4473, 2014.

[8] P. Anastas and N. Eghbali, "Green chemistry: Principles and practice," *Chemical Society Reviews*, vol. 39, no. 1, pp. 301–312, 2010.

[9] Y. Hartanto, M. Corvilain, H. Marien, J. Janssen, and I. F. Vankelecom, "Interfacial polymerization of thin-film composite forward osmosis membranes using ionic liquids as organic reagent phase," *Journal of Membrane Science*, vol. 601, p. 117 869, 2020.

[10] L. Xiao *et al.*, "Ionic liquid regulated interfacial polymerization process to improve acid-resistant nanofiltration membrane permeance," *Journal of Membrane Science*, p. 119 882, 2021.

[11] H. Gao, T. Jiang, B. Han, *et al.*, "Aqueous/ionic liquid interfacial polymerization for preparing polyaniline nanoparticles," *Polymer*, vol. 45, no. 9, pp. 3017–3019, 2004.

[12] F. Yan and J. Texter, "Surfactant ionic liquid-based microemulsions for polymerization," *Chemical communications*, no. 25, pp. 2696–2698, 2006.

[13] P.-R. Van den Mooter, L. Dedvukaj, and I. F. Vankelecom, "Use of ionic liquids and co-solvents for synthesis of thin-film composite membranes," *Membranes*, vol. 11, no. 4, p. 297, 2021.

[14] G. Falca, V. E. Musteata, S. Chisca, M. N. Hedhili, C. Ong, and S. P. Nunes, "Naturally extracted hydrophobic solvent and self-assembly in interfacial polymerization," *ACS Applied Materials and Interfaces*, 2021.

[15] C. Ong, G. Falca, T. Huang, *et al.*, "Green synthesis of thin-film composite membranes for organic solvent nanofiltration," *ACS Sustainable Chemistry and Engineering*, vol. 8, no. 31, pp. 11 541–11 548, 2020.

[16] E. Yara-Varon, A.-S. Fabiano-Tixier, M. Balcells, R. Canela-Garayoa, A. Bily, and F. Chemat, "Is it possible to substitute hexane with green solvents for extraction of carotenoids? a theoretical versus experimental solubility study," *RSC Advances*, vol. 6, no. 33, pp. 27 750–27 759, 2016.

[17] A.-G. Sicaire, M. A. Vian, A. Filly, Y. Li, A. Bily, and F. Chemat, "2-methyltetrahydrofuran: Main properties, production processes, and application in extraction of natural products," in *Alternative Solvents for Natural Products Extraction*, Springer, 2014, pp. 253–268.

[18] F. Yuan, Z. Wang, X. Yu, *et al.*, "Visualization of the formation of interfacially polymerized film by an optical contact angle measuring device," *The Journal of Physical Chemistry C*, vol. 116, no. 21, pp. 11 496–11 506, 2012.

[19] C. Y. Tang, Y.-N. Kwon, and J. O. Leckie, "Effect of membrane chemistry and coating layer on physiochemical properties of thin film composite polyamide ro and nf membranes: I. ftir and xps characterization of polyamide and coating layer chemistry," *Desalination*, vol. 242, no. 1-3, pp. 149–167, 2009.

[20] A. K. Ghosh, B.-H. Jeong, X. Huang, and E. M. Hoek, "Impacts of reaction and curing conditions on polyamide composite reverse osmosis membrane properties," *Journal of Membrane Science*, vol. 311, no. 1-2, pp. 34–45, 2008.

[21] J. P. Coates and P. H. Shelley, "Infrared spectroscopy in process analysis," *Encyclopedia of Analytical Chemistry: Applications, Theory and Instrumentation*, 2006.

[22] D. Sachdev, P. H. Maheshwari, and A. Dubey, "Piperazine functionalized mesoporous silica for selective and sensitive detection of ascorbic acid," *Journal of Porous Materials*, vol. 23, no. 1, pp. 123–129, 2016.

[23] V. T. Do, C. Y. Tang, M. Reinhard, and J. O. Leckie, "Degradation of polyamide nanofiltration and reverse osmosis membranes by hypochlorite," *Environmental science and technology*, vol. 46, no. 2, pp. 852–859, 2012.

[24] B.-M. Jun, H. K. Lee, Y.-I. Park, and Y.-N. Kwon, "Degradation of full aromatic polyamide nf membrane by sulfuric acid and hydrogen halides: Change of the surface/permeability properties," *Polymer Degradation and Stability*, vol. 162, pp. 1–11, 2019.

[25] M. F. J. Solomon, Y. Bhole, and A. G. Livingston, "High flux membranes for organic solvent nanofiltration (osn)—interfacial polymerization with solvent activation," *Journal of membrane science*, vol. 423, pp. 371–382, 2012.

[26] T.-D. Lu, B.-Z. Chen, J. Wang, *et al.*, "Electrospun nanofiber substrates that enhance polar solvent separation from organic compounds in thin-film composites," *Journal of Materials Chemistry A*, vol. 6, no. 31, pp. 15 047–15 056, 2018.

[27] J. Aburabie, P. Neelakanda, M. Karunakaran, and K.-V. Peinemann, "Thin-film composite crosslinked polythiosemicarbazide membranes for organic solvent nanofiltration (osn)," *Reactive and Functional Polymers*, vol. 86, pp. 225–232, 2015.

[28] N. Misdan, W. Lau, A. Ismail, T. Matsuura, and D. Rana, "Study on the thin film composite poly (piperazine-amide) nanofiltration membrane: Impacts of physicochemical properties of substrate on interfacial polymerization formation," *Desalination*, vol. 344, pp. 198–205, 2014.

[29] L. Li, S. Zhang, X. Zhang, and G. Zheng, "Polyamide thin film composite membranes prepared from 3, 4, 5-biphenyl triacyl chloride, 3, 3, 5, 5-biphenyl tetraacyl chloride and m-phenylenediamine," *Journal of Membrane Science*, vol. 289, no. 1-2, pp. 258–267, 2007.

[30] D. T. Padavan, A. M. Hamilton, L. E. Millon, D. R. Boughner, and W. Wan, "Synthesis, characterization and in vitro cell compatibility study of a poly (amic acid) graft/cross-linked poly (vinyl alcohol) hydrogel," *Acta biomaterialia*, vol. 7, no. 1, pp. 258–267, 2011.

[31] M. Gussoni, F. Greco, P. Ferruti, E. Ranucci, A. Ponti, and L. Zetta, "Poly (amidoamine) s carrying tempo residues for nmr imaging applications," *New Journal of Chemistry*, vol. 32, no. 2, pp. 323–332, 2008.

[32] H. Komber, B. Voit, O. Monticelli, and S. Russo, "H and 13c nmr spectra of a hyperbranched aromatic polyamide from p-phenylenediamine and trimesic acid," *Macromolecules*, vol. 34, no. 16, pp. 5487–5493, 2001.

[33] C. Kong, T. Kamada, T. Shintani, M. Kanezashi, T. Yoshioka, T. Tsuru, *et al.*, "Enhanced performance of inorganic-polyamide nanocomposite membranes prepared by metal-alkoxide-assisted interfacial polymerization,"

[34] N. Hadei, G. T. Achonduh, C. Valente, C. J. O'Brien, and M. G. Organ, "Differentiating c- br and c-cl bond activation by using solvent polarity: Applications to orthogonal alkyl–alkyl negishi reactions," *Angewandte Chemie*, vol. 123, no. 17, pp. 3982–3985, 2011.

[35] W. Lau, A. Ismail, N. Misdan, and M. Kassim, "A recent progress in thin film composite membrane: A review," *Desalination*, vol. 287, pp. 190–199, 2012.

[36] S. Mondal and N. Das, "Triptycene based organosoluble polyamides: Synthesis, characterization and study of the effect of chain flexibility on morphology," *RSC Advances*, vol. 4, no. 106, pp. 61 383–61 393, 2014.

[37] S. H. Dale and M. R. Elsegood, "Hydrogen-bonding adducts of benzenepolycarboxylic acids with n, n-dimethylformamide: Benzene-1, 4-dicarboxylic acid n, n-dimethylformamide disolvate, benzene-1, 2, 4, 5-tetracarboxylic acid n, n-dimethylformamide tetrasolvate and benzene-1, 2, 3-tricarboxylic acid n, n-dimethylformamide disolvate monohydrate," *Acta Crystallographica Section C: Crystal Structure Communications*, vol. 60, no. 6, o444–o448, 2004.

[38] A. Miao, M. Wei, F. Xu, and Y. Wang, "Influence of membrane hydrophilicity on water permeability: An experimental study bridging simulations," *Journal of Membrane Science*, vol. 604, p. 118 087, 2020.

[39] S.-H. Chen, D.-J. Chang, R.-M. Liou, C.-S. Hsu, and S.-S. Lin, "Preparation and separation properties of polyamide nanofiltration membrane," *Journal of Applied Polymer Science*, vol. 83, no. 5, pp. 1112–1118, 2002.

[40] J. Cadotte, R. King, R. Majerle, and R. Petersen, "Interfacial synthesis in the preparation of reverse osmosis membranes," *Journal of Macromolecular Science—Chemistry*, vol. 15, no. 5, pp. 727–755, 1981.

[41] H. A. Le Phuong, C. F. Blanford, and G. Szekely, "Reporting the unreported: The reliability and comparability of the literature on organic solvent nanofiltration," *Green Chemistry*, 2020.

[42] P. Marchetti, M. F. Jimenez Solomon, G. Szekely, and A. G. Livingston, "Molecular separation with organic solvent nanofiltration: A critical review," *Chemical reviews*, vol. 114, no. 21, pp. 10 735–10 806, 2014.

[43] K. Chen, P. Li, H. Zhang, *et al.*, "Organic solvent nanofiltration membrane with improved permeability by in-situ growth of metal-organic frameworks interlayer on the surface of polyimide substrate," *Separation and Purification Technology*, vol. 251, p. 117 387, 2020.

[44] D. Chen, J. R. Werber, X. Zhao, and M. Elimelech, "A facile method to quantify the carboxyl group areal density in the active layer of polyamide thin-film composite membranes," *Journal of Membrane Science*, vol. 534, pp. 100–108, 2017.

[45] M. Paul and S. D. Jons, "Chemistry and fabrication of polymeric nanofiltration membranes: A review," *Polymer*, vol. 103, pp. 417–456, 2016.

[46] M. F. J. Solomon, Y. Bhole, and A. G. Livingston, "High flux hydrophobic membranes for organic solvent nanofiltration (osn)—interfacial polymerization, surface modification and solvent activation," *Journal of membrane science*, vol. 434, pp. 193–203, 2013.

[47] S. Hermans, E. Dom, H. Marien, G. Koeckelberghs, and I. F. Vankelecom, "Efficient synthesis of interfacially polymerized membranes for solvent resistant nanofiltration," *Journal of Membrane Science*, vol. 476, pp. 356–363, 2015.

[48] L. Paseta, M. Navarro, J. Coronas, and C. Tellez, "Greener processes in the preparation of thin film nanocomposite membranes with diverse metal-organic frameworks for organic solvent nanofiltration," *Journal of Industrial and Engineering Chemistry*, vol. 77, pp. 344–354, 2019.

[49] Y. Hai, J. Zhang, C. Shi, A. Zhou, C. Bian, and W. Li, "Thin film composite nanofiltration membrane prepared by the interfacial polymerization of 1, 2, 4, 5-benzene tetracarbonyl chloride on the mixed amines cross-linked poly (ether imide) support," *Journal of Membrane Science*, vol. 520, pp. 19–28, 2016.

[50] L. Xia, J. Ren, M. Weyd, and J. R. McCutcheon, "Ceramic-supported thin film composite membrane for organic solvent nanofiltration," *Journal of membrane science*, vol. 563, pp. 857–863, 2018.

[51] S. Karan, Z. Jiang, and A. G. Livingston, "Sub–10 nm polyamide nanofilms with ultrafast solvent transport for molecular separation," *Science*, vol. 348, no. 6241, pp. 1347–1351, 2015.

[52] I. C. Adaka and P. F. Uzor, "Cyrene as a green solvent in the pharmaceutical industry," in *Green Sustainable Process for Chemical and Environmental Engineering and Science*, Elsevier, 2021, pp. 243–248.

[53] Y. Wan, J. Luo, and Z. Cui, "Membrane application in soy sauce processing," in *Membrane Technology*, Elsevier, 2010, pp. 45–62.

[54] Y. Li, L. H. Wee, A. Volodin, J. A. Martens, and I. F. Vankelecom, "Polymer supported zif-8 membranes prepared via an interfacial synthesis method," *Chemical Communications*, vol. 51, no. 5, pp. 918–920, 2015.

[55] Y. Xu, F. You, H. Sun, and L. Shao, "Realizing mussel-inspired polydopamine selective layer with strong solvent resistance in nanofiltration toward sustainable reclamation," *ACS Sustainable Chemistry and Engineering*, vol. 5, no. 6, pp. 5520–5528, 2017.

[56] Y. C. Xu, Y. P. Tang, L. F. Liu, Z. H. Guo, and L. Shao, "Nanocomposite organic solvent nanofiltration membranes by a highly-efficient mussel-inspired co-deposition strategy," *Journal of Membrane Science*, vol. 526, pp. 32–42, 2017.

[57] A. A. Tashvigh, L. Luo, T.-S. Chung, M. Weber, and C. Maletzko, "A novel ionically cross-linked sulfonated polyphenylsulfone (sppsu) membrane for organic solvent nanofiltration (osn)," *Journal of Membrane Science*, vol. 545, pp. 221–228, 2018.

[58] D. Hua and T.-S. Chung, "Polyelectrolyte functionalized lamellar graphene oxide membranes on polypropylene support for organic solvent nanofiltration," *Carbon*, vol. 122, pp. 604–613, 2017.

[59] S. Yang, H. Zhen, and B. Su, "Polyimide thin film composite (tfc) membranes via interfacial polymerization on hydrolyzed polyacrylonitrile support for solvent resistant nanofiltration," *Rsc Advances*, vol. 7, no. 68, pp. 42 800–42 810, 2017.

[60] D. Y. Xing, S. Y. Chan, and T.-S. Chung, "The ionic liquid [emim] oac as a solvent to fabricate stable polybenzimidazole membranes for organic solvent nanofiltration," *Green Chemistry*, vol. 16, no. 3, pp. 1383–1392, 2014.

Chapter 6

Accessing the suitability of thin film composite membranes fabricated using bio-renewable solvents for applications in aqueous nanofiltration

6.1 Introduction

The first asymmetric membrane was fabricated using cellulose triacetate, a functionalised natural polymer, in 1955 by Reid *et al.* [1]. Cellulose triacetate was dissolved in acetone and the dope solution was used to prepare membranes that were not fit for application as they experienced very low flux in the units of μ L/cm^2 h with an operating pressure of 58 bar and NaCl rejection was determined to be 98 % [2]. This polymer, cellulose triacetate which is cellulose acetate with a higher degree of acylation was later replaced to cellulose diacetate by Loeb *et al.* in 1963 to produce membranes that had experienced higher flux than the previously reported membranes but were prone to biological attack [2], [3].

Cellulose acetate (CA) membranes were the first high-performance membrane used for reverse osmosis, nanofiltration and microfiltration processes [2]. CA membranes are easy to produce, mechanically tough, and resistant to degradation by chlorine and other oxidants [2]. However, CA membranes have a dense skin layer and a low porous sub-layer, resulting in an extremely low flux and compaction under high temperatures [2]. Haddada *et al.* reported the use of an asymmetric CA membrane fabricated using an acetone and formamide dope solution with a water flux of 7.1 L m^{-2} h^{-1} and 86 % NaCl salt rejection [4]. The development of new thin film composite membranes in the 1960s led to this form of membrane being predominantly chosen over asymmetric CA membranes, as a higher water flux of 51 L m^{-2} h^{-1} was experienced with 99.5 % NaCl salt rejection [2].

Cellulose acetate membranes were initially preferred for commercial settings, however, the production of cellulose acetate was difficult compared to synthetic polymer and today TFC membranes are predominately produced using PES [5]–[12] and PSf [13]–[19]. These fossil fuel-derived synthetic polymers are widely used as these polymers exhibit superior chemical and mechanical stability [20]. Today, as the need for sustainable membrane fabrication increases as fossil fuel resources become depleted, there is a need to revisit

the use of natural, renewable materials for optimising the green benefits of membrane separation.

In this work, the traditional polymer used for membrane fabrication, cellulose acetate, was explored to produce a TFC membrane. The work in this project looked at CA rather than the traditional petroleum-derived polymers PES or PSf as CA is a renewable biopolymer and the use of this polymer is in line with principles of Green Chemistry. Cellulose acetate membranes have been fabricated and tested for NF applications previously and have been reported by Sun *et al.*, Haddada *et al.*, and Idrees *et al.*, [4], [21]–[28]. An asymmetric membrane produced via cellulose acetate has a polymer concentration ranging from 20-22 wt.% and this produces a very dense skin layer for the rejection of contaminants. As this skin layer is not required for a TFC membrane as a selective layer was prepared, a polymer concentration of 10 wt.% was used.

In this chapter, the work looked at the two selective layers PA(n-hexane) and PA(2-MeTHF) that were prepared in Chapter 5 and the two layers were deposited onto the CA support and the performance of the membranes: water flux, molecular weight cut-off, dye and salt rejection properties of the two TFC membranes were investigated. In addition to this, solvent activation was carried out using ethanol to investigate the effect, if any, ethanol activation had on these membranes. The results were compared with NF 270 a commercial nanofiltration membrane with a semi-aromatic polyamide selective layer that has the same chemistry as the selective layers produced in this work and a different support layer. The results were compared to see how the TFC membranes produced in this work using the bio-renewable solvents (2-MeTHF for the selective layer and Cyrene™ for the support) compared to a commercially available membrane.

6.2 Support fabrication

6.2.1 Hansen solubility parameters

The Hansen solubility parameters for cellulose acetate and Cyrene™ were explored in Chapter 4 and the relative energy difference (RED) was calculated using Equation 4.2 in Chapter 4. A RED value less than 1 indicates that the polymer and solvent are alike and will dissolve. The RED value of Cyrene™ and CA was 1.05 and as this is close to 1 a polymer dope solution was formed to successfully produce supports. The CA-Cyrene™ polymer dope solution was stirred and heated to 80 °C and left overnight to prepare the polymer solution. A similar solution was prepared and was left overnight to stir with no heating to see if the polymer would dissolve at room temperature, however, the polymer only dissolved when heating was applied to the solution and this could be attributed to the high RED value of the solvent and polymer solution. A solvent mixture was then investigated to lower the heat consumption of the polymer dope solution in line with the principles of Green Chemistry. Acetone was chosen as this solvent is the traditional solvent used for CA membrane fabrication, and it also has a yellow ranking on the CHEM21 scheme. Acetone was added to the dope solution at a 50:50 ratio to Cyrene™ [4], [22], [28], [29].

Table 6.1: Hansen solubility parameters of CA membranes cast using Cyrene™ and solvent mixtures methanol and acetone, values taken from [30], [31]

	$\delta_D(MPa^{1/2})$	$\delta_P(MPa^{1/2})$	$\delta_H(MPa^{1/2})$	RED
Cellulose Acetate	18.6	12.7	11	-
Cyrene™	15.5	10.4	7	1.05
Acetone	18.8	10.6	6.9	-
Methanol	14.7	12.3	22.3	-
Cyrene™/acetone mixture	10.9	10.5	6.9	0.52
Cyrene™/methanol mixture	12.1	11.4	14.6	0.9

The RED value for the solvent mixture was calculated to be 0.52, lower than that of the CA-Cyrene™ solution at 1.05. The dissolution temperature of the polymer in the solvent mixture could not be 80 °C, the temperature previously used with the Cyrene™ solution, as the boiling point of acetone is 56 °C. The addition of acetone at a 50:50 ratio to Cyrene™ lowered the energy consumption associated to the fabrication of these membranes, as polymer dissolution could take place at room temperature with stirring. This dissolution at room temperature without the need for any heat could possibly be due to the lower RED value of the solvent and polymer solution, indicating a higher affinity between the two [30]. Further to this, the cost of acetone is currently £45.50 per litre at Sigma Aldrich, while the cost of Cyrene™ is £182.00 per litre, the use of the solvent mixture also lowered the cost of the fabricated support.

The use of this polymer solvent mixture dope solution with a DI water coagulation bath, produced rough supports, see Figure 6.1. During interfacial polymerisation, the polyamide layer did not stick to the surface of the support and would fall off, thus deeming this support not fit for the required application.

Figure 6.1: Cellulose acetate support fabricated using a polymer dope solution of CA, Cyrene™ and acetone (50:50) using water as the non-solvent

Methanol was then used as a co-solvent mixture and added to the Cyrene™ dope solution at a 50:50 ratio, and the addition of methanol produced smooth supports suitable for filtration, see Figure 6.2. The boiling point of methanol is 64 °C, and the polymer dope solution was mixed at room temperature to successfully produce the solvent mixture polymer solution. The cost of methanol is currently £26.50 per Litre at Sigma Aldrich, cheaper than acetone, further reducing the cost associated with the fabrication of these membranes. In addition to this, methanol is also ranked as yellow on the CHEM21 list of solvents, [29].

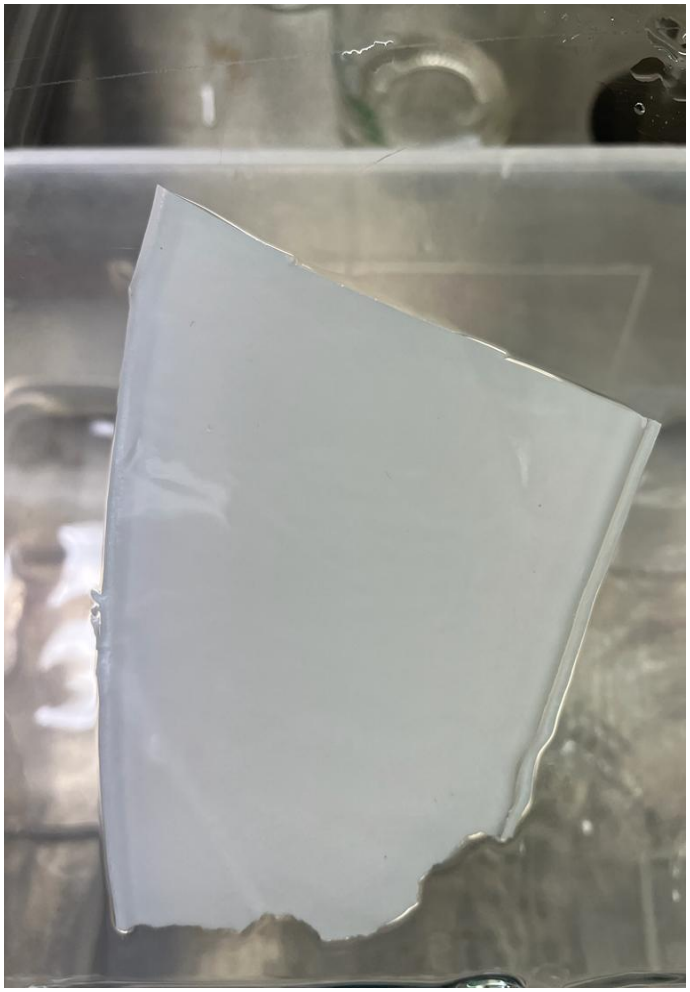

Figure 6.2: Cellulose acetate support fabricated using a polymer dope solution of CA, Cyrene™ and methanol (50:50) using water as the non-solvent

A CA-Cyrene™ dope solution was prepared, and a membrane was cast using this solution. The pure water permeance of the support was tested and found to be 190 L m^{-2} h^{-1} bar^{-1}. The pure water permeance of the 50:50 ratio of methanol and Cyrene™ support was tested and found to be 152 L m^{-2} h^{-1} bar^{-1}. The addition of methanol reduced the PWP from 190 L m^{-2} h^{-1} bar^{-1} to 152 L m^{-2} h^{-1} bar^{-1}, however, with the fabrication material and energy cost lowered for fabrication, the lower permeance value is acceptable as the selective layer will determine and affect the pure water flux.

6.2.2 Morphology

Cloud point measurements were conducted to characterise the thermodynamics of the polymer solutions. The points were plotted in a ternary phase diagram as shown in Figure 6.3. The CA-Cyrene™/methanol polymer solution was titrated with the non-solvent water by visualising the turbidity in the polymer solution. The binodal curve for the CA-Cyrene™/methanol-non-solvent system is closer to the polymer-non-solvent axis, indicating that the CA-Cyrene™/methanol solution can tolerate a higher non-solvent content. Similar to the supports fabricated in Chapter 4, the Cyrene™ based supports experienced a long phase inversion process of 5 minutes, but produced a porous support with macrovoids.

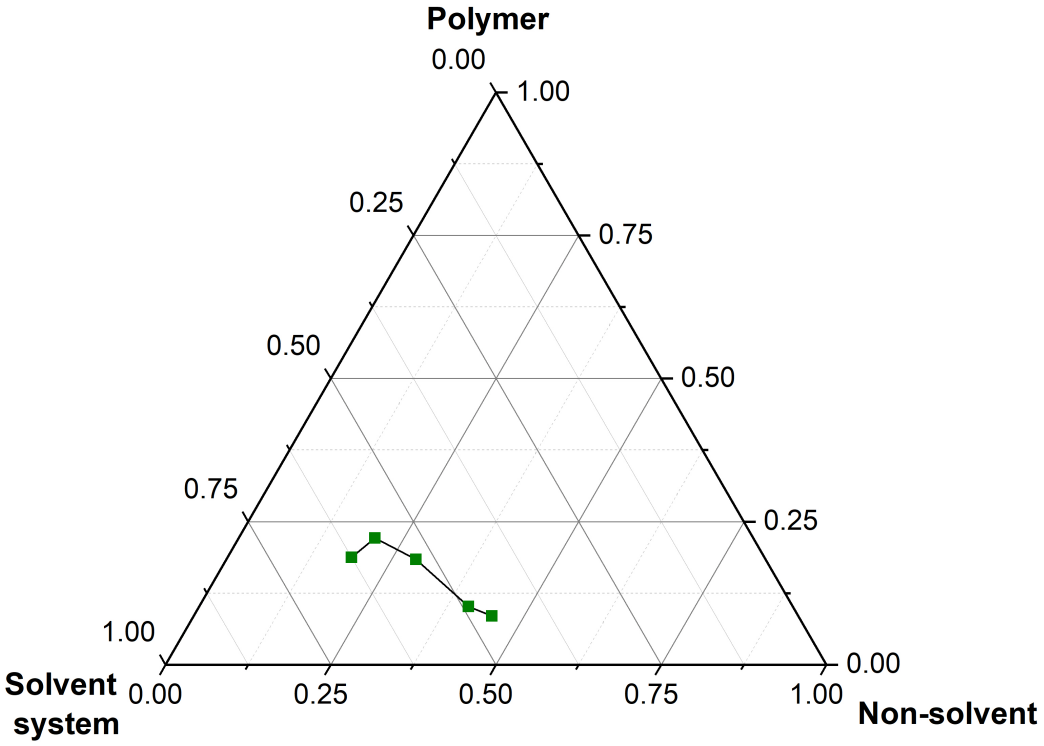

Figure 6.3: Ternary phase diagram of CA-Cyrene™/methanol-water polymer/solvent/non-solvent system

SEM was conducted to characterise the CA-Cyrene™/methanol support. The polymer dope solution produced asymmetric supports that had a porous spongy macro void structure, see Figure 6.4. The molecular weight cut off for the CA support was investigated using PEG molecular markers of different molecular weights ranging from 200-20,000 g/mol in an aqueous solution. The MWCO for the CA-Cyrene™/methanol was tested and found to be, 17,500 g/mol from the 90 % mark on the graph, see Figure 6.5. The combination of Cyrene™/methanol also produced supports in the microfiltration range, just as the Cyrene™/AA supports fabricated in Chapter 4.

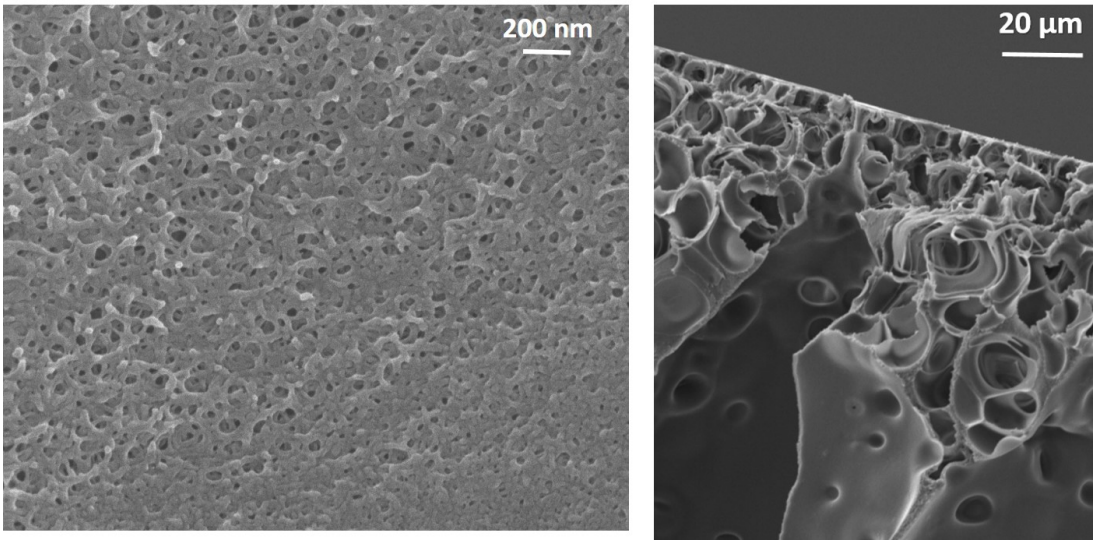

Figure 6.4: SEM images of the surface and cross-section of the CA- Cyrene™/methanol support

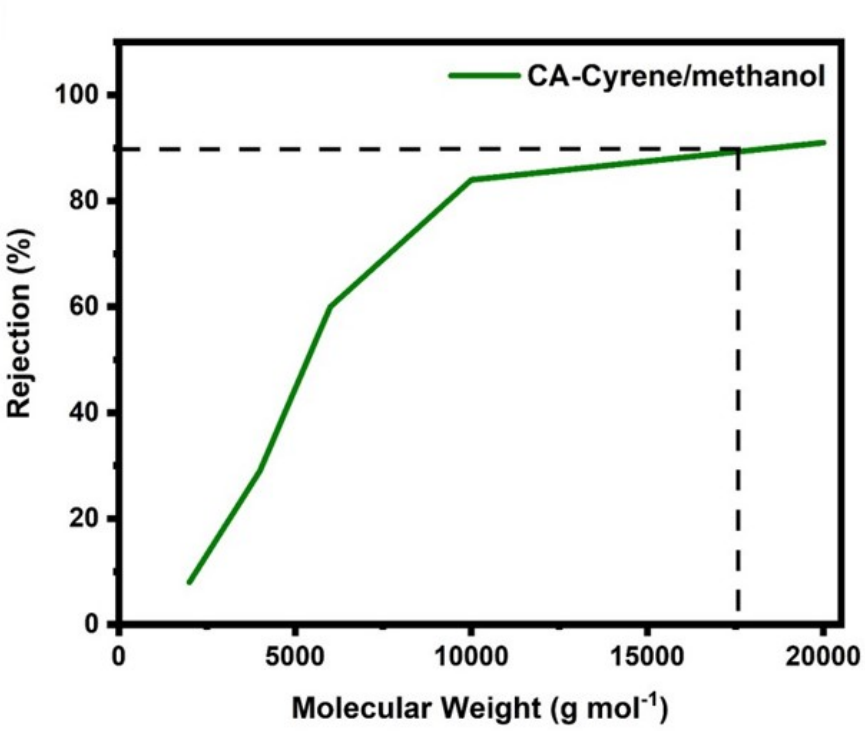

Figure 6.5: Molecular weight cut off for the CA-Cyrene™/methanol support, (MWCO= 17,500 g/mol)

6.3 Nanofiltration experiments

6.3.1 Pure water permeance

A TFC membrane was fabricated using the two selective layers, PA(n-hexane) and PA(2-MeTHF) developed in Chapter 5 and were deposited onto the CA-Cyrene™/methanol support. The pure water permeability of the two TFC membranes and NF 270 a commercial nanofiltration membrane was tested over 3-7 bar. The PA(2-MeTHF)/TFC experienced the highest pure water permeance compared to NF 270 and the PA(n-hexane)/TFC at 17.8 L m^{-2} h^{-1} bar^{-1}, 11.8 L m^{-2} h^{-1} bar^{-1} and 8.5 L m^{-2} h^{-1} bar^{-1} respectively at 7 bar.

The trend in the water permeance follows PA(2-MeTHF) > NF 270 > PA(n-hexane). The NF 270 pure water permeance was higher than the works reported by Kim *et al.,* at 11.8 L m^{-2} h^{-1} bar^{-1} and 8.9 L m^{-2} h^{-1} bar^{-1} respectively [32]. The trend of water permeance increase in the bio-renewable TFC was also experienced in Chapter 5, and can be ascribed to the looser structure of the PA(2-MeTHF) compared to the PA(n-hexane) as the former had a lower O/N ratio indicating a less cross-linked structure compared to the latter.

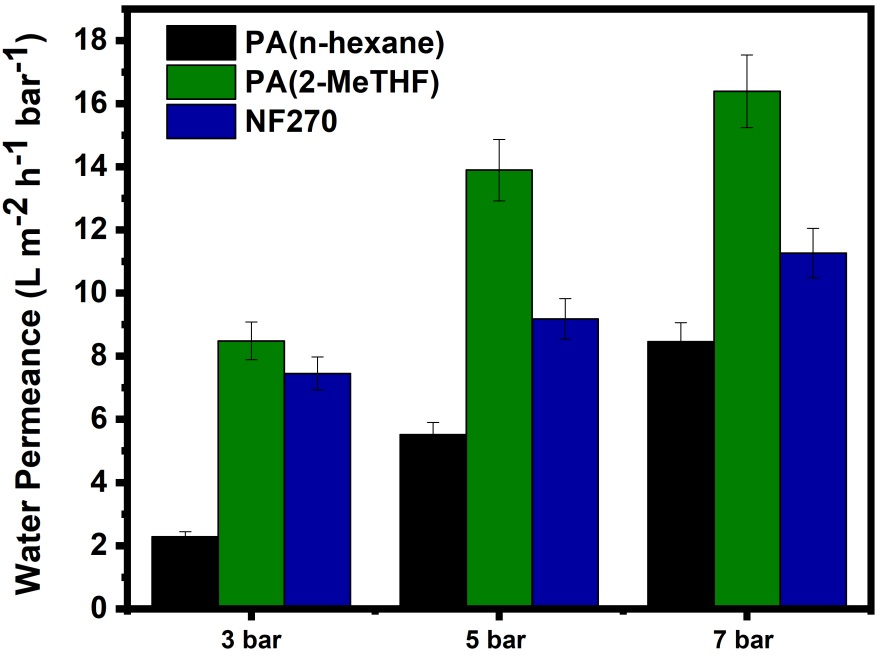

Figure 6.6: Pure water permeability of the membranes used in this work at different pressures

The molecular weight cut off for the three TFC membranes was investigated using PEG molecular markers of different molecular weights ranging from 200-20,000 g/mol in an aqueous solution. The MWCO for the PA(n-hexane) was found to be 300 g/mol from the 90 % rejection point at Figure 6.7 and the lower pore size of the membrane could contribute to the low pure water permeance that this membrane experienced. The MWCO for the PA(2-MeTHF)/TFC was found to be 800 g/mol and NF270 membrane was tested and found to be 580 g/mol. The NF 270 value reported here was higher than that reported by Kim *et al.,* and also that which is presented in the DOW data sheet of 200-300 g/mol [32], [33]. A possible reason for the increase in the MWCO for this membrane is that the sheet in which the membrane was taken from had a higher MWCO as there is sheet to sheet variation. This increase in the MWCO in the NF 270, could have contributed to the higher water permeance through the NF 270 TFC membrane. The trend in the MWCO

for the three membranes is in accordance with the pure water permeance at PA(2-MeTHF) > NF 270 > PA(n-hexane).

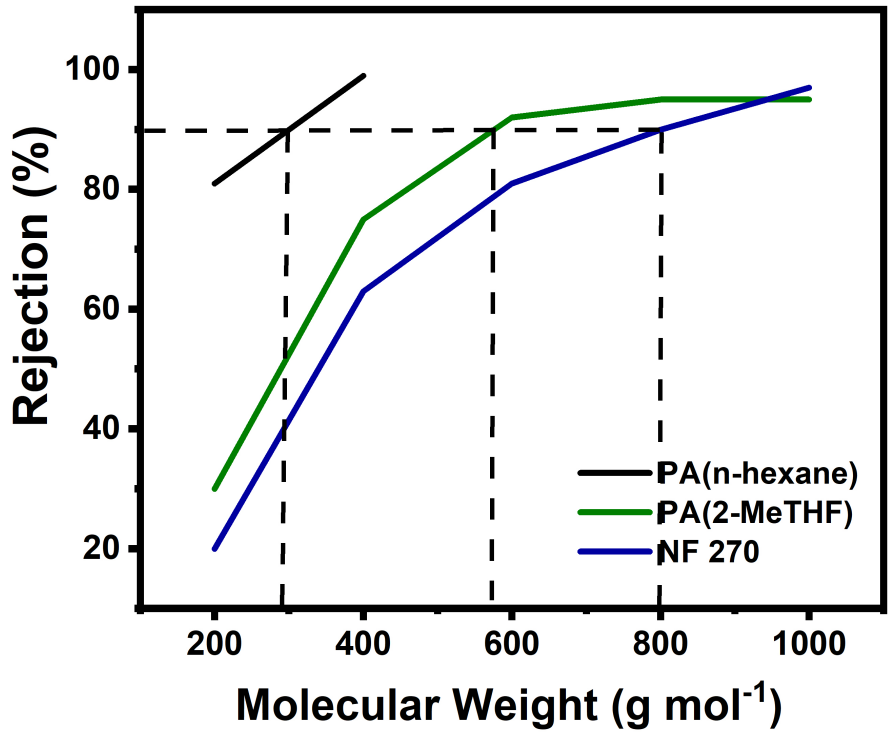

Figure 6.7: Molecular weight cut off for three TFC membranes used in this work, (PA(n-hexane)/TFC MWCO 300 g/mol, PA(2-MeTHF)/TFC MWCO 800 g/mol, NF 270 MWCO 800 g/mol)

The hydrophilicity of the three membranes was evaluated using contact angle measurements. This was carried out to investigate the wettability of the membrane surface as a lower value of contact angle often enhances water permeation through the membrane, as it experiences greater hydrophilicity [34]. The PA(2-MeTHF)/TFC experienced the greatest hydrophilicity at 23°, the PA(n-hexane)/TFC had a lower hydrophilicity of 47° and NF 270 exhibited the lowest water contact angle at 53°, see Figure 6.8.

The addition of the PA(2-MeTHF) selective layer onto the support increased the hydrophilicity of the support and aided the water permeance through the TFC membrane.

The trend in the contact angle measurements is not in accordance with the trend of the water permeance in the TFC membranes, PA(2-MeTHF) > PA(n-hexane) > NF 270 rather than, PA(2-MeTHF) > NF 270 > PA(n-hexane) the trend followed in water permeation. The results indicate that although the hydrophilicity of the membrane plays a role in water permeation through the membrane, the biggest contributing factor is the pore size of the membrane, as a higher pore size will allow for greater permeation through the membrane.

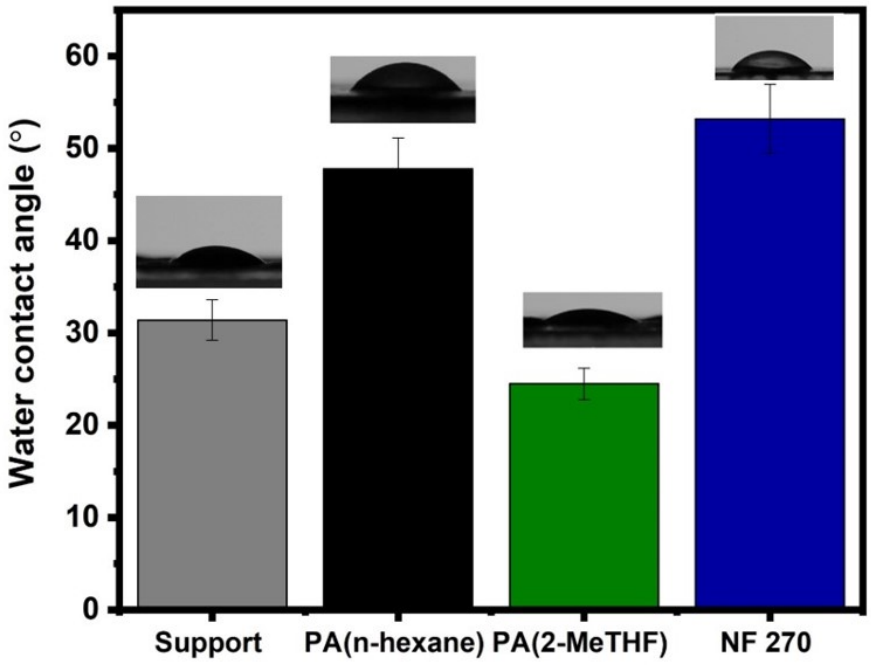

Figure 6.8: Water contact angle of the different membranes used in this work

6.3.2 Dye removal

The three TFC membranes, PA(2-MeTHF)/TFC and PA(n-hexane)/TFC and the NF 270 were tested for dye removal using five dyes of different molecular weights ranging from 1000 g/mol to 300 g/mol and varying positive and negative charges. A 50 ppm dye/water solution was used for filtration experiments, with an operating pressure of 5 bar. The properties of the dyes used in the experiment are found in Table 5.5. The feed solution

was constantly stirred at 700 rpm to avoid concentration polarisation. Figure 6.9 shows the dye removal of the three membranes.

The NF 270 membrane was able to exhibit 99.9 % rejection for all dyes, irrespective of the molecular weight and the charge. The rejection of the dyes increased as the molecular weight increased and all the dye rejections are above 99 %. The PA(2-MeTHF)/TFC membrane experienced a higher dye rejection than the PA(n-hexane)/TFC membrane, for example, Rose Bengal dye experienced a 99.8 % and 99.6 % rejection in the two respective membranes. The increase in dye rejection for the PA(2-MeTHF)/TFC compared to the PA(n-hexane)/TFC was also experienced in Chapter 5, and this could be ascribed to the presence of additional C=O groups in the membrane, see Figure 5.2 and Figure 5.3 in Section 5.1.2. The presence of additional C=O groups in the PA(2-MeTHF) caused further negativity in the charge of the selective layer [35]. This increase in charge allowed for a greater electrostatic repulsion from the dye and the selective layer and enhanced dye rejection [35], [36]. The selectivity between the NF 270 and PA(2-MeTHF)/TFC membranes are comparable, at 99.9 % and 99.8 % for Rose Bengal rejection and from this data, it can be concluded that the bio-renewable membrane could possibly compete with the commercial membrane on an industrial level.

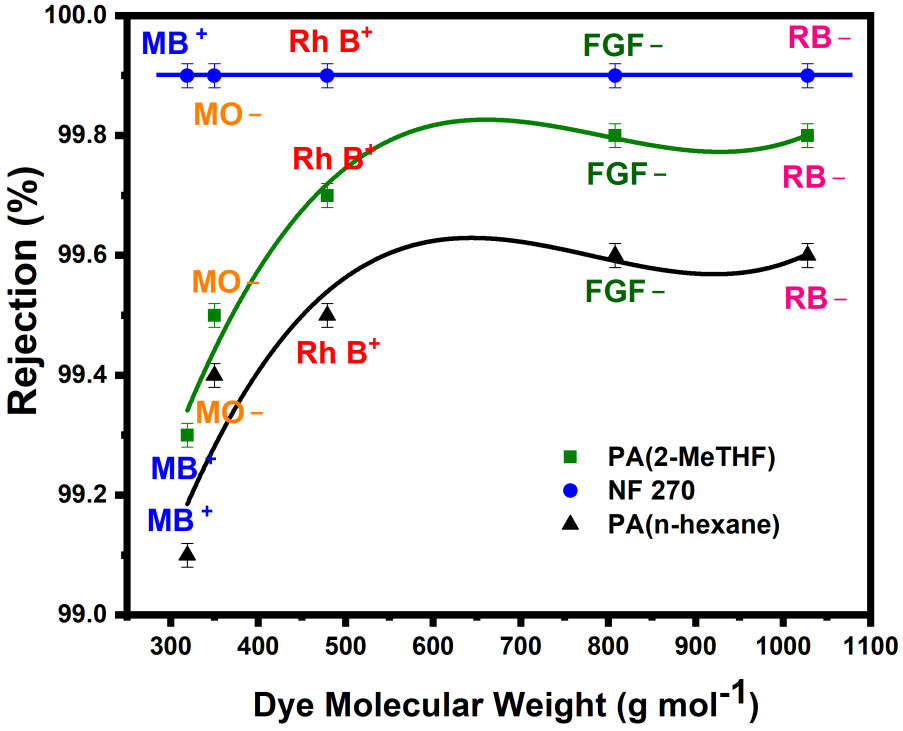

Figure 6.9: NF separation performance of the two membranes consisting of PA(n-hexane) and PA(2-MeTHF) selective layers and the NF 270 membrane (feed: 50 ppm dyes in water; pressure: 5bar)

6.3.3 Salt rejection

Different aqueous salt solutions consisting of Na_2SO_4, $MgSO_4$, $MgCl_2$, and NaCl at 1000 ppm were filtered through both TFC membranes at a pressure of 5 bar and tested for rejection, the molecular weight of these salts is given in Table 6.2.

Table 6.2: Molecular weight of salts

Salt	Molecular Weight (g mol^{-1})
Na_2SO_4	142.0
$MgSO_4$	120.3
$MgCl_2$	95.2
NaCl	54.4

The separation of the salts with the membranes was dominated mainly by size exclusion effects due to the molecular weight of the salts [13], [20], [37]. The molecular weights of the salts used in this experiment are listed in Table 6.2. For each salt, the PA(n-hexane)/TFC membrane performed better than the PA(2-MeTHF)/TFC membrane with higher salt rejection, for example for the salt Na_2SO_4 the two membranes experienced a rejection of 91 % and 63 % respectively. The order of rejection for salts for the two membranes was $Na_2SO_4 > MgSO_4 > MgCl_2 > NaCl$, which is also the order of the molecular weight.

The lower salt rejection for the PA(2-MeTHF)/TFC membrane can be attributed to the looser structure of the selective layer. Different characterisation techniques that were carried out in Chapter 5 for the two polyamides showed that the PA(n-hexane) had a more cross-linked structure than the PA(2-MeTHF) layer. This was validated with XPS and BET analysis, see Figure 5.4 and Figure 5.3 and Table 5.2 in Section 5.1.2. The looser structure was also determined through the MWCO for the two TFC membranes as the PA(n-hexane)/TFC exhibited a MWCO of 300 g/mol compared to the 800 g/mol, the MWCO for the PA(2-MeTHF). The molecular weight of the dyes that were used for dye removal experiments were high and in the range of 300-1000 g/mol. The salts used in this experiment had a lower molecular weight, ranging from 50-140 g/mol indicating that the selective layer is not able to reject lower molecular weight molecules and the rejection is governed by size exclusion for salt rejection as the rejection of both membranes decreased as the salt size decreased [37].

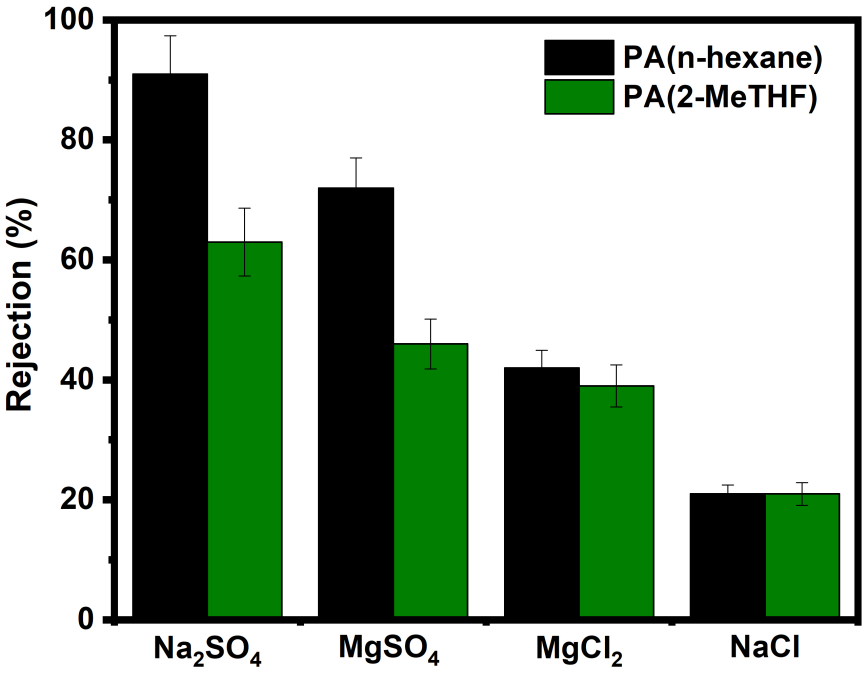

Figure 6.10: NF separation performance of the two membranes consisting of PA(n-hexane) and PA(2-MeTHF) selective layers (feed: 1000 ppm aqueous salt solution; pressure: 5bar)

Feed solutions consisting of $MgCl_2$ and NaCl were tested with the NF 270 membrane to compare the performance of the TFC membranes. The TFC membranes fabricated in this work experienced a higher rejection of $MgCl_2$ regardless of the selective layer at 42 % PA(n-hexane)/TFC, 39 % PA(2-MeTHF)/TFC and 36 % for the NF 270 TFC membrane. For NaCl however, NF 270 TFC membrane performed better, outperforming the PA(n-hexane) and PA(2-MeTHF) at 24 %, 21 % and 20 % respectively. The difference in rejection between the two salts can be ascribed to the difference in the valency of the salts. NaCl a monovalent salt and $MgCl_2$ a multivalent ion, nanofiltration membranes with the poly(piperazineamide) chemistry are able to reject organics such as dyes at high concentrations which was shown in section 6.3.2 and are able to reject divalent salts well which has been shown in the rejection of $MgCl_2$ [38].

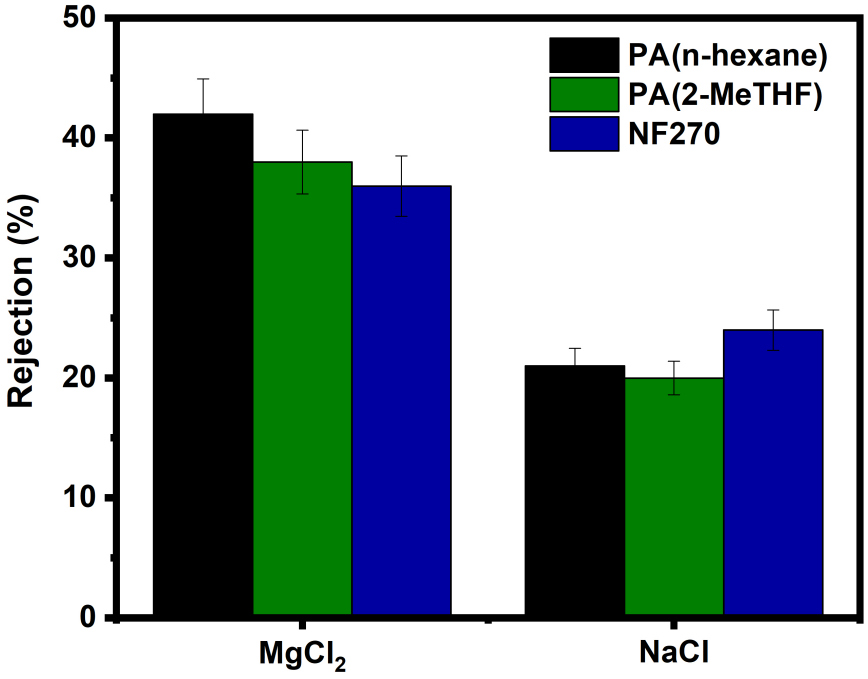

Figure 6.11: NF separation performance of the two membranes comprising of PA(n-hexane) and PA(2-MeTHF) selective layers and the NF 270 membrane (feed: 1000 ppm aqueous salt solution; pressure: 5bar)

6.3.4 Solvent activation

Solvent activation was employed on the three membranes using ethanol as the activation solvent, as the membranes were not stable in DMF or DMSO. Solvent activation was carried out to remove any contaminants or oligomers present within the membranes and to investigate the permeance and rejection increase that ethanol would present with the two selective layers produced in this work [39]. The Hildebrand solubility parameters of ethanol is similar to that of PA at 26.2 $MPa^{1/2}$ and 23 $MPa^{1/2}$ respectively indicating that it is a good activating solvent for the membranes [40], [41]. Ethanol was filtered through each membrane at 5 bar for 10 min for activation, the pure water permeance was tested at

different pressures and the salt rejection was measured using $MgCl_2$.

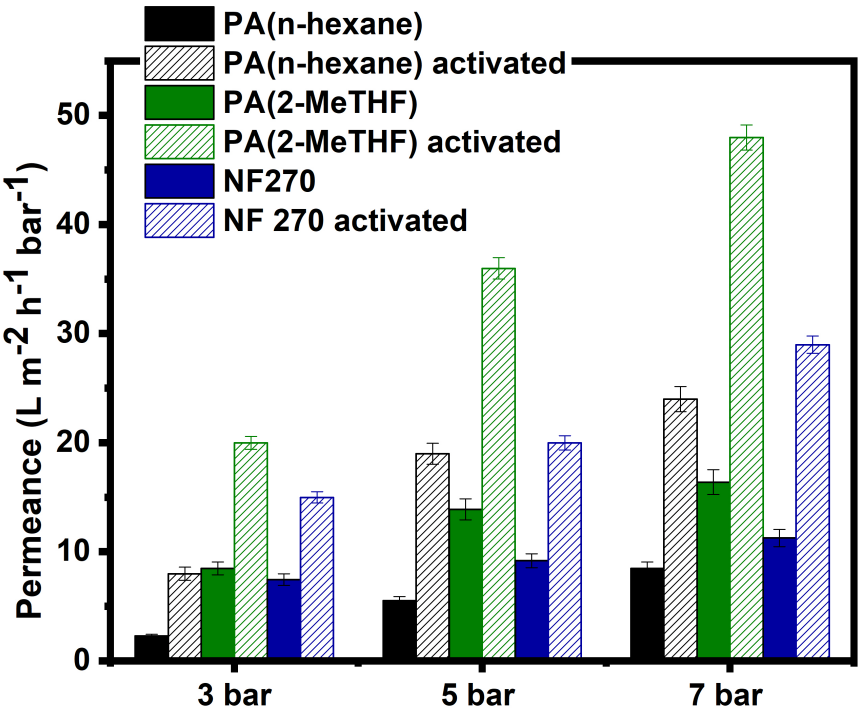

Figure 6.12: Pure water permeability of the membranes used in this work at different pressures before and after ethanol activation

The pure water permeability was tested at 3, 5 and 7 bar and for all the membranes the permeability increased considerably after activation. At 7 bar, each membrane experienced an increase of over 60 % and permeances reached 29 L m^{-2} h^{-1} bar^{-1} , 48 L m^{-2} h^{-1} bar^{-1} and 24 L m^{-2} h^{-1} bar^{-1} for the PA(n-hexane)/TFC, PA(2-MeTHF)/TFC and NF 270 TFC membrane respectively. This increase in water permeance is a common phenomenon that occurs after solvent activation that can be attributed to the opening of membrane pores that could have been blocked and the removal of any uncrosslinked polymer fragments in the PA layer before activation [42], [43]. Increase in water permeances when using ethanol for solvent activation was also experienced by Kulkarni *et al.* where water permeance increased by 70 % after activation [40].

The three membranes were tested with $MgCl_2$ and NaCl feed solutions after activation. The PA(n-hexane)/TFC experienced no change in salt rejection for both salts, and this was also experienced with dye rejection in Chapter 5 as the rejection remained the same after activation. The PA(2-MeTHF)/TFC experienced a slight decrease in salt rejection from 21 % in NaCl to 20 % after activation, this was also experienced in $MgCl_2$ as the salt rejection decreased from 39 % to 38 %. This was also experienced for the dye rejection in Chapter 5, the swelling of PA(2-MeTHF) was lower in solvents compared to PA(n-hexane) so the same effect could not be experienced. The NF 270 TFC membrane experienced a slight increase in salt rejection, as $MgCl_2$ salt rejection increased slightly from 36 % to 37 %, and this phenomena was also experienced by Kulkarni *et al.*, where the salt rejection increased slightly from 70 % to 75 % after ethanol activation [40].

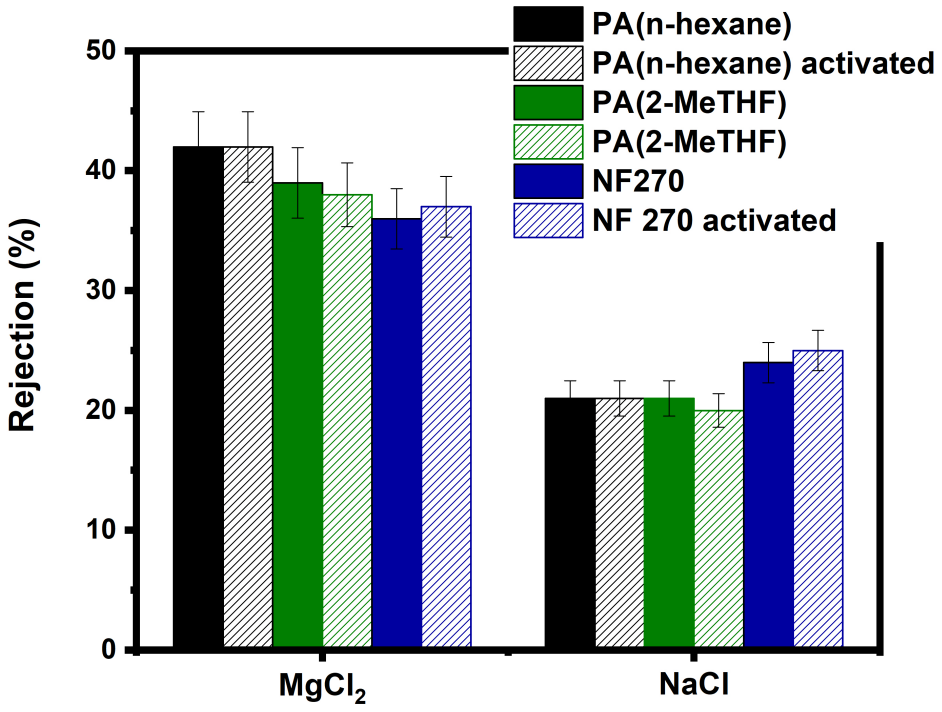

Figure 6.13: NF separation performance of the two membranes consisting of PA(n-hexane) and PA(2-MeTHF) selective layers and the NF 270 membrane before and after ethanol activation (feed: 1000 ppm aqueous salt solution; pressure: 5bar)

6.4 Conclusion

The work presented in this chapter looked at producing a TFC membrane devoid of heating, as membrane fabrication was able to proceed at room temperature. Polymer dope solutions were formed with two solvents were used that were both ranked as yellow, (problematic) on the CHEM21 ranking and this is a step change from solvents that are primarily used that ranked as hazardous. The selective layers that were established in Chapter 5 were deposited onto the support to produce a TFC membrane. A commercial NF 270 membrane with the same selective layer polyamide chemistry was used to compare the bio-renewable membrane produced in this work to current commercially available membranes. The TFC membranes were characterised using pure water permeance, water contact angle and the molecular weight cut off. Nanofiltration experiments were carried out containing various dye solutions and also various salt solutions.

The study found that the size exclusion effect was the major governing factor for separation in the three membranes. Dyes with a molecular weight ranging from 300-1000 g/mol experienced higher rejections compared to salts of molecular weights 50-140 g/mol. The selectivity of Rose Bengal dye between the NF 270 and PA(2-MeTHF)/TFC membranes were comparable, at 99.9 % and 99.8 % for Rose Bengal, indicating that the bio-renewable membrane could compete with the commercial membrane. For the multivalent salt, $MgCl_2$ the PA(2-MeTHF)/TFC membranes performed better than the commercial NF 270 TFC membrane and rejection reached 39 % and 36 % respectively. Further to this, the pure water permeation reached 17.8 L m^{-2} h^{-1} bar^{-1} for the PA(2-MeTHF)/TFC membrane, compared to 11.8 L m^{-2} h^{-1} bar^{-1} for the commercial NF 270 TFC membrane. Ethanol activation was also explored and the permeance for all three membranes increased by 60 % and the salt rejection for the PA(n-hexane)/TFC remained constant, the rejection slightly decreased for the PA(2-MeTHF)/TFC membrane and slightly increased for the NF 270 membrane.

6.4. Conclusion

The results presented in this chapter indicate that the combination of the bio-renewable solvents used for TFC membrane fabrication outperforms the commercial NF 270 membrane in terms of greater selectivity in both dye and salts. Higher throughputs in terms of water permeation could be experienced if the commercial membranes were substituted with the bio-renewable TFC membrane.

References

[1] J. Glater, "The early history of reverse osmosis membrane development," *Desalination*, vol. 117, no. 1-3, pp. 297–309, 1998.

[2] R. W. Baker, *Membrane technology and applications*. John Wiley and Sons, 2012.

[3] S. Loeb and S. Sourirajan, "Sea water demineralization by means of an osmotic membrane," in ACS Publications, 1962.

[4] R. Haddada, E. Ferjani, M. S. Roudesli, and A. Deratani, "Properties of cellulose acetate nanofiltration membranes. application to brackish water desalination," *Desalination*, vol. 167, pp. 403–409, 2004.

[5] M. Safarpour, V. Vatanpour, and A. Khataee, "Preparation and characterization of graphene oxide/tio2 blended pes nanofiltration membrane with improved antifouling and separation performance," *Desalination*, vol. 393, pp. 65–78, 2016.

[6] S. Amiri, A. Asghari, V. Vatanpour, and M. Rajabi, "Fabrication and characterization of a novel polyvinyl alcohol-graphene oxide-sodium alginate nanocomposite hydrogel blended pes nanofiltration membrane for improved water purification," *Separation and Purification Technology*, vol. 250, p. 117 216, 2020.

[7] M. Peydayesh, T. Mohammadi, and S. K. Nikouzad, "A positively charged composite loose nanofiltration membrane for water purification from heavy metals," *Journal of Membrane Science*, vol. 611, p. 118 205, 2020.

[8] P. Daraei, S. S. Madaeni, N. Ghaemi, H. A. Monfared, and M. A. Khadivi, "Fabrication of pes nanofiltration membrane by simultaneous use of multi-walled carbon nanotube and surface graft polymerization method: Comparison of mwcnt and paa modified mwcnt," *Separation and purification technology*, vol. 104, pp. 32–44, 2013.

[9] C. Liu, W. Wang, L. Zhu, *et al.*, "High-performance nanofiltration membrane with structurally controlled pes substrate containing electrically aligned cnts," *Journal of Membrane Science*, vol. 605, p. 118 104, 2020.

[10] S. Pourjafar, A. Rahimpour, and M. Jahanshahi, "Synthesis and characterization of pva/pes thin film composite nanofiltration membrane modified with tio2 nanoparticles for better performance and surface properties," *Journal of Industrial and Engineering Chemistry*, vol. 18, no. 4, pp. 1398–1405, 2012.

[11] S. Hosseini, M. Afshari, A. Fazlali, *et al.*, "Mixed matrix pes-based nanofiltration membrane decorated by (fe3o4–polyvinylpyrrolidone) composite nanoparticles with intensified antifouling and separation characteristics," *Chemical Engineering Research and Design*, vol. 147, pp. 390–398, 2019.

[12] N. Zaghbani, A. Hafiane, and M. Dhahbi, "Removal of safranin t from wastewater using micellar enhanced ultrafiltration," *Desalination*, vol. 222, no. 1-3, pp. 348–356, 2008.

[13] N. Misdan, W. Lau, A. Ismail, and T. Matsuura, "Formation of thin film composite nanofiltration membrane: Effect of polysulfone substrate characteristics," *Desalination*, vol. 329, pp. 9–18, 2013.

[14] R. Du and J. Zhao, "Properties of poly (n, n-dimethylaminoethyl methacrylate)/polysulfone positively charged composite nanofiltration membrane," *Journal of membrane science*, vol. 239, no. 2, pp. 183–188, 2004.

[15] N. Ghaemi, S. S. Madaeni, A. Alizadeh, *et al.*, "Fabrication and modification of polysulfone nanofiltration membrane using organic acids: Morphology, characterization and performance in removal of xenobiotics," *Separation and purification technology*, vol. 96, pp. 214–228, 2012.

[16] R. Du and J. Zhao, "Positively charged composite nanofiltration membrane prepared by poly (n, n-dimethylaminoethyl methacrylate)/polysulfone," *Journal of applied polymer science*, vol. 91, no. 4, pp. 2721–2728, 2004.

[17] R. Derakhsheshpoor, M. Homayoonfal, A. Akbari, and M. R. Mehrnia, "Amoxicillin separation from pharmaceutical wastewater by high permeability polysulfone nanofiltration membrane," *Journal of Environmental Health Science and Engineering*, vol. 11, no. 1, pp. 1–10, 2013.

[18] A. Mollahosseini and A. Rahimpour, "Interfacially polymerized thin film nanofiltration membranes on tio2 coated polysulfone substrate," *Journal of Industrial and Engineering Chemistry*, vol. 20, no. 4, pp. 1261–1268, 2014.

[19] F. Peng, X. Huang, A. Jawor, and E. M. Hoek, "Transport, structural, and interfacial properties of poly (vinyl alcohol)–polysulfone composite nanofiltration membranes," *Journal of Membrane Science*, vol. 353, no. 1-2, pp. 169–176, 2010.

[20] N. Misdan, W. Lau, A. Ismail, T. Matsuura, and D. Rana, "Study on the thin film composite poly (piperazine-amide) nanofiltration membrane: Impacts of physicochemical properties of substrate on interfacial polymerization formation," *Desalination*, vol. 344, pp. 198–205, 2014.

[21] S. P. Sun, K. Y. Wang, N. Peng, T. A. Hatton, and T.-S. Chung, "Novel polyamide-imide/cellulose acetate dual-layer hollow fiber membranes for nanofiltration," *Journal of Membrane Science*, vol. 363, no. 1-2, pp. 232–242, 2010.

[22] R. M. Narbaitz, D. Rana, H. T. Dang, *et al.*, "Pharmaceutical and personal care products removal from drinking water by modified cellulose acetate membrane: Field testing," *Chemical Engineering Journal*, vol. 225, pp. 848–856, 2013.

[23] J. Caloca, L. Z. Flores-Lopez, H. Espinoza-Gomez, E. L. Sotelo-Barrera, A. Nunez-Rivera, and R. D. Cadena-Nava, "Silver nanoparticles supported on polyethylene glycol/cellulose acetate ultrafiltration membranes: Preparation and characterization of composite," *Cellulose*, vol. 24, no. 11, pp. 4997–5012, 2017.

[24] H. Kaur, V. K. Bulasara, and R. K. Gupta, "Influence of ph and temperature of dip-coating solution on the properties of cellulose acetate-ceramic composite membrane for ultrafiltration," *Carbohydrate polymers*, vol. 195, pp. 613–621, 2018.

[25] B. Tarus, N. Fadel, A. Al-Oufy, and M. El-Messiry, "Effect of polymer concentration on the morphology and mechanical characteristics of electrospun cellulose acetate and poly (vinyl chloride) nanofiber mats," *Alexandria Engineering Journal*, vol. 55, no. 3, pp. 2975–2984, 2016.

[26] H. Idress, S. Zaidi, A. Sabir, *et al.*, "Cellulose acetate based complexation-nf membranes for the removal of pb (ii) from waste water," *Scientific Reports*, vol. 11, no. 1, pp. 1–14, 2021.

[27] J.-H. Choi, K. Fukushi, and K. Yamamoto, "A submerged nanofiltration membrane bioreactor for domestic wastewater treatment: The performance of cellulose acetate nanofiltration membranes for long-term operation," *Separation and purification technology*, vol. 52, no. 3, pp. 470–477, 2007.

[28] A. Figoli, C. Ursino, S. Santoro, *et al.*, "Cellulose acetate nanofiltration membranes for cadmium remediation," *Journal of Membrane Science and Research*, vol. 6, no. 2, pp. 226–234, 2020.

[29] D. Prat, A. Wells, J. Hayler, *et al.*, "Chem21 selection guide of classical-and less classical-solvents," *Green Chemistry*, vol. 18, no. 1, pp. 288–296, 2015.

[30] M. A. Rasool, P. P. Pescarmona, and I. F. Vankelecom, "Applicability of organic carbonates as green solvents for membrane preparation," *ACS Sustainable Chemistry and Engineering*, vol. 7, no. 16, pp. 13 774–13 785, 2019.

[31] T. Marino, F. Galiano, A. Molino, and A. Figoli, "New frontiers in sustainable membrane preparation: Cyrene as green bioderived solvent," *Journal of membrane science*, vol. 580, pp. 224–234, 2019.

[32] D. W. Kim, J. Choi, D. Kim, and H.-T. Jung, "Enhanced water permeation based on nanoporous multilayer graphene membranes: The role of pore size and density," *Journal of Materials Chemistry A*, vol. 4, no. 45, pp. 17 773–17 781, 2016.

[33] E. Kurt, D. Y. Koseoglu-Imer, N. Dizge, S. Chellam, and I. Koyuncu, "Pilot-scale evaluation of nanofiltration and reverse osmosis for process reuse of segregated textile dyewash wastewater," *Desalination*, vol. 302, pp. 24–32, 2012.

[34] A. Miao, M. Wei, F. Xu, and Y. Wang, "Influence of membrane hydrophilicity on water permeability: An experimental study bridging simulations," *Journal of Membrane Science*, vol. 604, p. 118 087, 2020.

[35] D. Chen, J. R. Werber, X. Zhao, and M. Elimelech, "A facile method to quantify the carboxyl group areal density in the active layer of polyamide thin-film composite membranes," *Journal of Membrane Science*, vol. 534, pp. 100–108, 2017.

[36] M. Paul and S. D. Jons, "Chemistry and fabrication of polymeric nanofiltration membranes: A review," *Polymer*, vol. 103, pp. 417–456, 2016.

[37] A. W. Mohammad, Y. Teow, W. Ang, Y. Chung, D. Oatley-Radcliffe, and N. Hilal, "Nanofiltration membranes review: Recent advances and future prospects," *Desalination*, vol. 356, pp. 226–254, 2015.

[38] C. Y. Tang, Y.-N. Kwon, and J. O. Leckie, "Effect of membrane chemistry and coating layer on physiochemical properties of thin film composite polyamide ro and nf membranes: I. ftir and xps characterization of polyamide and coating layer chemistry," *Desalination*, vol. 242, no. 1-3, pp. 149–167, 2009.

[39] T.-D. Lu, B.-Z. Chen, J. Wang, *et al.*, "Electrospun nanofiber substrates that enhance polar solvent separation from organic compounds in thin-film composites," *Journal of Materials Chemistry A*, vol. 6, no. 31, pp. 15 047–15 056, 2018.

[40] A. Kulkarni, D. Mukherjee, and W. N. Gill, "Flux enhancement by hydrophilization of thin film composite reverse osmosis membranes," *Journal of Membrane Science*, vol. 114, no. 1, pp. 39–50, 1996.

[41] S.-J. Xu, Q. Shen, Z.-L. Xu, and Z.-Q. Dong, "Novel designed tfc membrane based on host-guest interaction for organic solvent nanofiltration (osn)," *Journal of Membrane Science*, vol. 588, p. 117 227, 2019.

[42] M. F. J. Solomon, Y. Bhole, and A. G. Livingston, "High flux membranes for organic solvent nanofiltration (osn)—interfacial polymerization with solvent activation," *Journal of membrane science*, vol. 423, pp. 371–382, 2012.

[43] J. H. Kim, S. J. Moon, S. H. Park, M. Cook, A. G. Livingston, and Y. M. Lee, "A robust thin film composite membrane incorporating thermally rearranged polymer support for organic solvent nanofiltration and pressure retarded osmosis," *Journal of Membrane Science*, vol. 550, pp. 322–331, 2018.

Chapter 7

Conclusion and Future Work

In recent years, works reported in the literature have been invested in embedding sustainability into membrane fabrication and designing new membrane materials. The works have been detailed in Chapter 2, the Literature Review section of this thesis and the work carried out in this thesis extended the current work. This thesis looked at the replacement of hazardous and toxic petroleum-derived solvents with benign bio-renewable alternatives in thin film composite membrane fabrication, in line with several principles of Green Chemistry. Membranes were successfully fabricated and applied in both organic and aqueous nanofiltration applications.

An ideal green solvent for fabrication should have reduced hazards associated with the solvent and be produced with renewable resources. The solvents should be easily degradable and have little to no toxicity and also little to no volatile organic compounds. Further to this, an ideal green solvent should be available worldwide at a low cost. The two solvents used in this work, Cyrene™ and 2-MeTHF, both fit into the description of an ideal green solvent.

The biggest disadvantage with the use of bio-renewable solvents is the cost associated with them, today (June 2022) at Sigma Aldrich solvent prices for 1 Litre are: n-hexane £61, 2-MeTHF £167, DMF £96.30 and Cyrene™ at £182. The bio-renewable solvents are substantially more expensive than petroleum-derived solvents. As membrane fabrication is solvent-intensive, the costs associated with the production of membranes produced using bio-renewable solvents are significant. The availability of the solvents however is better as they are available worldwide with next-day delivery through Sigma Aldrich. When the work in this thesis first started in 2018, Cyrene™ was only available through the Circa Group with a lead time of six months, and this has now come a long way since then. As the use of the solvents increases and the applications for them increases, the cost associated with them will reduce, making them an affordable option.

In this work, a comparative study was carried out changing the solvents from petroleum derived to bio-renewable alternatives, the fabrication conditions, however, were identical.

Because of this, the e factor and the solvent intensity were not calculated [1]. However, the health, safety and environmental scores from the CHEM21 solvent selection guide were investigated to see how the change in solvent affected the scores and the green metrics of TFC membrane fabrication are shown in Table 7.1. The total score for Cyrene™ is 10, which is the same as "Recommended" solvents such as ethanol, isopropanol and butanol suggested by the CHEM21 solvent selection guide [2]. Similar to NMP, the high boiling point of Cyrene™ (Cyrene™: 226 °C and NMP: 202 °C), makes it difficult to treat and recover, hence it is classified as a "problematic" solvent. However, the health and safety score for Cyrene™ and DMF is 2 and 1 respectively and the use of this solvent reduces the health implications considerably, which is highly favourable.

The use of 2-MeTHF for the polyamide selective layer reduces the total score from 18 (n-hexane) to 14, where 2-MeTHF is more environmentally friendly. The safety score of n-hexane and 2-MeTHF, two solvents with low boiling points, is identical, as these solvents can vaporise easily, forming flammable mixtures. Amongst the organic solvents suitable for IP, such as n-hexane and heptane, 2-MeTHF is the ideal candidate with the lowest total score. The work in this thesis demonstrates that it is feasible to replace petroleum-derived solvents with bio-renewable alternatives to improve the green metric of these processes. For example, the total solvent score for the traditional TFC fabrication protocol is 35 (18 for hexane, and 17 for DMF). The sole use of bio-solvents in the same process was calculated to be 24 and the total solvent score was reduced by 45 % indicating that the health and safety and environmental are many with the change in solvents.

Table 7.1: Comparison of the green metrics from the CHEM21 Solvent Selection Guide for the replacement solvents, 2-MeTHF and Cyrene, with petroleum-derived solvents deployed in a typical TFC membrane fabrication protocol – hexane and NMP or DMF, all values taken from [2]

	Solvents	Safety score	Health score	Environmental score	Total	Category
Selective layer	Hexane	8	3	7	18	Hazardous
	Heptane	6	2	7	15	Problematic
	2-MeTHF	6	5	3	14	Problematic
Support	DMF	3	9	5	17	Hazardous
	NMP	1	9	7	17	Hazardous
	Cyrene™	1	2	7	10	Problematic

The key findings of each chapter will be presented here. The advantages of deploying bio-renewable solvents for membrane fabrication that were experienced during this work will also be presented. Recommendations will also be given on how the work in each chapter could be further progressed.

7.1 Key findings in Chapter 4

Cyrene™, a bio-renewable solvent, was used as an alternative to petroleum-derived DMF to fabricate a support for organic solvent nanofiltration applications. Firstly, the most conventional polymer used for OSN applications, polyimide, was dissolved in Cyrene™ and a rough support was produced. This support could not be used as the foundation for interfacial polymerisation, therefore it could not be utilised for thin film composite membrane fabrication. Cellulose acetate was the polymer that was later explored and successfully produced smooth supports.

The study showed that Cyrene™, a bio-renewable solvent, can be used as an alternative for petroleum-derived DMF to successfully produce a cellulose acatate support. A quick (90 mins) low alkali (0.05 M KOH) deacetylation process was used to produce supports that were stable in harsh organic solvent systems, thus deeming them appropriate for use in OSN applications. The combination of Cyrene™ and acetic acid produced supports that exhibited excellent permeance of solvents, and a 115% increase was experienced for water permeation compared to the RC-DMF support. The bio-renewable solvent-derived support exhibited better thermal stability compared to RC-DMF at high temperatures. Protocols were established that produced supports that maintained structural integrity and excellent stability in DMF immersion at 100 °C. The supports were stable in harsh organic solvents and performed well in different solvent environments. Further to the performance of the support, the health and safety and environmental benefits of changing the solvents are also highly advantageous, as the hazards and risks associated with the use

of Cyrene™ are lower compared to DMF.

7.1.1 Future work for Chapter 4

The most commonly used polymer PI for OSN membrane fabrication was not able to produce supports with the solvent Cyrene™. Although substantial experimental work was carried out to mitigate the wrinkles that were produced on the support, they were all unsuccessful as wrinkles were always produced despite changing different fabrication parameters. In addition to the experimental work, the Hansen solubility parameters suggested that the polymer/solvent/non-solvent system was favourable. Further work could be carried out to investigate how the polymer, solvent and non-solvent interact and why this system in particular (PI/Cyrene™/water) was not compatible.

The work in this chapter presented a few interesting results. Supports that are predominantly produced using a high polymer concentration (17.5 wt.%) are usually in the nanofiltration range in terms of pore size [3], [4]. However, supports produced in this work with the Cyrene™ solvent system exhibited microfiltration pore sizes of 790 nm [3]. Further to this, a delayed demixing during phase inversion predominantly produces supports that have less porosity and exhibit a nodular structure [3], [5], [6]. However, this was not the case for the Cyrene™ based membranes, the phase inversion time was considerably longer for the Cyrene™ based supports compared to the DMF-based supports at 663 s and 53 s respectively. The Cyrene™ based support exhibited higher porosity compared to the DMF support with an MWCO of 10,500 g/mol and 590 g/mol respectively. The kinetics of phase inversion with Cyrene™ could be investigated to explore how the solvent adds porosity to the supports fabricated using this solvent. Other green solvents such as methyl lactate, G-Valerolactone, glycerol formal and diacetin have been reported, and they all produce supports that are suitable for nanofiltration [4], [7]–[9].

The use of Cyrene™ has opened a whole avenue of exploration in membrane fabrication.

Future work building on this chapter could include the investigation of a wide range of polymers such as PES, PVDF, PSf, PAN, PANi and PBI support fabrication. Different thin film composite membranes could be fabricated to investigate the feasibility of these different polymer membranes in both aqueous and organic solvent nanofiltration applications. The cross-linking step that is required for OSN membranes could be altered with a focus on sustainability and can possibly redefine the conventional protocols that are used. Further to this, the supports could be used in microfiltration applications without the addition of a selective layer and the use of the Cyrene™ based supports could be investigated to see how they compare with the current state-of-the-art MF supports.

Finally, the support produced with the Cyrene™ solvent system was unstable in chlorinated environments. The results from the solvent immersion tests showed that the supports dissolved quicker in the chlorinated solvents at 8.1 % for the Cyrene™ based solvent compared to 1.9 % for the DMF-based support. In addition to this, the permeation of the chlorinated solvents was less through the Cyrene™ supports at 7 L m^{-2} h^{-1} bar^{-1} compared to 5.6 L m^{-2} h^{-1} bar^{-1} for the DMF based support in chloroform. All other solvents experienced at least a 100 % increase in solvent permeation through the Cyrene™ based support. Further work could be carried out to explore why the Cyrene™ based support is unstable in the chlorinated solvents and if this extends to other polymers or only cellulose acetate.

7.2 Key findings in Chapter 5

In this chapter, the solvent for interfacial polymerisation was changed from n-hexane, a hazardous petroleum-derived solvent to a benign bio-renewable solvent, 2-MeTHF. The resultant film produced using 2-MeTHF exhibited greater chemical resistance in DMF and THF compared to the n-hexane-derived film. However, the 2-MeTHF derived polymer had less microporosity, the yields of the films were 22 times less than the conventional films

and the O/N ratio indicated that the film was less cross-linked compared to the n-hexane derived film indicating that n-hexane is a better solvent for interfacial polymerisation [10].

The addition of these films onto the regenerated cellulose support produced in Chapter 4 created a thin film composite membrane produced solely from green solvents. Optimal IP parameters were explored for the 2-MeTHF polymer to find a trade-off between selectivity and permeability and the TFC membranes PA(2-MeTHF)/RC and PA(n-hexane)/RC were tested for OSN applications. The PA(2-MeTHF)/RC TFC membrane exhibited increased hydrophilicity due to additional carboxylic acid groups that were present in the film, allowing for greater ethanol permeance at 11.2 L m^{-2} h^{-1} bar^{-1} compared to 2.5 L m^{-2} h^{-1} bar^{-1} experienced with PA(n-hexane)/RC TFC membrane. The permeance further increased to reach 25 L m^{-2} h^{-1} bar^{-1} after DMF activation and 20 L m^{-2} h^{-1} bar^{-1} after DMSO activation for the bio-renewable solvent based TFC membrane. The bio-renewable membrane experienced higher dye rejections compared to PA(n-hexane) over a molecular weight range from 300 to 1000 g/mol and all rejections were above 90 %.

The separation performance of TFC membranes fabricated solely using bio-renewable solvents in this chapter outperformed the polymer membranes produced using petroleum-derived solvents and different OSN membranes that have been reported in literature using the same ethanol and Rose Bengal feed stream. The work showed that the bio-renewable solvent-based TFC membrane surpassed not only the current protocols used for TFC membrane fabrication but also mixed matrix membranes that have fillers such as metal-organic frameworks embedded in them to enhance permeance and selectivity.

7.2.1 Future work for Chapter 5

The work carried out in this chapter provided a foundation for a new polyamide fabricated using 2-MeTHF via interfacial polymerisation. Although the PA(2-MeTHF) polymer has been characterised well, there can be other characterisation that can be carried

out that was outside the scope of this work. This includes: finding the molecular weight of the two polymers, and further investigation into the different yields of the two polymers. The formation of the film differs as the PA(n-hexane) is produced as a thin film and the remnants of the film are in the organic phase, on the other hand, the PA(2-MeTHF) is produced as microbubbles with the remnants in the aqueous phase. Further exploration into the interfacial polymerisation kinetics when using 2-MeTHF would give an indication as to why a bubble was produced rather than a film and what factors affect interfacial polymerisation film formation.

7.3 Key findings in Chapter 6

The work presented in this chapter looked at producing a TFC membrane devoid of heating, as membrane fabrication was able to proceed at room temperature. The selective layers that were established in Chapter 5 were deposited onto the support to produce a TFC membrane, and the performance of this membrane was tested against a commercially available DOW NF 270 TFC membrane.

The membranes were characterised with different salt and dye solutions to test the selectivity of the membrane. Further to this, the pure water permeability over a range of pressures was also tested. The study found that the size exclusion effect was the major governing factor for separation in the two membranes. Dyes with a molecular weight ranging from 300-1000 g/mol experienced higher rejections compared to salts of molecular weights 50-140 g/mol. Dye rejection reached 99.9 % for the NF 270 TFC membrane, and this was comparable to the bio-renewable based TFC membrane at 99.8 %. For the multivalent salt, $MgCl_2$ the PA(2-MeTHF)/TFC membranes performed better than the commercial NF 270 TFC membrane and rejection 39 % and 36 % respectively. The pure water permeance in the PA(2-MeTHF)/TFC membranes was also higher than the NF 270 TFC membrane at 17.8 L m^{-2} h^{-1} bar^{-1} and 11.8 L m^{-2} h^{-1} bar^{-1} respectively. Ethanol

activation was also explored and the permeance for all three membranes increased by 60 % and the salt rejection for the PA(n-hexane)/TFC remained constant, the rejection slightly decreased for the PA(2-MeTHF)/TFC membrane and slightly increased for the NF 270 membrane.

7.3.1 Future work for Chapter 6

The comparison between NF 270 and the bio-renewable TFC produced using Cyrene™ and 2-MeTHF proved to be very promising. The bio-renewable TFC membrane exhibited better water permeance, comparable dye rejection and better divalent salt rejection, indicating that the latter membrane could possibly compete with the commercially available membrane. However, further investigation would be required to see just how well the membrane performs in different solutions. Additional testing comprising of salts such as sodium bicarbonate, sodium sulphate and calcium carbonate could be tested for the rejection capabilities of this membrane compared to the NF 270 TFC membrane.

Further to this, the cost associated with the fabrication of bio-renewable membranes is currently higher than the petroleum derived membranes. For the bio-renewable membranes to be considered beneficial, the economical aspect of these membranes would need to be considered. The higher permeance, comparable dye rejection and slightly higher salt rejections of the bio-renewable should be advantageous for the current systems to be replaced.

In addition to this, investigation into the fouling and flux decline of the PA(2-MeTHF) selective layer membrane could be examined to see how well this selective layer is compared to the traditional PA(n-hexane). As the work in this thesis was proof of concept work and all tests were carried out using a dead end cell, with operating times of a few hours. Long term filtration tests could be carried out using a cross-flow cell to investigate how the membranes perform over longer durations of 10-20 hours. The performance of the

membranes at longer times would give an indication of how well they are able to perform in industrial applications.

References

[1] P. Silva, S. Han, and A. G. Livingston, "Solvent transport in organic solvent nanofiltration membranes," *Journal of Membrane Science*, vol. 262, no. 1-2, pp. 49–59, 2005.

[2] D. Prat, A. Wells, J. Hayler, *et al.*, "Chem21 selection guide of classical-and less classical-solvents," *Green Chemistry*, vol. 18, no. 1, pp. 288–296, 2015.

[3] R. W. Baker, *Membrane technology and applications*. John Wiley and Sons, 2012.

[4] M. A. Rasool, P. P. Pescarmona, and I. F. Vankelecom, "Applicability of organic carbonates as green solvents for membrane preparation," *ACS Sustainable Chemistry and Engineering*, vol. 7, no. 16, pp. 13 774–13 785, 2019.

[5] D. Y. Xing, N. Peng, and T.-S. Chung, "Formation of cellulose acetate membranes via phase inversion using ionic liquid,[bmim] scn, as the solvent," *Industrial and Engineering Chemistry Research*, vol. 49, no. 18, pp. 8761–8769, 2010.

[6] D. Y. Xing, S. Y. Chan, and T.-S. Chung, "The ionic liquid [emim] oac as a solvent to fabricate stable polybenzimidazole membranes for organic solvent nanofiltration," *Green Chemistry*, vol. 16, no. 3, pp. 1383–1392, 2014.

[7] M. A. Rasool and I. Vankelecom, "Use of γ-valerolactone and glycerol derivatives as bio-based renewable solvents for membrane preparation," *Green chemistry*, vol. 21, no. 5, pp. 1054–1064, 2019.

[8] M. A. Rasool, C. Van Goethem, and I. F. Vankelecom, "Green preparation process using methyl lactate for cellulose-acetate-based nanofiltration membranes," *Separation and Purification Technology*, vol. 232, p. 115 903, 2020.

[9] M. A. Rasool and I. F. Vankelecom, "Preparation of full-bio-based nanofiltration membranes," *Journal of Membrane Science*, vol. 618, p. 118 674, 2021.

[10] J. Jegal, S. G. Min, and K.-H. Lee, "Factors affecting the interfacial polymerization of polyamide active layers for the formation of polyamide composite membranes," *Journal of Applied Polymer Science*, vol. 86, no. 11, pp. 2781–2787, 2002.

Chapter 8

Appendix

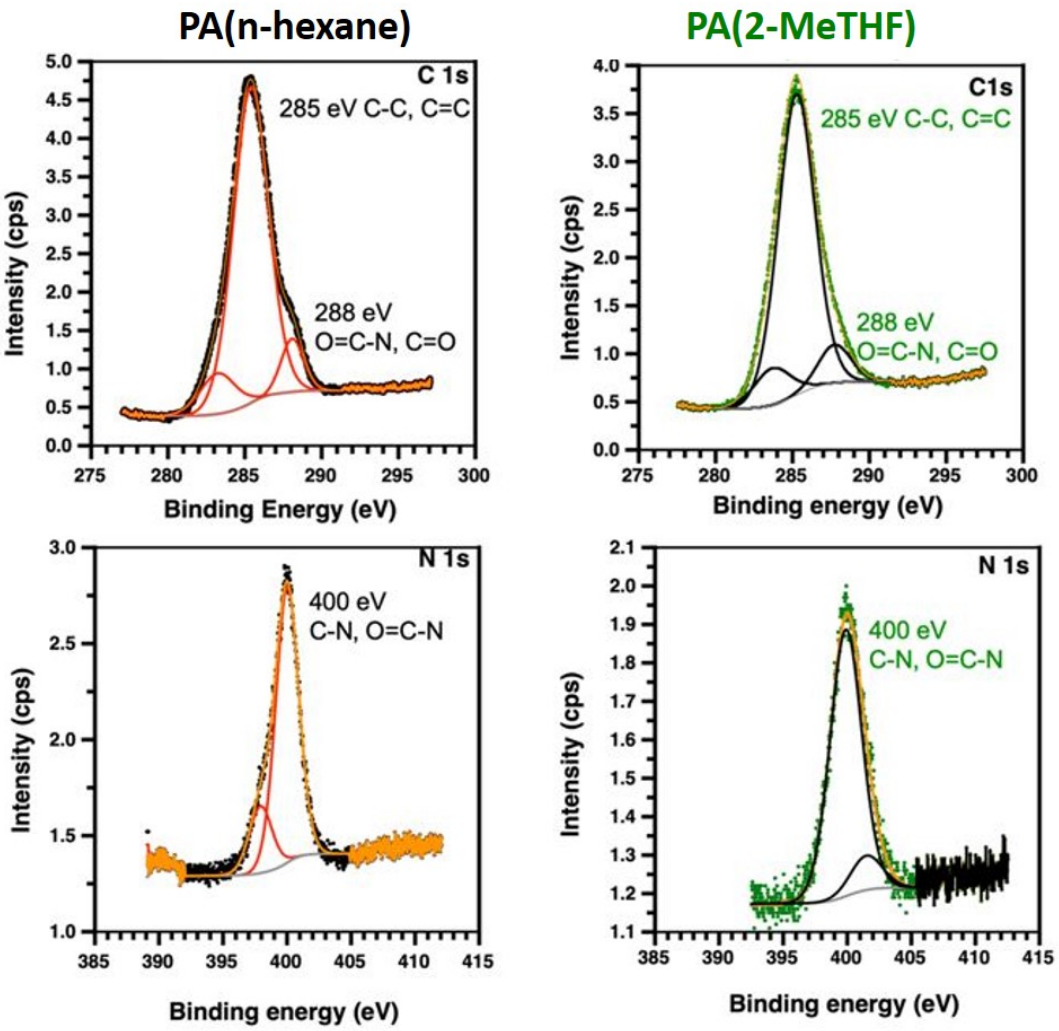

Figure 8.1: Deconvoluted high resolution C 1s and N 1s spectra

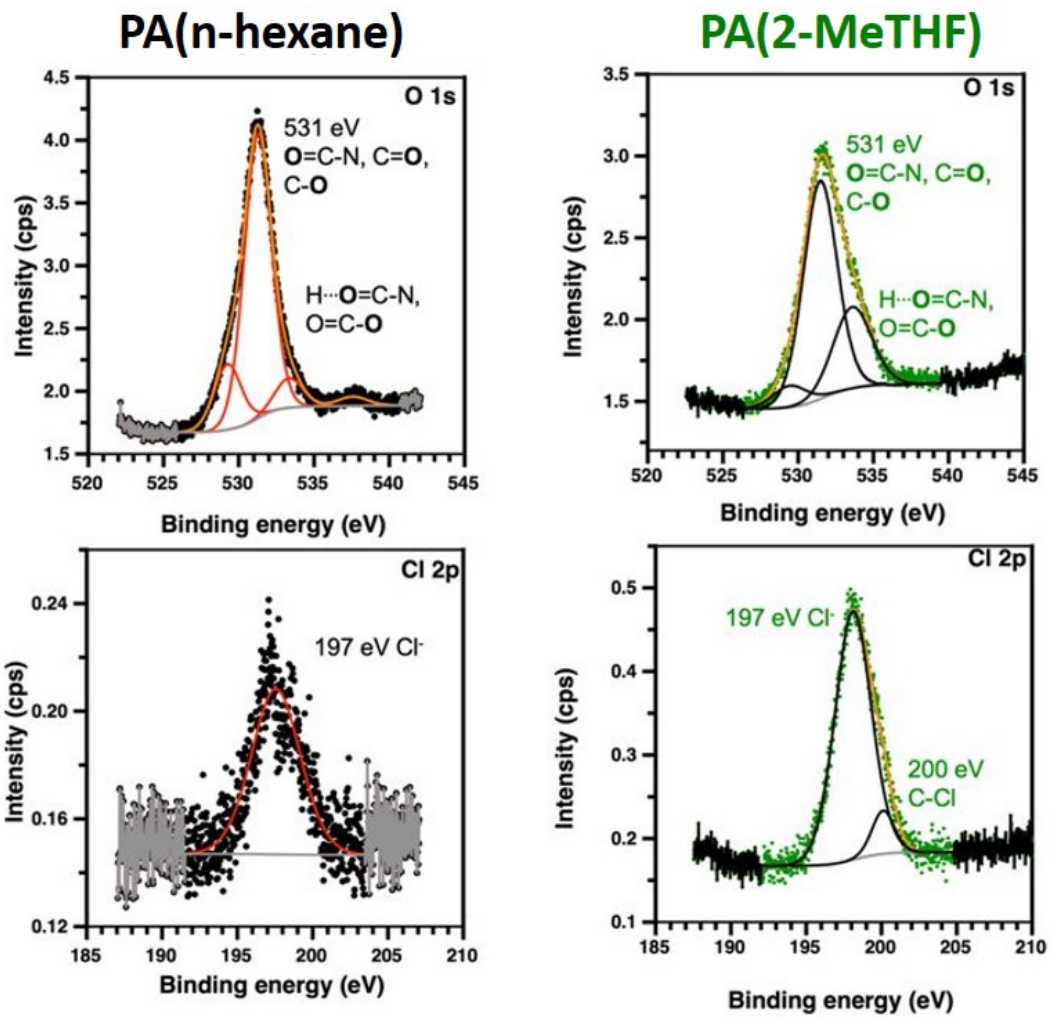

Figure 8.2: Deconvoluted high resolution O 1s and Cl 2p spectra